



**Lymph node heterogeneity is imprinted by unconventional
T cells that are organized in functional units**

**Lymphknoten Heterogenität ist durch unkonventionelle
T Zellen reguliert, welche in funktionellen Einheiten
organisiert sind**

Doctoral thesis for a doctoral degree
at the Graduate School of Life Sciences,
Julius-Maximilians-Universität Würzburg,

Section Infection and Immunity

submitted by

Konrad Knöpper

from

Bonn, Germany

Würzburg, 2022



Submitted on:

Office stamp

Members of the Thesis Committee

Chairperson: Prof. Dr. Jürgen Seibel

Primary Supervisor: Prof. Dr. Wolfgang Kastenmüller

Supervisor (Second): Prof. Dr. Markus Sauer

Supervisor (Third): Prof. Dr. Georg Gasteiger

Date of Public Defence:

Date of Receipt of Certificates:



Table of Contents

Table of Figures	III
Summary	1
Zusammenfassung	2
Introduction	3
The immune system	3
The innate immune system	3
The adaptive immune system	4
T cells	5
Cytokines	6
Lymphatic organs	7
Unconventional T cells	8
Niches	10
Results	11
Lymph nodes display unique cytokine profiles	11
Differentially expressed cytokines are largely produced by UTC	13
UTC TCR-based lineage composition differs across lymph nodes	15
scRNA-sequencing uncovers transcriptional heterogeneity among UTC	16
scRNA-sequencing reveals two major cluster of circulating and non-circulating UTC	19
Phenotype of non-circulating UTC is reflected in the draining tissue	25
TCR-dependent lineage enrichment across mouse facilities	26
Functional unit concept of UTC	28
Th17-like UTC localize in the interfollicular area in sdLN	29
Th17-like UTC encompass distinct TCR-based lineages in sdLN	32
Th17-like UTC produce IL-17 across TCR-based lineages in sdLN	32
Th17-like UTC are compensated in numbers and function in sdLN	33
All UTC units are compensated in single TCR-based lineage deficient strains	36
Discussion	38
Summary	38
Lymph node heterogeneity	39
Functional unit concept of UTC	40
Dedicated Th2-like UTC are absent outside the thymus of naïve mice	42
Translation to humans	43
Clinical relevance	44

Limitations of the study	45
Future directions	46
Material and Methods	47
Material	47
Mouse strains	52
Methods	53
Virus preparation	53
Bacteria preparation	53
Treatment of mice	53
Footpad infection	53
Intranasal infection	53
Isolation of lymphocytes from organs	53
Lymph nodes	53
Spleen	54
Skin	54
Lung	54
Intestine	55
Ex vivo stimulation of lymphocytes	55
Histology	55
Fixation and embedding	55
Microscopy	56
Flow cytometry	56
Tetramer staining	56
scRNA-sequencing	57
Cell sorting	57
Hash tagging for scRNA-sequencing	57
Dropseq	57
scRNA-sequencing analysis	57
Sample demultiplexing and doublet identification	57
scRNA-sequencing analysis workflow	58
Pathway and Gene set enrichment analysis	58
Visualization	58
Statistical analysis	58
Abbreviations	59
Publication list	61
References	62
Acknowledgement	71

Table of Figures

Figure 1: <i>Ex vivo</i> stimulation demonstrates lymph node-specific cytokine profile	12
Figure 2: Site-specific cytokine response is imprinted by UTC	14
Figure 3: Site-specific IL-4 production <i>in vivo</i>	15
Figure 4: UTC TCR-based lineage composition differs across lymph nodes	16
Figure 5: scRNA-sequencing of UTC across distinct lymph nodes uncovers transcriptional heterogeneity	18
Figure 6: Cluster distribution across lymph nodes identified circulating and non-circulating subsets	20
Figure 7: Th1, Th2 and Th17 associated gene expression across clusters	22
Figure 8: Th2-like UTC are not detected in lymph nodes	23
Figure 9: Transcriptional comparison between cluster 2 vs 3 and cluster 1 vs 4	24
Figure 10: Phenotype comparison of UTC in tissues and their draining lymph node	26
Figure 11: UTC comparison of different mouse facilities	27
Figure 12: Schematic representation of the functional unit concept	29
Figure 13: Th17-like UTC in skin draining lymph node have a specific localization	30
Figure 14: Transcriptional heterogeneity of Th17-like UTC does not represent TCR-based lineage identity	31
Figure 15: Th17-like UTC produce IL-17F after stimulation across TCR-based lineage identity	33
Figure 16: Numbers and subsets of Th17-like UTC are compensated in single TCR-based lineage deficient mice	34
Figure 17: IL-17F response is compensated in single TCR-based lineage deficient mice	35
Figure 18: All UTC subsets are compensated in single TCR-based lineage deficient mice	37

Summary

The immune system has the function to defend organisms against a variety of pathogens and malignancies. To perform this task, different parts of the immune system work in concert and influence each other to balance and optimize its functional output upon activation. One aspect that determines this output and ultimately the outcome of the infection is the tissue context in which the activation takes place. As such, it has been shown that dendritic cells can relay information from the infection sites to draining lymph nodes. This way, the ensuing adaptive immune response that is initiated by dendritic cells, is optimized to the tissue context in which the infection needs to be cleared.

Here, we set out to investigate whether unconventional T cells (UTC) could have a similar function in directing a site-specific immune response. Using flow cytometry, scRNA-sequencing and functional assays we demonstrated that UTC indeed drive a characteristic immune response in lymph nodes depending on the drained tissues. This function of UTC was directly connected to their lymphatic migration from tissues to draining lymph nodes reminiscent of dendritic cells. Besides these tissue-derived UTC that migrated via the lymph, we further identified circulatory UTC that migrated between lymph nodes via the blood. Functional characterization of UTC following bacterial infection in wt and single TCR-based lineage deficient mice that lacked subgroups of UTC further revealed that both tissue-derived and circulatory UTC were organized in functional units independent of their TCR-based lineage-affiliation (MAIT, NKT, $\gamma\delta$ T cells). Specific reporter mouse models revealed that UTC within the same functional unit were also located in the same microanatomical areas of lymph nodes, further supporting their shared function. Our data show that the numbers and function of UTC were compensated in single TCR-based lineage deficient mice that lacked subgroups of UTC.

Taken together, our results characterize the transcriptional landscape and migrational behavior of UTC in different lymph nodes. UTC contribute to a functional heterogeneity of lymph nodes, which in turn guides optimized, site-specific immune responses. Additionally, we propose the classification of UTC within functional units independent of their TCR-based lineage. These results add significantly to our understanding of UTC biology and have direct clinical implications. We hope that our data will guide targeted vaccination approaches and cell-based therapies to optimize immune responses against pathogens and cancer.

Zusammenfassung

Das Immunsystem verteidigt den Wirt gegen eine Vielzahl an Pathogenen und malignen Transformationen. Um diese Aufgabe effizient zu erfüllen, arbeiten verschiedene Bereiche des Immunsystems zusammen, um bei Aktivierung optimal zu funktionieren. Einen potenziellen Einfluss auf die Immunantwort hat der Gewebekontext, in dem die Aktivierung stattfindet. Es konnte gezeigt werden, dass dendritische Zellen Informationen von der Infektionsstelle im Gewebe zum drainierenden Lymphknoten transportieren. Auf diese Weise kann die adaptive Immunantwort, initiiert von den dendritischen Zellen, auf die Situation im Gewebe optimiert werden, um die Infektion zu bekämpfen.

In dieser Arbeit wollten wir die Rolle der unkonventionellen T Zellen (UTC) in der Generierung der ortsspezifischen Immunantwort untersuchen. Durch die Verwendung der Durchflusszytometrie, der Einzelzell-RNS Sequenzierung und funktioneller Analysemethoden, konnten wir zeigen, dass diese Zellen eine Lymphknoten-spezifische Immunantwort generieren, die vom drainierenden Gewebe abhängt. Diese Eigenschaft der UTC war direkt mit ihrer Fähigkeit geknüpft, vom Gewebe zu den Lymphknoten zu wandern – wie dendritische Zellen. Neben dieser Gewebe-abstammenden UTC Population konnten wir auch eine im Blut zirkulierende Gruppe dieser Zellen identifizieren. Die Analyse von UTC nach bakterieller Infektion von wild Typ und einzelnen Gen-defizienten Mäusen, denen bestimmte Gruppen an UTC fehlen, zeigte, dass UTC als funktionelle Einheiten agieren, unabhängig von ihrer auf T Zell Rezeptor basierenden Subgruppen (MAIT, NKT, $\gamma\delta$ T Zellen). Mit spezifischen Reporter Maus Linien konnten wir zeigen, dass sich verschiedene Subgruppen von UTC gemeinsam in spezifischen mikroanatomischen Nischen in Lymphknoten befinden, was eine überlappende Funktion andeutet. Außerdem war die Anzahl und Funktion der UTC insgesamt unverändert, auch wenn einzelne Subgruppen in Gen-defizienten Mäusen fehlten.

Zusammengefasst charakterisieren unsere Ergebnisse das Transkriptionsprofil und Migrationsverhalten der UTC in verschiedenen Lymphknoten. Wir zeigen, dass UTC zum Teil für die Lymphknoten spezifischen Unterschiede ursächlich sind und damit eine spezifische, optimierte Immunantwort steuern. Diese Ergebnisse erweitern unser Wissen über die Biologie von UTC signifikant und haben direkte klinische Relevanz. Auf der Basis dieses Wissens können neue Impfansätze oder Zelltherapie Strategien zielgenau entwickelt werden.

Introduction

The immune system

The immune system is responsible for defending the host against a variety of threats, ranging from pathogens such as viruses, bacteria, or parasites, to malignant diseases like cancer. Its importance is probably best recognized in times where the immune system is suppressed or dysfunctional. Patients undergoing radiotherapy to treat cancer, taking immune suppressive medication after organ transplantation, or being born with mutations causing dysfunctionality in parts of the immune system suffer from re-occurring infection and would, in most cases, succumb to them without medical intervention¹. As much as a missing or weakened immune response can be fatal for patients, an overshooting or even unnecessary activation of the immune system can have detrimental effects as well, ranging from pathologies like allergies to severe autoimmune diseases². These two extreme scenarios of a dysfunctional and misguided immune response visualize how essential it is for the immune system to maintain a balance and react appropriately. Based on certain characteristics the immune system is classically divided into the innate and the adaptive arms of the immune system.

The innate immune system

In order to fulfill its purpose in reacting in a balanced and appropriate manner, the most essential task of the immune system is to differentiate between self and non-self³. Therefore, immune cells are equipped with a variety of receptors that can specifically recognize pathogen associated molecular patterns (PAMP) or danger associated molecular patterns (DAMP)⁴. The molecules that can be recognized by these receptors are either an integral part of pathogens like lipo-polysaccharide (LPS), a cell membrane building block of Gram-negative bacteria⁵, or indicate stressed, damaged or dying cells like the presence of adenosine-triphosphate (ATP) in the extra-cellular space⁶. The recognition of these molecular patterns by germline encoded receptors is classically facilitated by receptors of the innate immune system.

Once an innate immune receptor recognizes its ligand, for example LPS and its corresponding receptor toll-like receptor (TLR)-4⁷, an intracellular signaling cascade is initiated. Next to the TLR-family of receptors, other innate immune receptors like the retinoic acid-inducible gene I (RIG-I)-like receptors⁸, C-type lectin receptors⁹, and nucleotide-binding and oligomerization domain (NOD)-like receptors¹⁰ exist. All these receptors commonly recognize different evolutionary conserved ligands and upon activation initiate a signaling cascade and transcriptional activity. For TLRs this cascade is initiated with the recruitment of a toll/interleukin-1 receptor (TIR)-domain containing proteins like myeloid differentiation primary response 88 (MyD88) or TIR-domain-containing adapter-inducing interferon- β (TRIF) to the TLR signaling scaffold¹¹. This recruitment activates signaling pathways like the nuclear factor 'kappa-light-chain-enhancer' of activated B-

cells (NF κ B) or mitogen-activated protein (MAP) kinase pathway¹¹, inducing the transcription of cytokines fulfilling an immunological function. This efficient signaling cascade and rapid response kinetic endows the innate part of the immune system to immediately react upon activation and therefore forms the first line of defense against invading pathogens.

To appropriately react to the diverse innate immune stimuli, given the multitude of contexts in which they can be recognized, the innate arm of the immune system is divided into specialized cells which all fulfill one or multiple functions to coordinate the immune response. Examples of these cells are macrophages, innate lymphoid cells (ILC), natural killer (NK) cells, which have been classified as a group 1 ILC subpopulation¹² and neutrophils. Macrophages are present in basically every tissue including the lung, liver, brain, and heart. As an integral part of the tissue structure, these cells fulfill functions beyond immunological defense, ranging from tissue repair and maintenance to support of the physiological function. For example, it was shown that cardiac macrophages play a role in conducting the electrical current that drives the heartbeat¹³. As local resident immune cells, macrophages also form the first line of defense. Equipped with a variety of innate immune receptors, macrophages sense DAMPs and PAMPs in the tissue and initiate the immune response by secreting factors that activate other local immune cells, such as ILC¹⁴.

ILC are usually located in barrier tissues where they act as resident immune sentinels as in the lung, intestine, liver and other organs¹⁵. Upon activation they react with the production of local cytokines, which activate and direct the functionality of other immune cells¹⁶. Neutrophils are short-lived cells that circulate in the blood throughout the body until local activation signals, potentially produced by ILC, induce their extravasation and migration into barrier tissues. There, neutrophils are directed to the site of danger where they migrate in swarms¹⁷ and release effector molecules like proteases and can undergo NETosis to fight the infection¹⁸. NETosis is a process by which neutrophils release their DNA and nuclear proteins to entrap pathogens and actively kill them¹⁹. NK cells can also be recruited from the blood stream, participating in active killing of malignant or infected target cells²⁰, as well as guiding the recruitment of further specialized immune cells like dendritic cells (DC), which initiate the specialized adaptive immune response²¹.

The adaptive immune system

The large breadth of patterns and stimuli that are recognized by innate immune cells gives them the advantage to react immediately and in a pathogen- or damage-specific manner that is appropriate to the situation. Nevertheless, to achieve complete protection against pathogens or malignant transformed cells a response limited towards these patterns is insufficient, which is likely why the adaptive immune system has developed as an additional layer of defense²². One hallmark of the adaptive immune system is the use of non-germline encoded receptors. The recognition of foreign molecules is facilitated via randomly assembled receptors, like T and B cell receptors. During the maturation of these cells from bone marrow progenitors, their receptor encoding genes

undergo random recombination and/ or somatic hypermutation²³⁻²⁵, processes that lead to the generation of a unique receptor per cell²⁶. Looking at the overall population of T cells, around 10¹⁵ receptors with unique binding capacities can theoretically be formed, allowing for a specialized the recognition of the same number of different antigens²⁷. This number of specialized receptors exceeds by far the repertoire of innate immune receptors, but also causes difficulties in particular the danger of autoimmunity.

T cells

As previously stated, the main task of the immune system is to differentiate self from non-self. For germline encoded receptors, this task is solved by evolutionary pressure. If genetic mutations in the genes encoding for innate receptors cause them to recognize self, the individuals harboring aforementioned mutations suffer from autoimmune diseases and will in most cases die early in life. This selection avoids the inheritance of these mutations and therefore selects against innate immune receptors that recognize self. Randomly recombined receptors, like the T cell receptor (TCR), on the other hand, are not inherited and need to be selected after maturation of the cells, therefore the chances to form a self-recognizing receptor is high and can have detrimental consequences²⁸. To control for these consequences, T cells mature in the thymus, where, upon TCR recombination, the cells undergo positive and negative selection²⁹.

Double negative (DN) thymocytes, referring to their expression pattern of cluster of differentiation (CD4 and CD8 co-receptors), develop into double positive T cells, and get selected for recognition and interaction with antigen presenting molecules like major histocompatibility complex (MHC I and MHC II)³⁰. These thymocytes can be subdivided into stage 1 to 4 DN cells, based on their expression level of CD44 and CD25³¹, marking different maturation steps in their development in the thymus. In the DN3 stage, the pre-TCR is formed and shuffled to the surface³². Signaling through this receptor provides the thymocytes with survival signals to induce the recombination of the TCR and forming a mature receptor^{33,34}. Successfully recombined receptors can then interact with MHC molecules present on the cortical thymic epithelial cells. Thymocytes failing to interact with MHC molecules succumb to apoptosis, a process referred to as positive selection³⁵. This selection ensures that only thymocytes survive that have a recombined TCR capable of interacting with their antigen presenting molecule.

During the following maturation step in the thymic medulla, thymocytes develop into single positive T cells and undergo a process referred to as negative selection³⁵. In the medulla, the cells are exposed to a variety of host derived antigens. In the case of MHC I and MHC II the presented antigens are processed peptides derived from endogenously produced proteins. Other classes of antigens, like lipids and metabolites, are presented by other specialized antigen presenting molecules. High affinity recognition of these peptide self-antigens induces cell death, to avoid the

maturation of highly auto-reactive T cells. Conventional T cells can either interact with MHCI or MHCII, maturing into CD8 or CD4 single positive T cells, respectively³⁶. This division of cell fates further determines the function of these cells during an immune response. CD4 T cells, interacting with MHCII, get their antigen presented solely by professional antigen presenting cells (APC) like DCs or macrophages in peripheral tissues³⁷. This antigen is primarily, although not exclusively, derived from extracellular sources obtained via phagocytosis³⁸. Upon recognition of their cognate antigen in the periphery presented by APCs, naïve CD4 T cells polarize into either T helper cell type (Th)1, Th2 or Th17 cells, depending on the flavor of inflammatory response driven by innate receptors, and guide the immune response and the maturation of antibody producing B cells or other immune cells³⁹.

In brief, Th1, Th2 and Th17 directed immune responses develop to defend against different classes of pathogens. Th1 polarized CD4 T cells produce primarily interferon- γ (IFN γ) to defend against viruses and intracellular bacteria⁴⁰. Th2 polarized CD4 T cells express interleukin (IL)-4 and IL-13 guiding the immune response against parasites⁴¹, while Th17 CD4 T cells secrete IL-17 in order to defend the host against extracellular bacteria and fungi⁴².

CD8 T cells recognize antigens that are presented via MHCI, an antigen presenting molecule that is expressed by nearly every nucleated cell in the body. The antigen source is primarily intracellularly produced protein that is further degraded via proteasomes^{43,44}. Upon viral infection or malignant transformation of cells, viral or tumor antigens get presented via MHCI and CD8 T cells have the capacity to directly target and kill these cells⁴⁵. However, before being able to fulfill this effector function, naïve CD8 T cells need to be properly activated by professional antigen presenting cells like DCs^{46,47}. This activation induces the CD8 T cells to proliferate and further differentiate into either memory or short-lived effector cells^{48,49}.

Next to the usage of randomly recombined receptors, the formation of memory cells with the capacity to mount a more intense and faster secondary immune response, is another hall mark of the adaptive immune system, although it is debated whether innate cells can have memory features as well⁵⁰. In contrast to naïve CD8 T cells, memory cells can be activated via cytokines and partially reside in barrier tissues, being integrated in the first line of defense and monitoring the local cells for infection or malignancies via the antigens presented on their MHCI molecules⁵¹.

Cytokines

Thymic selection is an essential step in ensuring that T cells, limited to being fully activated upon non-self recognition, are present in the periphery. Nevertheless, there are multiple mechanisms in place to ensure that naïve conventional T cells only get activated in appropriate situations. As such, naïve T cells need to acquire three types of signals to become fully activated. First, the TCR is required to engage and recognize an antigen presented via MHC. Second, the

antigen presenting cell needs to provide costimulatory molecules, primarily in form of CD80 or CD86, which interact with CD28 on the T cell^{52,53}. Third, the antigen presenting cell, or surrounding cells have to produce inflammatory cytokines which are recognized by dedicated receptors on the T cell and provide confirmation that a non-self-antigen was detected in an inflammatory context^{54,55}.

Cytokines are the most common form for immune cells to communicate in a contact independent manner. They can be used as survival signals like IL-7 or IL-15, which are expressed during homeostasis. Activating cytokines like IFN γ and IL-18 are mainly secreted during an ongoing inflammatory immune response. Furthermore, suppressive cytokines like transforming-growth-factor (TGF)- β and IL-10 can dampen or resolve the immune activation and often counteract the action of inflammatory cytokines. Overall, cytokines play an essential role in every step of the immune response. As an example, the cytokines received by a naïve CD4 T cell during activation determine whether it matures into a Th1, Th2 or Th17 effector cell⁵⁶. The context of cytokine signaling and integration into a plethora of multiple signals determines the functional outcome of cytokine signaling. Cytokines bind to dedicated receptors on the cellular surface of the target cells. These receptors are mainly made of two or three trans-membrane proteins, which together form the signaling complex and high affinity receptor⁵⁷. Binding of the cytokine induces structural changes, which allow the recruitment of intracellular signaling molecules and the induction of the signaling cascade⁵⁸. Commonly used signaling pathways downstream of cytokine receptors are the Janus-kinase or tyrosine-kinase pathway⁵⁷,

The availability of cytokines is often a rate limiting step for cells upon activation but also during homeostasis. This limitation is controlled by tightly regulated production and scavenging mechanisms in the tissue. The importance of this limitation is best exemplified with the cytokine IL-18. IL-18 is a highly inflammatory cytokine⁵⁹ that is produced mainly by macrophages after inflammasome activation⁶⁰ and binds to a receptor complex consisting of IL-18R1 and IL-18rap⁶¹. To limit the inflammatory effects of IL-18 to a local response, a binding protein for IL-18, IL-18BP, is secreted into the circulation, buffering excessively produced cytokine, without signal transduction or cell activation⁶². Deficiency of this binding protein leads to increased inflammation under inflammatory conditions⁶³. Also, constantly produced survival cytokines like IL-7 can be a limiting factor that determines the cell pool size. Increasing the access to IL-7 can lead to increased numbers of T cells, while reducing its abundance would adjust the T cell population size to a smaller number⁶⁴.

Lymphatic organs

Positive and negative selection of T cells during their maturation in the thymus gives the adaptive immune system the capacity to reliably differentiate between self and non-self. Nevertheless, the created number of antigen-specific receptors causes another difficulty that needs

to be overcome for the adaptive immune response to be effective in protecting the host. Neutrophils, a type of innate immune cell, can be used as an example to compare the adaptive and the innate immune system characteristics and visualize the arising problems. Three subpopulations of mature neutrophils have been described, which might differ in their function and contribution to the immune response⁶⁵. Having three functionally distinct subsets means there are millions of cells for each subset present in the bloodstream, which in absolute numbers is sufficient to mount a significant immune response. Since roughly each T cell possesses a unique TCR, it is estimated that there are only around 100 T cells specific for a certain antigen present at once in mice and around one in 10^6 T cells in human²⁷. In order to limit or clear an infection the antigen-specific T cells need to expand to reach sufficient absolute numbers⁶⁶. Therefore, the adaptive immune system reacts slower and fulfills its function in a delayed manner compared to the innate immune response.

Furthermore, the adaptive immune system faces the problem on how to protect each barrier site of the body with the limited number of specific adaptive immune cells. To coordinate the immune response and ensure that a T cell finds its matching antigen in a reasonable amount of time, these cells constantly migrate and recirculate through the blood, entering and exiting lymphatic organs such as the lymph nodes and spleen⁶⁷. One function of these organs is to provide a meeting spot for T cells and their antigen presenting cells, mainly DCs⁶⁸. Antigen obtained at barrier sites, like the skin, is transported via the lymphatic vessels by DCs to the draining lymph node⁶⁹. There, DCs interact with antigen-specific T cells that are present in the draining lymph node. Following this interaction, DCs activate the T cell and thereby initiate the adaptive immune response and clonal expansion of the T cells.

To facilitate this process, T cells recirculate through lymph nodes, entering from the blood via high-endothelial venules and exiting via the lymph to re-enter the blood stream, until they find their cognate antigen being presented. To coordinate this migrational behavior as efficiently as possible, the recirculation of lymphocytes through the blood and the exit of DCs from tissues are additionally regulated by the circadian rhythm^{70,71}.

Unconventional T cells

Antigen presentation via MHCI and MHCII is limited to proteins. Since not only proteins, but also other macro-molecules can be pathogen derived antigens, additional antigen presenting complexes and T cells restricted to these, exist. As a group, these T cells are referred to as unconventional T cells (UTC) and consist of several TCR-based lineages, defined by their restriction to other antigen-presenting molecules like CD1d and MR1. In mice, the majority of UTC lack the expression of the co-receptors CD4 and CD8⁷². CD1d is able to present lipid antigens like α -Galactosylceramid (GalCer) and interacts with the TCR of natural killer T (NKT) cells⁷³. Major

histocompatibility complex class I-related (MR1) is specialized in presenting vitamin B6 metabolites and thereby activates so called mucosal-associated invariant T (MAIT) cells⁷⁴. $\gamma\delta$ T cells are proposed to have a distinct mode of antigen recognition that is more similar to antibodies, which are not restricted to antigen presenting complexes. This could explain why typical antigen presenting molecules do not seem to be required for the development and function of this TCR lineage⁷⁵. The antigens recognized by $\gamma\delta$ T cells that have been identified so far, belong mainly to the class of phospho-antigens⁷⁶.

Aside from the class of antigens being recognized and the molecules interacting with their TCR, UTC differ in many other ways from conventional T cells. Most strikingly, they exit the thymus not as naïve T cells, that need to be properly activated to mount an immune response, but already with features of an effector cell. UTC polarize, like conventional CD4 T cells, into Th1-, Th2- and Th17-like phenotypes, which are classified based on the cytokines they produce upon activation^{77,78}. In line with that observation, only a fraction of these cells reside in the lymphatic organs or the blood, while a significant proportion seeds barrier-tissues like skin, lung and intestine, among others⁷⁷ and are considered to be tissue-resident⁷⁹. It has been described that the tissue seeding by UTC is not random process, but instead correlates with the TCR that is expressed by these cells and is further influenced by commensal bacteria that are present at distinct tissue sites^{80,81}.

In these barrier tissues UTC fulfill several functions, like regulating tissue homeostasis⁸², controlling commensal communities, protecting against invading pathogens⁸³ and promoting tissue healing⁸⁴. As an example, $\gamma\delta$ T cells have been shown to actively regulate thermogenesis via IL-17 production in the adipose tissue⁸². In the skin, they can specifically recognize *Staphylococcus aureus* (*S. aureus*) infections and contribute to bacterial clearance^{83,85}. Furthermore, $\gamma\delta$ T cells have been described to actively contribute to tissue healing, for example after muscle injury⁸⁶.

To fulfill this variety of functions appropriately, UTC have the capacity to be activated in multiple ways, some differing greatly from the mode of activation of conventional T cells. One important activation mechanism for T cells, including both conventional T cells and UTC, is TCR engagement with its cognate antigen. This interaction can induce the production of cytokines and proliferation of UTC⁸⁷. However, the TCR-dependent activation differs in several ways between UTC and conventional T cells. As described above, conventional T cells scan the lymphatic organs for the presence of their cognate antigen presented by DCs. DCs constantly present antigen to T cells via MHC I and MHC II. In contrast, some antigen presenting molecules for UTC are not constantly presenting antigen. For example, MR1 is only shuttled to the cell surface in the presence of presentable antigens, which are not constantly available during homeostasis⁸⁸. Therefore, in contrast to conventional T cells, the TCR of e.g. MAIT cells does not constantly interact with MR1 molecules. On the other end of the spectrum, it was recently described for a subset of UTC, the

dendritic epidermal T cells (DETC), a $\gamma\delta$ T cell subset specifically residing in the epidermis, that these cells have constant TCR engagement with their cognate antigen⁸⁹. This interaction during homeostasis was coined normality sensing by the authors because a temporal disruption of the signaling could partially activate the cells. Furthermore, this constant TCR engagement during homeostasis was required for the DETC to fulfill their function during inflammation.

Not only the context and regulation of antigen engagement differs between UTC and conventional T cells. For $\gamma\delta$ T cells it has also been described that the intracellular signaling cascade following TCR interaction with its cognate antigen and the TCR responsiveness differ significantly to conventional T cells⁹⁰. In line with that, a subset of $\gamma\delta$ T cells in the murine dermis is described to be lymphocyte-specific protein tyrosine kinase (LCK) negative⁹¹, which is an essential signaling molecule in the TCR signaling cascade⁹².

Next to the TCR-dependent activation, UTC have the potential to be stimulated in a TCR-independent manner via cytokines⁸⁷. During homeostasis UTC express a variety of cytokine receptors like IL-18R or IL-23R and upon a cytokine response can be induced. This is in stark contrast to conventional naïve T cells which are typically not activated via cytokines alone. Considering this activating mechanism, UTC seem to share certain aspects with ILCs which are primarily activated via cytokines⁹³.

Combining the observations that UTC are partially located in barrier tissues, have a pre-determined effector phenotype, and can react immediately to activating signals, led them to be classified in between the innate and the adaptive arms of the immune system, despite the fact that they are bona fide T cells that possess a recombined T cell receptor and undergo selection in the thymus.

Niches

When acting as survival factors, cytokines serve the essential role to control and limit the number of immune cells. As previously mentioned, the importance of the immune system becomes clearly apparent in conditions of its dysfunction, which justifies its evolution and the energetic costs invested in it. Nevertheless, evolutionary pressure also dictates the immune system to operate as efficiently as possible in terms of resources. To regulate immune cell presence in tissues and circulation, specific niches develop where immune cells are integrated into the tissue structure. This phenomenon is probably best described for macrophages, an innate immune cell type that resides in every organ of the body⁹⁴. In each specific organ, the number and phenotype of macrophages is adapted and controlled by locally produced factors like colony-stimulating factor 1 (CSF1) and IL-34. Local increase or decrease in survival cytokines controls the rate of proliferation and cell death, while other tissue specific factors can imprint the cell identity and cause the phenotype to be adapted to local requirements⁹⁵.

This site-specific presetting of the immune system is an integral mechanism to increase its efficiency. A site-specific preset immune system can react faster and limit energy consumption to where it is needed. Examples for this compartmentalization of the immune system are also detectable in the structures of lymph nodes. Distinct tissue draining lymph nodes harbor a specialized set of structural fibroblasts^{96,97}. Furthermore, the migration of DCs from distinct parts of the intestine and accompanied antigen transfer was shown to induce specific immune reactions in distinct intestine draining lymph nodes⁹⁸. Also, the site-specific environment seems to significantly influence the T cell response⁹⁹, and can directly impact the vaccination outcome in mice, non-human primates and humans based on the administration route¹⁰⁰⁻¹⁰².

These examples highlight the importance of local factors in guiding the immune response. Further research in identifying site-specific factors and cell types involved in the local shaping of the immune response is required to better understand the immune system and to develop targeted therapies.

In this study, we aimed to characterize which molecular factors define and differentiate site-specific immune responses in lymph nodes. We proposed that further site-specific factors and cell types beyond local fibroblasts and DCs are driving a divergent immune response in distinct lymph nodes.

Results

Lymph nodes display unique cytokine profiles

An increasing number of studies demonstrate the site-specificity of immune responses, implying potential therapeutic significance for vaccination. The molecular and cellular components responsible for these differences and how they are regulated are still an open question in the field.

We speculated that part of the underlying mechanism imprinting lymph node heterogeneity is found in the innate part of the immune response, since inflammatory cytokines produced early during infection are known to influence the adaptive cells and their phenotype^{56,103}. To circumvent potential confounding factors like timing or intensity of the inflammation, we set up an *ex vivo* system to activate the lymphocytes present in lymph nodes draining distinct tissues. We analyzed lung draining mediastinal lymph nodes (medLN), skin draining inguinal lymph nodes (iLN) and small intestine draining mesenteric lymph nodes (mesLN). Single cell suspensions were plated at a concentration of 5×10^6 cells per ml and stimulated with phorbol myristate acetate (PMA) and Ionomycin (Iono) for 4 h. To block the cytokine secretion and its loss over time, we treated the stimulated condition and non-stimulated control with Brefeldin A (BFA). Afterwards, the cytokine profile of different lymph nodes was analyzed via flow cytometry (Fig. 1A).

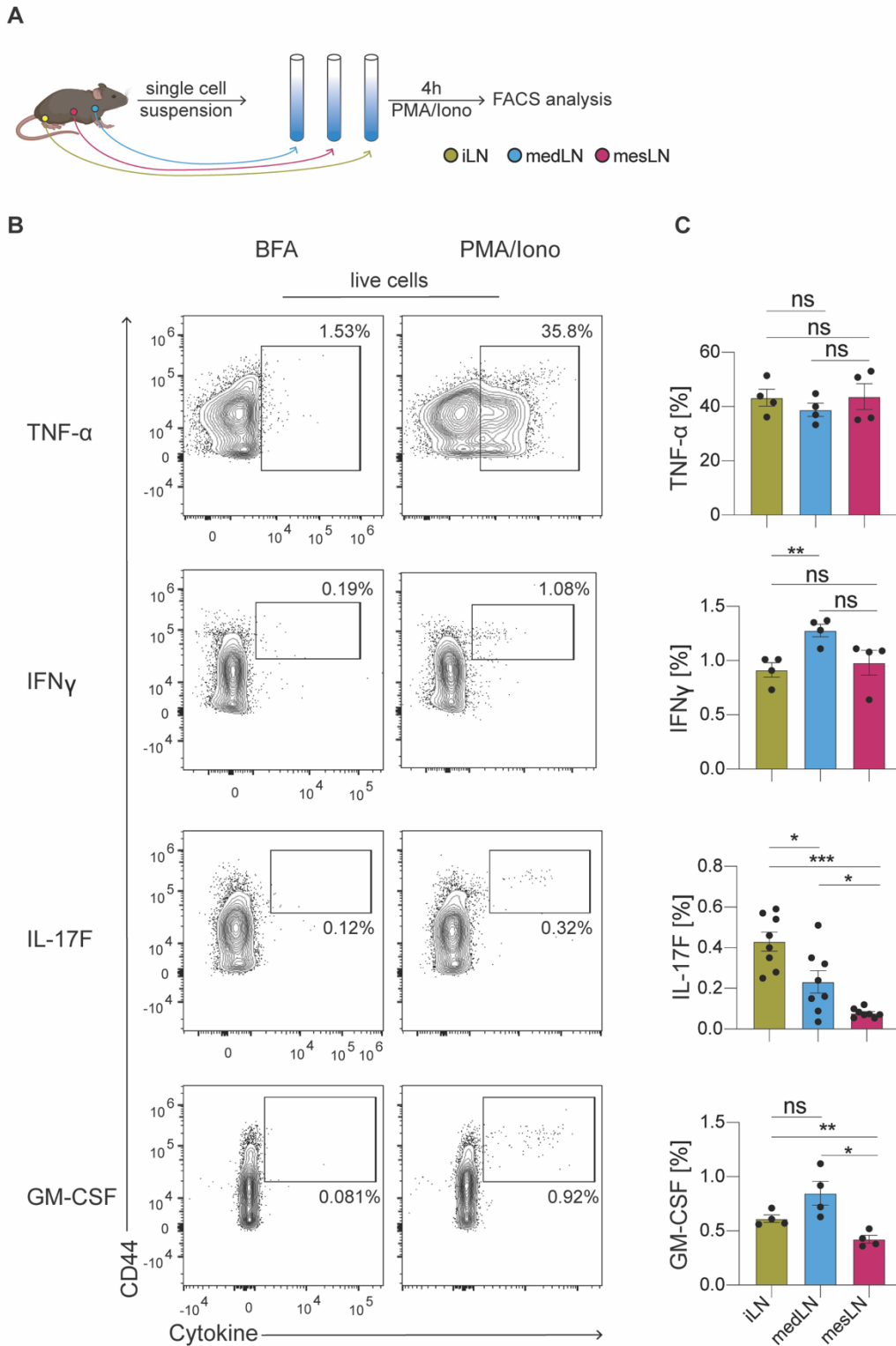


Figure 1: Ex vivo stimulation demonstrates lymph node-specific cytokine profile

A) Schematic representation of experimental set up. inguinal (iLN), mediastinal (medLN) and mesenteric (mesLN) lymph nodes (LNs) were isolated from B6 wt mice and single cell suspensions *ex vivo* stimulated for 4 h with phorbol myristate acetate/ Ionomycin (PMA/ Iono). Cytokine expression was analyzed using flow cytometry. B) Representative flow cytometry plot, pre-gated on live cells displaying cytokine production in control (BFA) and stimulated (PMA/ Iono) cells derived from medLN. C) Quantitative analysis of cytokine production comparing different lymph nodes. Data display 1 or 2 representative experiments with $n \geq 4$ mice. Bar graphs display mean

value and error bars represent SEM. Comparison between groups was calculated using non-paired student t-tests. ns $p > 0.05$; * $p < 0.05$; *** $p < 0.001$.

We observed a drastic increase in protein levels for all analyzed cytokines comparing the stimulated condition to the non-stimulated control, providing evidence that our experimental set-up is suitable to induce cytokine production (Fig. 1B). Tumor necrosis factor alpha (TNF- α) was most abundantly produced among the tested cytokines but was not differentially expressed between distinct lymph nodes (Fig. 1C). IFN γ on the other hand was expressed at a significantly higher frequency in the medLN than in the iLN (Fig. 1C). Even more pronounced differences were observed when analyzing the expression levels of IL-17F and granulocyte-macrophage colony-stimulating factor (GM-CSF) (Fig. 1C). IL-17F was highly induced in activated iLN-derived lymphocytes, while in medLN-derived and in particular the mesLN-derived lymphocytes, the production was significantly lower. The frequency of GM-CSF-producing cells was similarly reduced in mesLNs compared to medLNs or iLNs. In conclusion, these results demonstrate that the innate cytokine potential of the analyzed lymph nodes differs, which in turn could impact on the immune responses that are generated in these lymph nodes *in vivo*.

Differentially expressed cytokines are largely produced by UTC

Next, we wished to identify the source of the produced cytokines. Therefore, we used the same experimental set-up as before and additionally stained for cell type defining markers for consecutive single cell analysis using flow cytometry. When pre-gating on the cytokine producing cells, we observed that the main source for all analyzed cytokines is CD3 positive T cells (Fig. 2A). Quantifying the frequencies of subsets across the analyzed lymph nodes for TNF- α and IFN γ the main producers were conventional CD4/ CD8 positive T cells (Fig. 2B). Analyzing the source of IL-17F and GM-CSF, the cytokines showing the most heterogeneity across lymph nodes, we observed that most producing cells were CD4/ CD8 negative UTC (Fig. 2B).

To test for the *in vivo* relevance of our observation and to extend it also towards an additional cytokine, we infected *Ii4*^{GFP/wt} reporter mice with Vaccinia virus subcutaneously or intranasally. Three days later we compared the frequency and identity of green fluorescent protein (GFP) positive cells in popliteal lymph nodes (pLN) and medLNs. pLNs are skin draining lymph nodes similar to the iLN analyzed before. We observed that the frequency of GFP positive cells in the medLNs was significantly higher compared to the pLNs (Fig. 3A). In line with our results on IL-17F and GMCSF producing cells analyzed above using *in vitro* activation, the main cytokine producer for IL-4 (GFP positive cell population) in the medLN was also UTC (Fig. 3B). This result is in line with a previous study, showing that the early source of IL-4 after infection in the medLN is NKT cells¹⁰⁴, a subset of UTC.

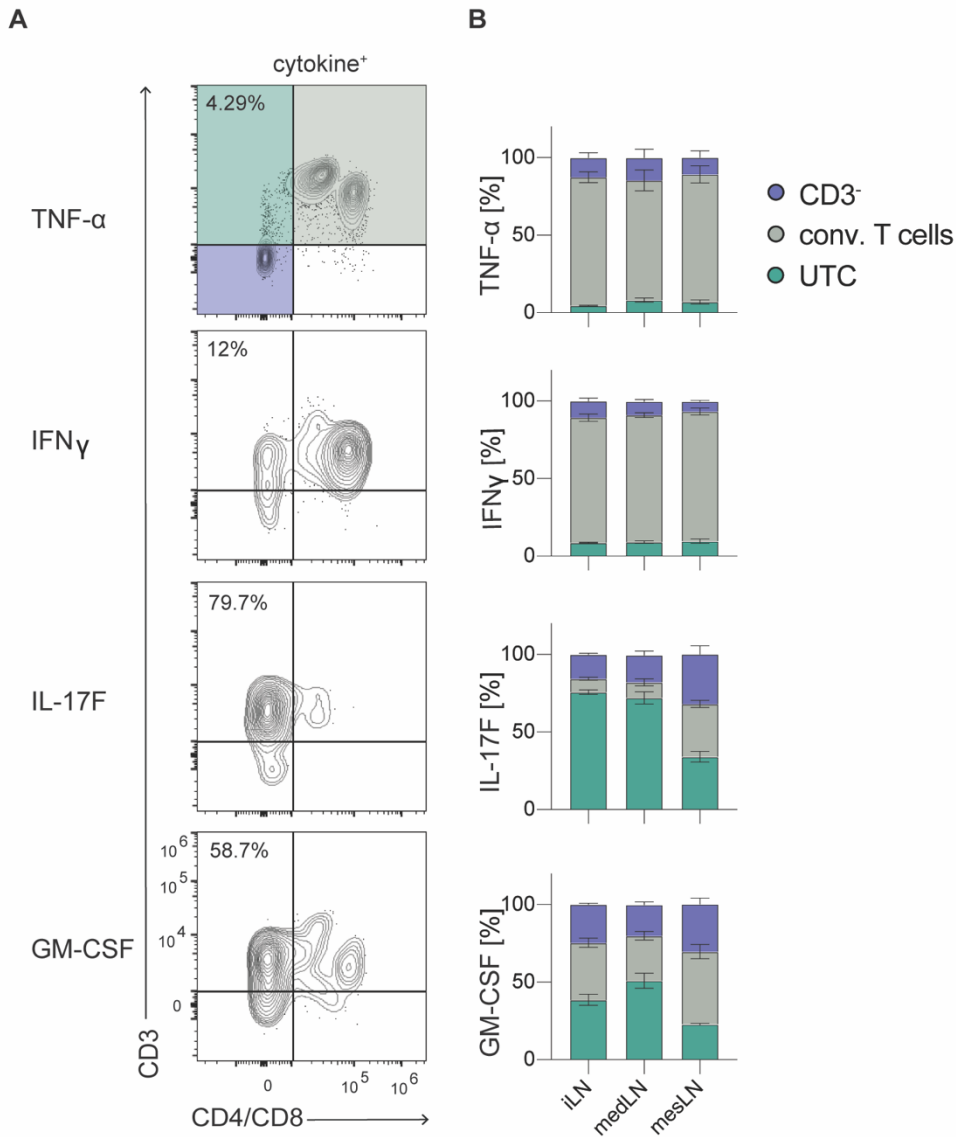


Figure 2: Site-specific cytokine response is imprinted by UTC

A) Representative flow cytometry plot of the identity of cytokine producing cells from medLN, pre-gated on all cytokine producers (cytokine⁺), after 4 h stimulation with PMA/ Iono. B) Quantitative analysis of cell type identity of cytokine producing cells comparing different lymph nodes. Data display 1 representative experiment with n ≥ 5 mice. Bar graphs display mean value and error bars represent SEM.

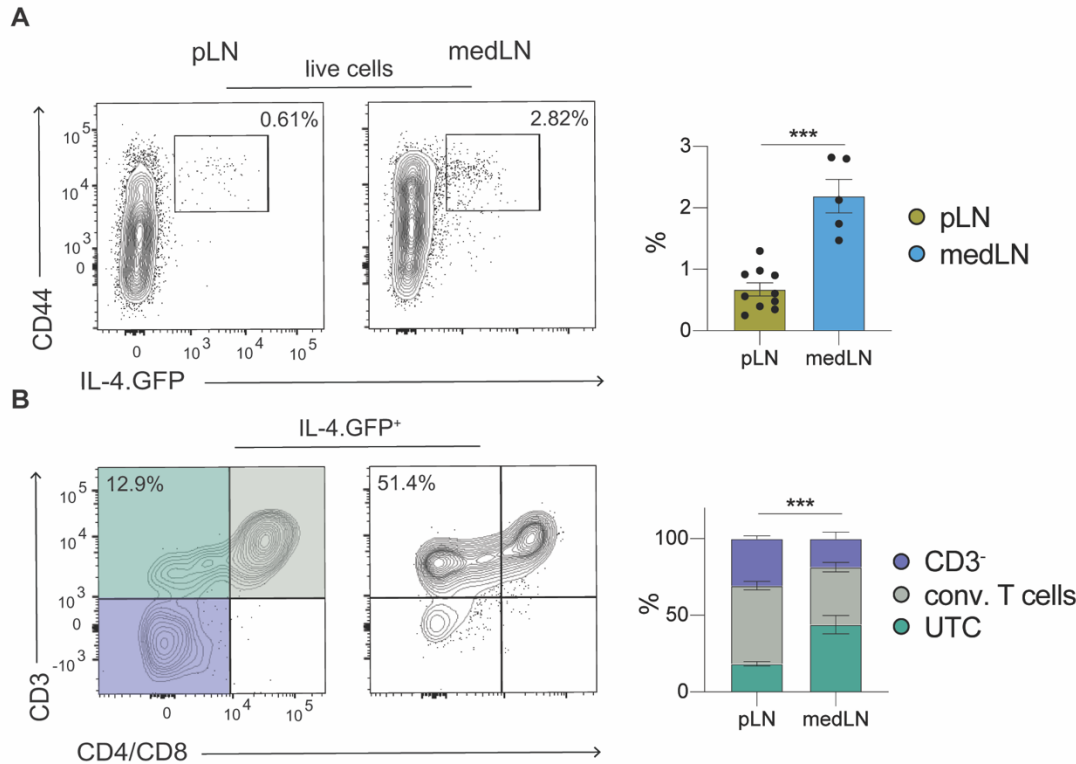


Figure 3: Site-specific IL-4 production *in vivo*

Ii4^{GFP/wt} reporter mice were infected either subcutaneously or intranasally with 200 PFU Vaccinia virus. 3 days post-infection the draining lymph node was analyzed via flow cytometry. A) Representative flow cytometry plots, pre-gated on live cells, and quantitative analysis of IL-4.GFP production in popliteal lymph node (pLN) and medLN. B) Representative flow cytometry plot, pre-gated on IL-4.GFP producers (IL-4.GFP⁺), and quantitative analysis of cell type identity of IL-4.GFP producers comparing pLN and medLN. The data display 2 experiments with $n = 5$ mice. Bar graphs display mean value and error bars represent SEM; dots display individual lymph nodes. Comparison between groups was calculated using a non-paired student t-test. *** $p < 0.001$. In B the frequency of UTC was tested for significance.

UTC TCR-based lineage composition differs across lymph nodes

Having determined that the major source of site-specific cytokines is UTC, we aimed to further characterize this cell population across lymph nodes. Since UTC are a heterogenous mix comprised of $\gamma\delta$ T cells, MAIT cells, NKT cells and other less well described non-MHC-restricted T cells⁷², we aimed to investigate the TCR-based lineage composition of UTC in distinct lymph nodes. The three major lineages can be readily identified via TCR-specific antibody staining ($\gamma\delta$ TCR, V β 6 and V β 8) or using antigen loaded tetramers (Fig. 4A). V β 6 and V β 8 TCR specific antibodies can be used to detect MR1-restricted MAIT cells⁷⁴, while CD1d tetramer loaded with PBS-57 specifically labels NKT cells¹⁰⁵. Quantification of the TCR-based lineage composition across lymph nodes revealed a striking heterogeneity. $\gamma\delta$ T cells were enriched in iLN and mesLN compared to medLN, while MAIT and more significantly NKT cells were prominent in the medLN (Fig. 4B). Together these results might offer an explanation for the site-specific cytokine production in LNs. The

heterogeneous cytokine profile was reflected by the heterogeneous UTC composition with regards to their TCR-based lineage affiliation.

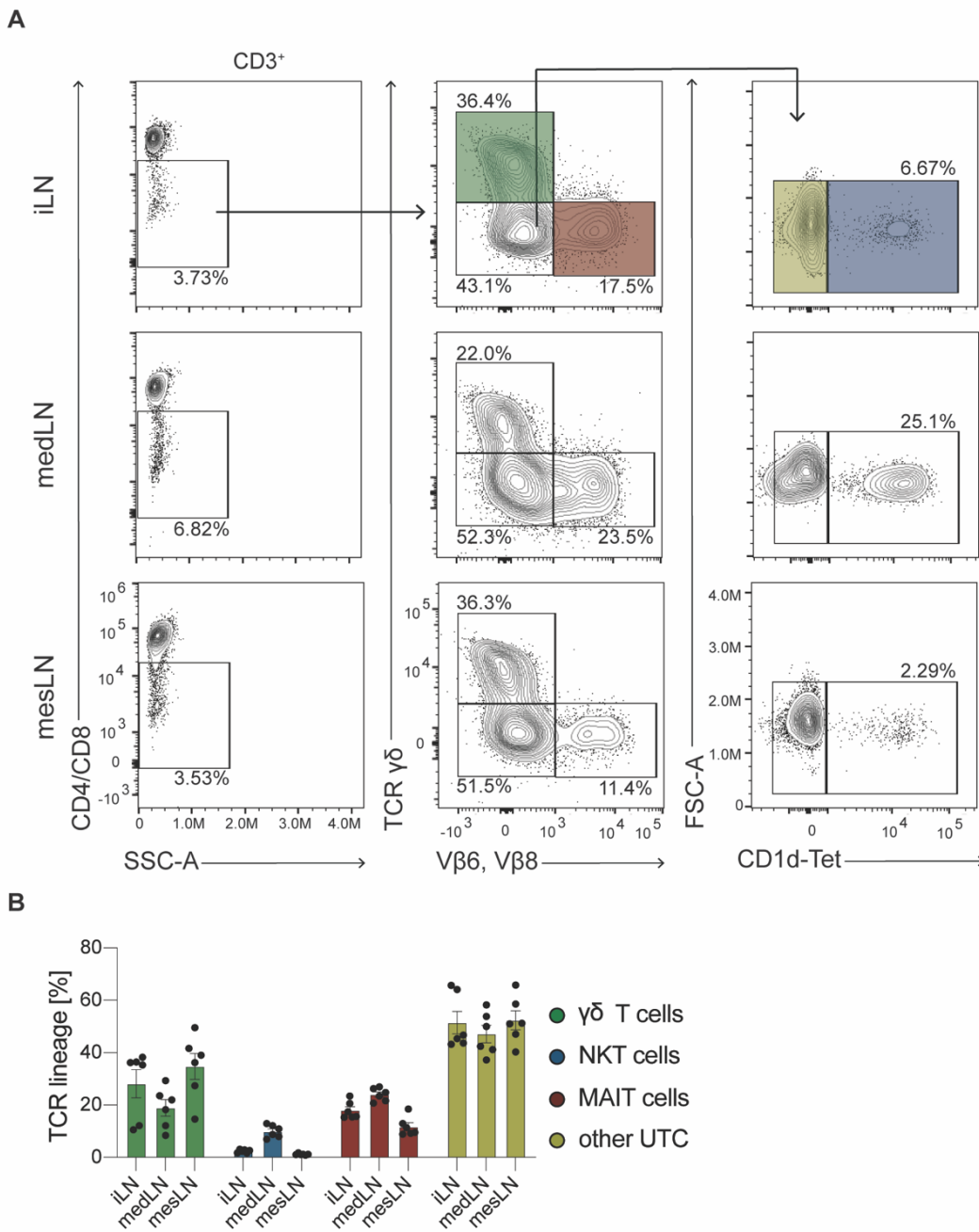


Figure 4: UTC TCR-based lineage composition differs across lymph nodes

A) Representative flow cytometry plots and gating strategy used to identify UTC, pre-gated on living $CD3^+$ cells. B) Quantitative analysis of TCR-based lineage subsets in different lymph nodes. Data display 2 experiments with $n = 6$ mice. Bar graphs display mean value and error bars represent SEM.

scRNA-sequencing uncovers transcriptional heterogeneity among UTC

Having described the TCR-based lineage composition of each lymph node and correlated it to a heterogeneous cytokine profile, we aimed to understand the molecular mechanism driving

these differences and linking certain cytokines to a corresponding TCR-based lineage. To this end, we analyzed the UTC compartment of different lymph nodes via single-cell ribonucleic acid (scRNA)-sequencing. To obtain an overview of these cells, we isolated distinct lymph nodes from mice, stained the single cell suspensions separately with the same antibody sorting mixture and individual hashtag antibodies (Fig. 5A). The hash tagging allows for later identification of the origin of each cell after transcriptomic sequencing¹⁰⁶. After sorting CD3 positive, CD4/ CD8 negative cells and subjecting them to scRNA-sequencing (see Methods), 12 separate clusters could be identified via unbiased analysis (Fig. 5B). Differentially expressed marker genes marked the individual clusters (Fig. 5C). Among these differentially expressed genes were counter regulated markers like *Sell* (coding for CD62L) and *Zbtb16* (coding for PLZF) which are expressed in clusters 0, 1, 5, 7, 8 and 2, 3, 4, 9, 11, respectively. Cluster 6 could be reliably identified by the lack of *Lck* expression, which is a member of the TCR signaling cascade. The *Sell* expressing clusters could be further subdivided by *Ccr9* expression for cluster 0, *Eomes* expression for cluster 7 and *Cxcr3* expression for cluster 1 and 5. The *Zbtb16* positive cluster could be separated further by *Cxcr3* expression in cluster 4, *Ccr6* expression in cluster 3 and 11, as well as *Slamf6* expression in cluster 9. To validate the sequencing results, cluster defining marker genes were analyzed on a protein level via flow cytometry (Fig. 5D). The gene expression profile of the clusters could be verified on a protein level, demonstrating significant heterogeneity among UTC. In line with the sequencing results, the markers analyzed via flow cytometry reliably identified distinct cell populations that represented the RNA-based subsets detected via scRNA-sequencing. To investigate whether the identified clusters reflect known TCR-based lineages, we quantified the contribution of each lineage for the distinct clusters via flow cytometry. Surprisingly, we observed that multiple TCR-based lineages were contributing to each cluster (Fig. 5E). Indeed, we were not able to identify a distinct $\gamma\delta$ T cell, MAIT cell or NKT cell cluster in our scRNA-sequencing validation analysis. These results argue that the correlation between TCR-based lineage heterogeneity and distinct cytokine profiles across lymph nodes is not causative as previously hypothesized. Therefore, the observed cytokine heterogeneity is driven by a distinct factor independent of TCR-based lineage affiliations of UTC.

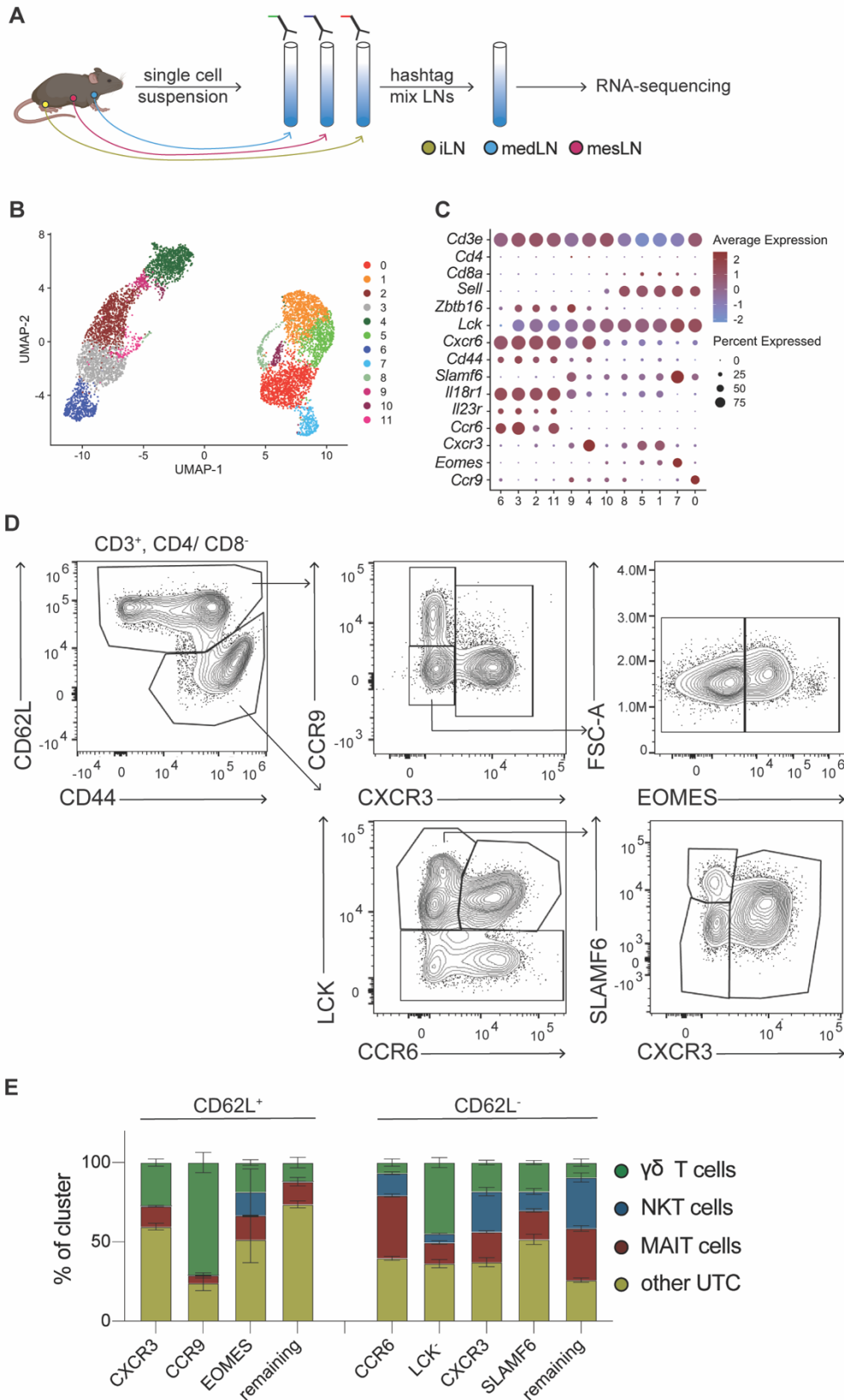


Figure 5: scRNA-sequencing of UTC across distinct lymph nodes uncovers transcriptional heterogeneity

A) Schematic representation of the experimental set up for comparative scRNA-sequencing of UTC from different LNs. iLN, medLN and mesLN were isolated, separately stained with antibodies for sorting and hashtagged. CD3⁺ and CD4/CD8⁻ cells were sorted, pooled and sequenced. B) UMAP

projection of 7041 single cells, color code based on cluster identity. C) Dot plot of selected marker genes associated with identified clusters. Color represents z-score mean expression values across clusters; dot size indicates the fraction of cells in the cluster expressing respective genes. D) Representative flow cytometry plots and gating strategy of iLN-, medLN- and mesLN-derived UTC, pre-gated on CD3⁺ and CD4/CD8⁻ cells, for marker genes validation at protein level. E) Quantitative analysis of TCR-based lineage subsets from the identified UTC clusters. Data represent 1 experiment with n = 10 mice (A-C) or display 2 experiments with n = 6 mice (D, E). Bar graphs display mean value and error bars represent SEM.

scRNA-sequencing reveals two major cluster of circulating and non-circulating UTC

To identify the mechanistic basis of the functional UTC heterogeneity among LNs draining distinct sites, we separated the uniform manifold approximation and projection (UMAP) by lymph nodes and analyzed the cluster distribution (Fig. 6A). The visual display readily showed an unequal cluster distribution when comparing distinct LNs. Comparing the two most separated groups of cells, it appeared, that the *Zbtb16* expressing group (cluster 2, 3, 4, 6, 9) had tissue of origin determined clustering of the cells. The group of clusters expressing *Sell* (cluster 0, 1, 5, 7, 8) displayed an equal distribution across analyzed lymph nodes. Quantification validated the visual impression (Fig. 6B), showing that cluster 3 and 6 are dominated by cells derived from iLN, while cluster 4 and 9 had an enrichment for cells from mesLN. Cluster 2 was enriched for cells derived from medLN. This observation, together with the selective expression of *Sell* in the homogeneous distributed clusters (Fig. 5C), led us to speculate that some cells recirculate between secondary lymphoid organs, while the other clusters represent non-circulating cells. *Sell* encodes for CD62L, which lymphocytes require to enter lymph nodes via interaction with glycosylation-dependent cell adhesion molecule-1 (GlyCAM-1) expressed on high endothelial venules¹⁰⁷.

To understand further differences between circulating and non-circulating UTC (Fig. 6C), we characterized differentially expressed genes (Fig. 6D) and subjected this gene list to pathway (Fig. 6E) and gene set enrichment analysis (Fig. 6F). In the circulating population *Ccl5*, *Klf2* and *Nkg7* were significantly upregulated. Enriched expression in the non-circulating cells was found for genes such as *Il7r*, *Rora* and *Blk* (Fig. 6D). Pathways enriched in the differentially expressed genes were associated with IL-2 signaling and Th1/ Th2 differentiation (Fig. 6E). Gene set enrichment analysis revealed that circulating UTC were enriched in a naïve CD4 T cell phenotype compared to central memory T cells (Fig. 6F). These results support the notion that the cells are circulating between secondary lymphoid organs like naïve CD4 T cells. Another significantly enriched gene set demonstrated the presence of Th17 markers in the non-circulating cell population, while Th1 associated genes are expressed in the circulatory pool.

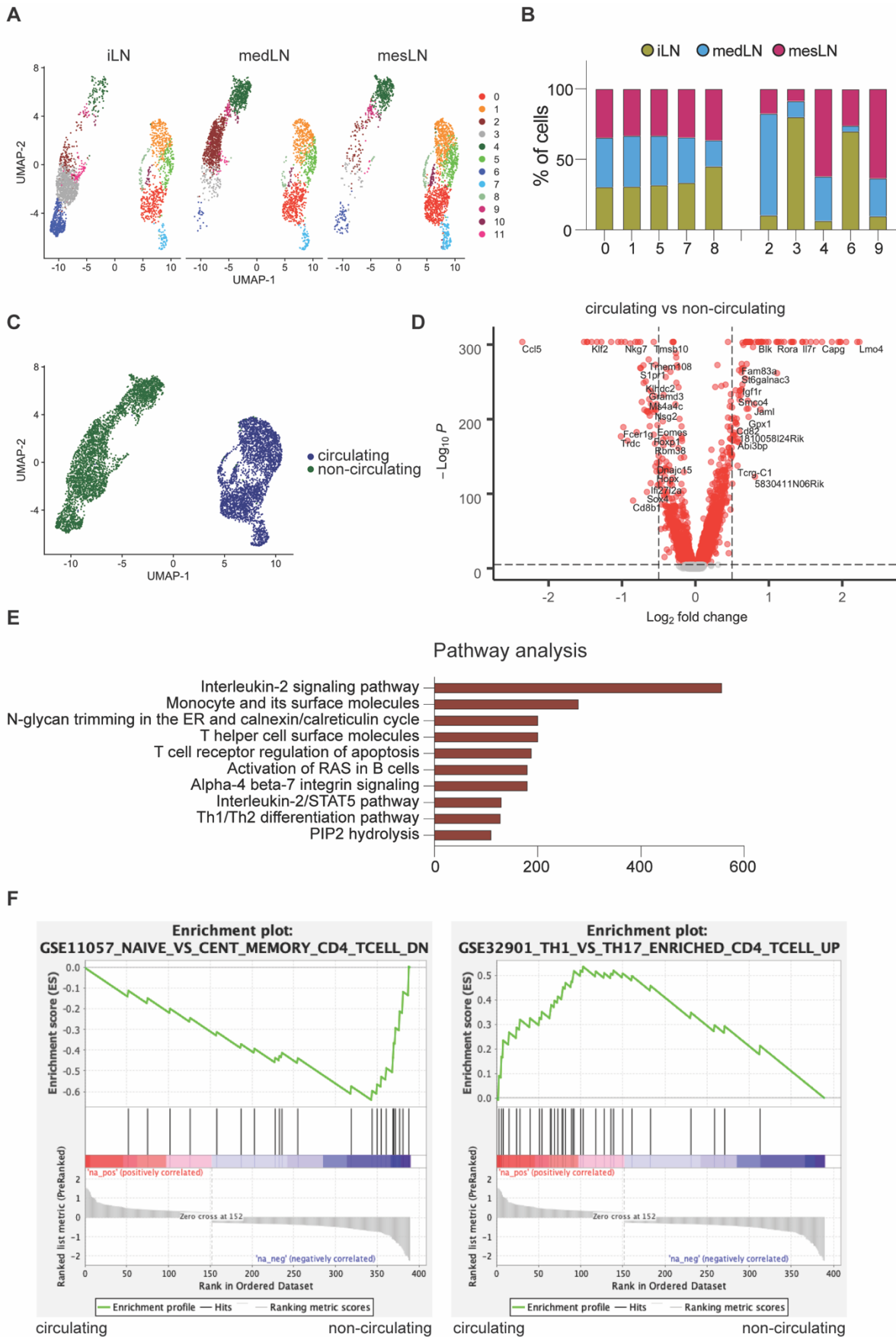


Figure 6: Cluster distribution across lymph nodes identified circulating and non-circulating subsets

A) UMAP projection of 7041 single cells, color code based on cluster identity and split by tissue of origin. B) Quantitative analysis of normalized lymph node contribution to the clusters. C) UMAP projection of 7041 single cells, color code based on circulating or non-circulating identity. D) Volcano plot displaying the log₂-fold change and adjusted p-value of genes comparing circulating and non-circulating UTC. E) Pathway analysis showing the top 10 pathways identified. The combined score calculated by taking the log of the p-value and multiplying it by the z-score of the deviation from the expected rank is displayed. F) Gene set enrichment analysis of differentially expressed genes comparing circulating and non-circulating cells.

Since the transcriptional identity of UTC show similarities to CD4 T-helper cell subsets (Th1, Th2, Th17)⁷⁷, we speculated that these known subsets might also be unevenly distributed comparing circulating and non-circulating UTC based on our pathway and gene set enrichment analysis. We projected the expression pattern of known associated marker genes onto the UMAP, to visualize the cluster association with the functional subsets (Fig. 7). As predicted by the gene set enrichment analysis, Th17-like cells, identified by the expression of *Rorc*, *Il17f* and *Ccr6*⁷⁸, were exclusively present in the non-circulating compartment. Th1-like UTC (*Tbx21*, *Ifng* and *Cxcr3*)⁷⁸ were present in circulating and non-circulating clusters. Therefore, it can be assumed that the significant enrichment of the Th1 compared to Th17 gene set rather resulted from the dominance of Th17-like cells being enriched in the non-circulating population. For Th2-like cells, it seemed like the described markers in the literature for T helper cells (*Gata3* and *Zbtb16*)⁷⁸ were less specific for UTC. *Zbtb16* was highly expressed in nearly all non-circulating clusters, while *Gata3* was expressed in all clusters, albeit to lower levels in the circulating cells. *Il4*, an additional marker for Th2-like cells, was only expressed in a few cells in the Th1-like cluster of the non-circulating population. The low detection of *Il4* transcripts can be either caused by technical difficulties, since only a minor fraction of transcripts is captured during scRNA-sequencing¹⁰⁸, or because we analyzed unstimulated cells. Therefore, it might be the case that without stimulation, Th1- and Th2-like cells of the non-circulating fraction are relatively similar and cluster together, or that we do not have enough Th2-like cells in numbers to form a separate cluster.

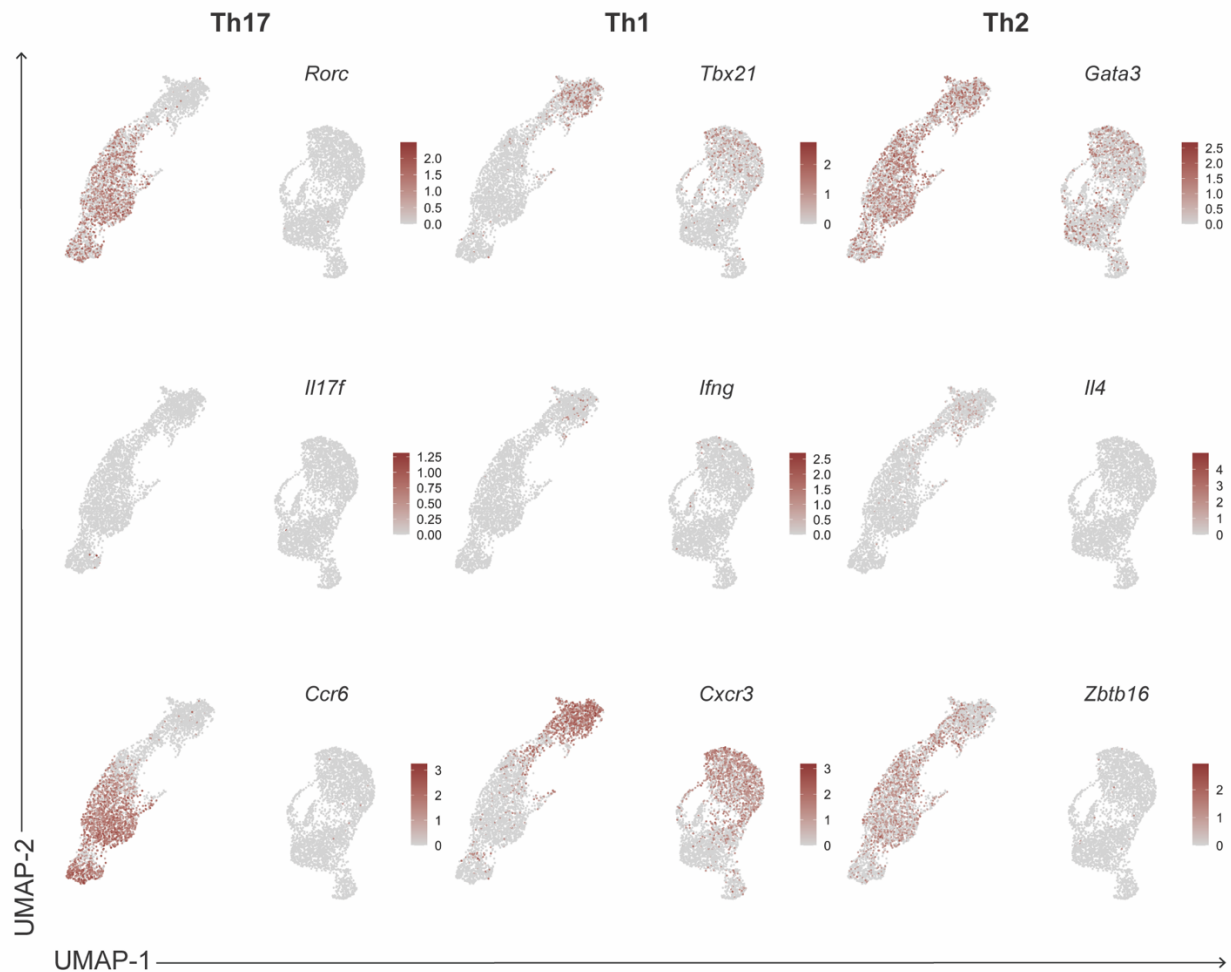


Figure 7: Th1, Th2 and Th17 associated gene expression across clusters
 UMAP projection of 7041 single cells, color code based on normalized gene expression.

To circumvent the technical limitation of having only non-activated UTC in our data set, we interrogated a publicly available scRNA-sequencing data set of IL-4 producing NKT cells derived from lung draining lymph node after influenza virus infection¹⁰⁴. Re-analysis of the data revealed two subsets of IL-4 positive NKT cells (Fig. 8A). The gene expression profile of the clusters, overlapped with marker genes of resident UTC (*Cd44* positive, *Sell* negative) (Fig. 8B). Furthermore, cluster 0 expressed high levels of *Tbx21* and cluster 1 expressed *Rorc* which are transcription factors defining Th1- and Th17-like cells, respectively (Fig. 8B). Taken together, we concluded that the IL-4 producing NKT cells in this data set represented a heterogeneous population of Th1- and Th17-like UTC, and not Th2-like cells. Since IL-4 expression did not reliably identify Th2-like cells in lymph nodes as it was previously reported in the thymus¹⁰⁹, we aimed to detect Th2-like UTC utilizing an IL-5 fate-mapping mouse model. This mouse model is the current gold standard to reliably detect type 2 ILC¹⁶. Under steady state condition, only a minor fraction of T cells was fate-map positive in the iLN (Fig. 8C). From the UTC compartment nearly all these cells were $\gamma\delta$ T cells expressing CCR6 (Fig. 8C), a Th17 marker. We therefore concluded that IL-5 fate-

mapping was not a suitable tool to identify Th2-like UTC. Taken together, these results question the existence of a bona-fide Th2-like UTC in peripheral lymph nodes in naïve animals. Indeed, three different state of the art techniques, scRNA-sequencing, IL-4 production and an IL-5 fate-mapping mouse model, were not able to distinguish them from Th1- or Th17-like UTC. Nevertheless, Th1- and Th17-like UTC were separated into distinct clusters.

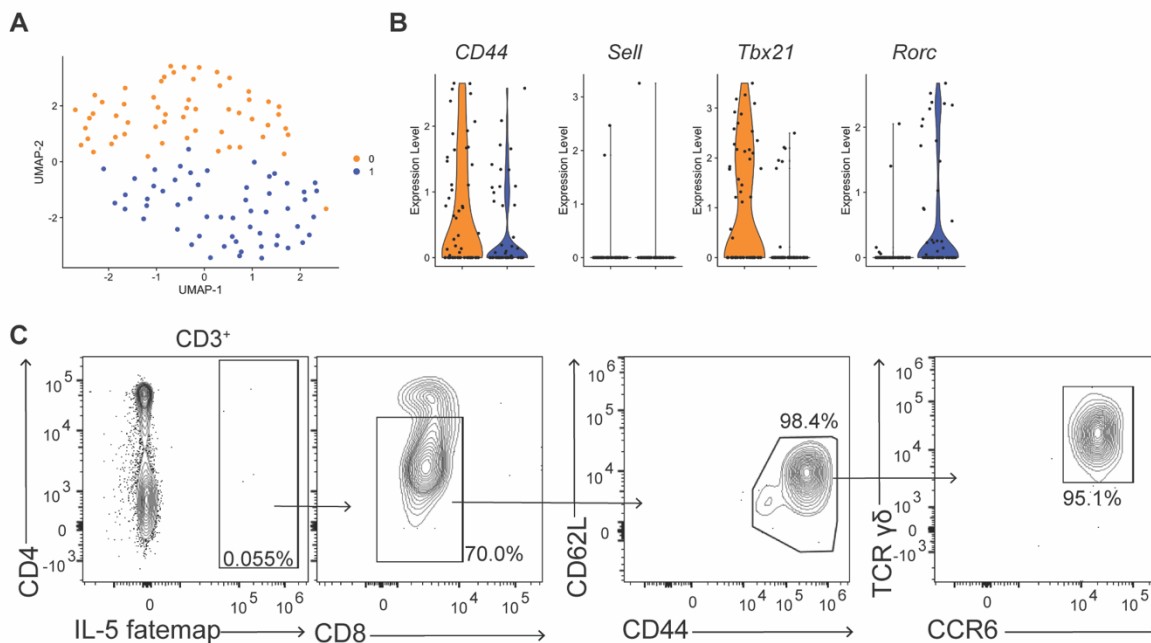


Figure 8: Th2-like UTC are not detected in lymph nodes

A-B) scRNA-sequencing transcriptomes of IL-4 producing, CD1d tetramer⁺ cells (medLN) were obtained from GSE103753 and analyzed. A) UMAP of 222 scRNA-sequencing transcriptomes were colored according to cluster classification. B) Violin plot of selected marker genes color coded by cluster identity. C) Representative flow cytometry plots, pre-gated on living cells derived from iLN of IL-5 fate map mouse. Data display 1 experiment.

To obtain a better understanding of the so far undescribed heterogeneity separating cells belonging to the same Th-like phenotype, we analyzed the Th17-like clusters 2 and 3 (Fig. 9A). We observed that these were derived from different lymph nodes (Fig. 6B). Cluster 2 harbored mainly iLN derived cells, while cluster 3 cells originated mainly from the medLN. That the cells clustered separately, despite having a similar Th17-like phenotype pointed towards a potential tissue imprinting, which was not that apparent for Th1-like cells. To understand the basis of this difference, we analyzed the differentially expressed genes comparing cluster 2 and 3 (Fig. 9B) and subjected the gene list to pathway analysis (Fig. 9C). The results revealed an enrichment of *S100a6*, *Vim* and *Cd7* expression in cluster 3 (medLN), while *Cd28* was upregulated in cluster 2 (iLN). Enriched pathways represented purine catabolism, as well as prostaglandin biosynthesis and regulation. These pathways might indicate altered metabolic requirements at distinct sites of the body.

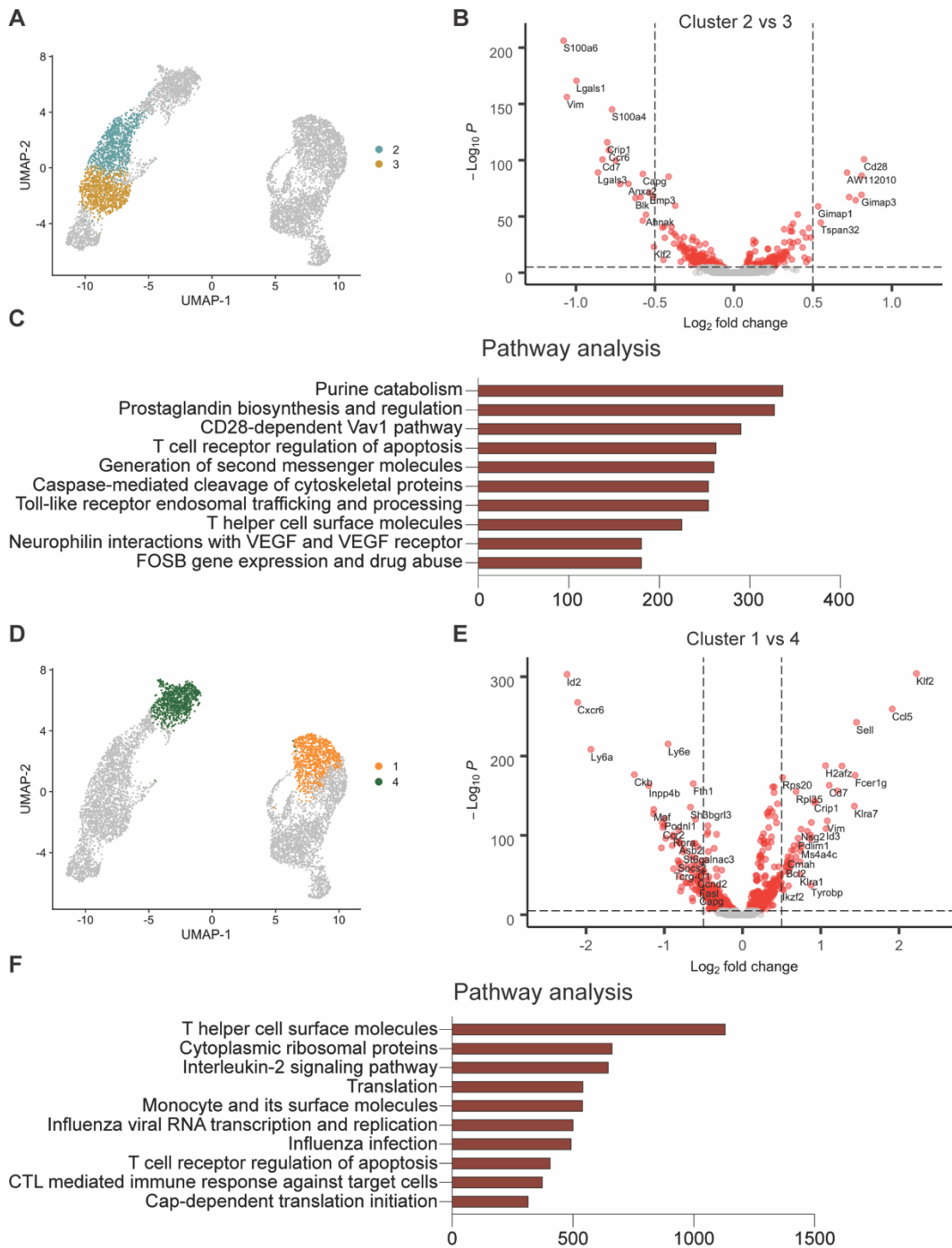


Figure 9: Transcriptional comparison between cluster 2 vs 3 and cluster 1 vs 4

A) UMAP projection of 7041 single cells, highlighted clusters 2 and 3 identity. B) Volcano plot displaying the \log_2 -fold change and adjusted p-value of genes comparing cluster 2 and 3. C) Pathway analysis showing the top 10 pathways identified. D) UMAP projection of 7041 single cells, highlighted clusters 1 and 4 identity. E) Volcano plot displaying the \log_2 -fold change and adjusted p-value of genes comparing cluster 1 and 4. F) Pathway analysis showing the top 10 pathways identified. The combined score calculated by taking the log of the p-value and multiplying that by the z-score of the deviation from the expected rank is displayed.

Although Th1-like cells were not distributed in distinct clusters across lymph nodes, there was a clear separation of circulating and non-circulating Th1-like cells. To further elucidate factors causing this difference, we compared cluster 1 (circulating) and cluster 4 (non-circulating) (Fig. 9D). Differentially expressed genes revealed that *Cxcr6*, *Id2* and *Ly6a* were enriched among cells in cluster 4 (non-circulating), while *Ccl5*, *Klf2* and *Fcer1g* were upregulated in cluster 1 (circulating) (Fig. 9E). Pathways associated with the differentially regulated genes encompassed translational regulation, T cell activation as well as surface marker expression (Fig. 9F). These results indicate that the translational regulation, as well as the activation status of these clusters differ, while both display genes associated with a Th1-like phenotype.

Phenotype of non-circulating UTC is reflected in the draining tissue

Transcriptional analysis of the different UTC clusters revealed heterogeneity at three different levels. First, the Th1- and Th17-like phenotype, as described in the literature before⁷⁷, could be distinguished, with exception of a Th2-like phenotype. Second, intermixed and lymph node-specific clusters revealed a heterogeneity between circulating and non-circulating cells across lymph nodes. Third, UTC with the same Th-like phenotype and probably similar circulation behavior cluster separately based on the lymph node they derive from (Fig. 8A-C). Metabolic pathway differences between these clusters indicate a potential tissue imprinting. Considering that all sequenced UTC were derived from lymph nodes, we wondered how these cells could differ to such an extent.

Recent publications demonstrated that a subset of UTC, $\gamma\delta$ T cells, is constantly migrating from the skin to skin-draining lymph nodes¹¹⁰⁻¹¹². Therefore, we speculated that the tissue imprinting that distinguishes Th17-like UTC from the iLN and medLN is happening in the skin and lung, rather than the lymph node itself. To test this hypothesis, we isolated UTC from the skin, lung and small intestine and compared their Th-like phenotype to their respective draining lymph node UTC counterparts. As markers we used CCR6, representing Th17-like cells and a *Cxcr3*^{GFP} reporter, identifying Th1-like cells. We observed major differences comparing the Th-like phenotypes across tissues. While we found nearly exclusive Th17-like cells in the skin, in the small intestine over 80% of UTC displayed a Th1-like phenotype (Fig. 10A and B). The lung represented a mixture of distinct Th phenotypes. Focusing on the non-circulating (CD62L negative) cells, the lymph nodes matched the draining tissue regarding the Th-like phenotype distribution of UTC. As already seen in the scRNA-sequencing distribution, the iLN harbored mainly Th17-like cells, while mesLN was enriched in Th1-like cells. The medLN had, like the lung, a mixture of the analyzed phenotypes.

Taken together, we concluded from the data that the non-circulating UTC retained their specific imprinting in the tissue and migrated to their draining lymph nodes. Thereby, the previous reports regarding the migratory behavior of $\gamma\delta$ T cells in the skin might be generalizable to other organs and UTC lineages.

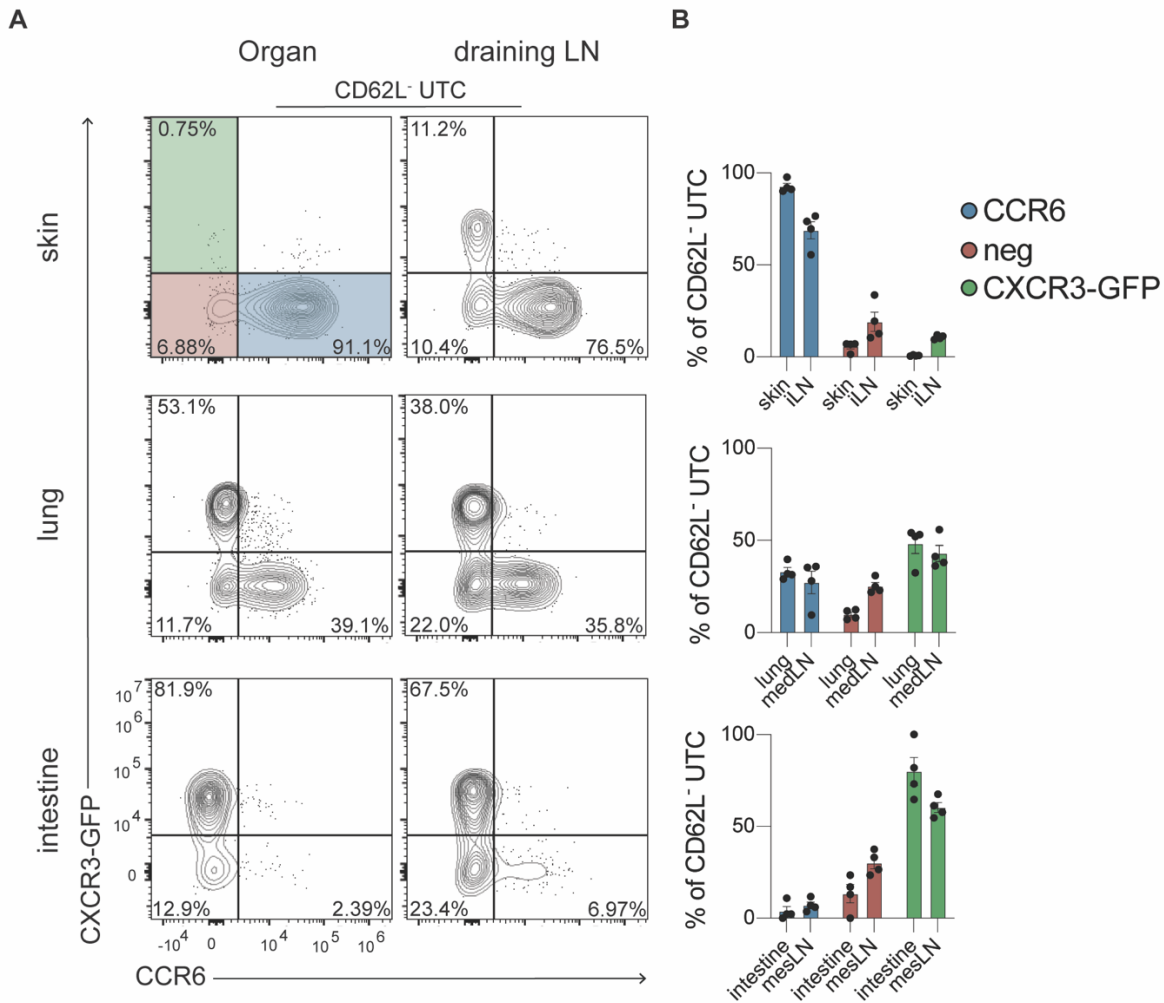


Figure 10: Phenotype comparison of UTC in tissues and their draining lymph node

A) Representative flow cytometry plots, pre-gated on living CD62L⁻ UTC, displaying CCR6 and CXCR3-GFP expression from *Cxcr3*^{GFP} hemizygous reporter mice. B) Quantitative analysis of phenotypic markers comparing tissue and draining lymph nodes. Data display 1 representative experiment with n = 4 mice. Bar graphs display mean value and error bars represent SEM.

TCR-dependent lineage enrichment across mouse facilities

Previous studies have shown that the tissue seeding of UTC, like MR1-restricted MAIT cells⁸⁰ and CD1d-restricted NKT cells⁸¹ is regulated early in life and depends on the presence of microbial antigens. These antigens are derived from the microbiome, which can differ greatly between mouse facilities and even vendors¹¹³. Since we demonstrated a direct correlation between lymph node and tissue phenotype of UTC, we speculated that microbiota caused changes in TCR-dependent tissue seeding are also reflected in the tissue draining lymph nodes.

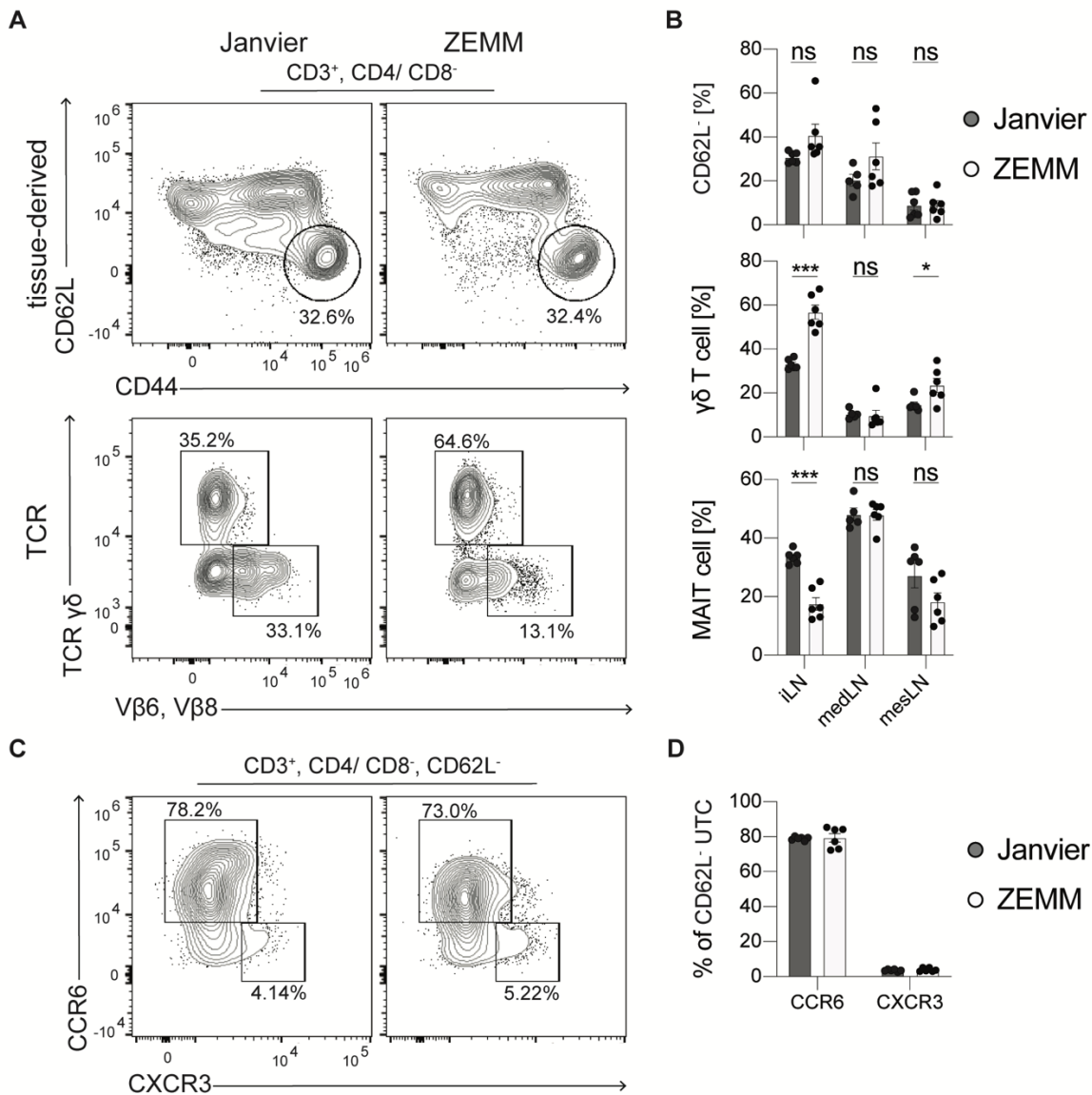


Figure 11: UTC comparison of different mouse facilities

Mice were housed in a facility in Würzburg (ZEMM) or ordered from a commercial vendor (Janvier). A) Representative flow cytometry plots, pre-gated on CD3⁺ CD4/CD8⁻ cells, displaying non-circulating (CD62L⁻) UTC from iLN, and their $\gamma\delta$ T cell and MAIT cell frequency. B) Quantitative analysis of CD62L⁻ UTC and their $\gamma\delta$ T cell and MAIT cell frequency comparing different lymph nodes. Data display 2 experiments with n = 6 mice. Bar graphs display mean value and error bars represent SEM. Comparison between groups was calculated using a non-paired student t-test. ns $p > 0.05$; * $p < 0.05$; *** $p < 0.001$.

Therefore, we analyzed the lymph nodes of mice bred in a facility at the campus Würzburg (ZEMM) and compared the UTC composition in mice from a commercial mouse vendor (Janvier) with the same specific pathogen free (SPF) hygiene status. The frequency of non-circulating UTC (CD62L negative, CD44 positive) did not differ comparing mice derived from the different facilities (Fig. 11A and B). Analyzing the TCR-based lineage composition of these cells, we observed that $\gamma\delta$ T cells were increased in Würzburg's mouse facility ZEMM, while MAIT cells were significantly

enriched in mice derived from Janvier (Fig. 11A and B). This difference was most obvious in the iLN. Next, we wanted to investigate whether in connection with the TCR-based lineage the Th-like phenotype was altered as well when comparing these two different mouse facilities. As before, we analyzed the Th1 and Th17 identifying markers CCR6 and CXCR3 in the iLN of non-circulating UTC. We observed no difference in comparing the mouse facilities (Fig. 11C and D). The majority, around 80% of CD62L negative UTC, expressed CCR6 while only a minor fraction of 3-5% was CXCR3 positive, independent of the facility the mice were maintained in. Therefore, we concluded that the alterations in microbiome only caused a shift in the UTC TCR-based lineage, while the Th phenotype showed the same tissue prevalence, independent of the microbiome.

Functional unit concept of UTC

The observed disconnection between the Th-like phenotype of the UTC and their TCR-based lineage, which was already indicated in our scRNA-sequencing analysis (Fig. 5), led us to speculate that innate immune imprinting of lymph nodes by UTC is evolutionarily preset and undisturbed by minor microbial and environmental changes. The observed innate cytokine differences between lymph nodes (Fig. 1) further seemed to be independent of the TCR-based lineage affiliation of UTC. We next wished to address which requirements a cell population would need to fulfil as a unit to ensure such a stability in imprinting of a lymph node, preserving the flexibility to adapt TCR-based lineage ratios. We assume that the cells need to be part of a functional unit and propose the following pillars of the functional unit concept.

- I) Specific localization. Even though all analyzed cells are located within a lymph node, it is a highly structured and organized tissue¹¹⁴. A functional unit is expected to reside within at a specific microanatomical location and not at different sites (Fig. 12A).
- II) Transcriptional homogeneity. Subsets of a functional niche, like TCR-based lineages, should not be distinguishable based on their transcriptome. This hypothesis can be tested utilizing scRNA-sequencing (Fig. 12B).
- III) Similar biological output. Parts of a functional unit should possess similar stimulation requirements for the same functional output. For example, the members of the functional unit should react to the same stimulation with the production of the same cytokine (Fig. 12C).
- IV) Redundancy. The absence of one subset of a functional unit, like the lack of NKT cells in *Cd1d*^{-/-} mice, should be compensated in numbers and functional output by the other members of the unit (Fig. 12D).

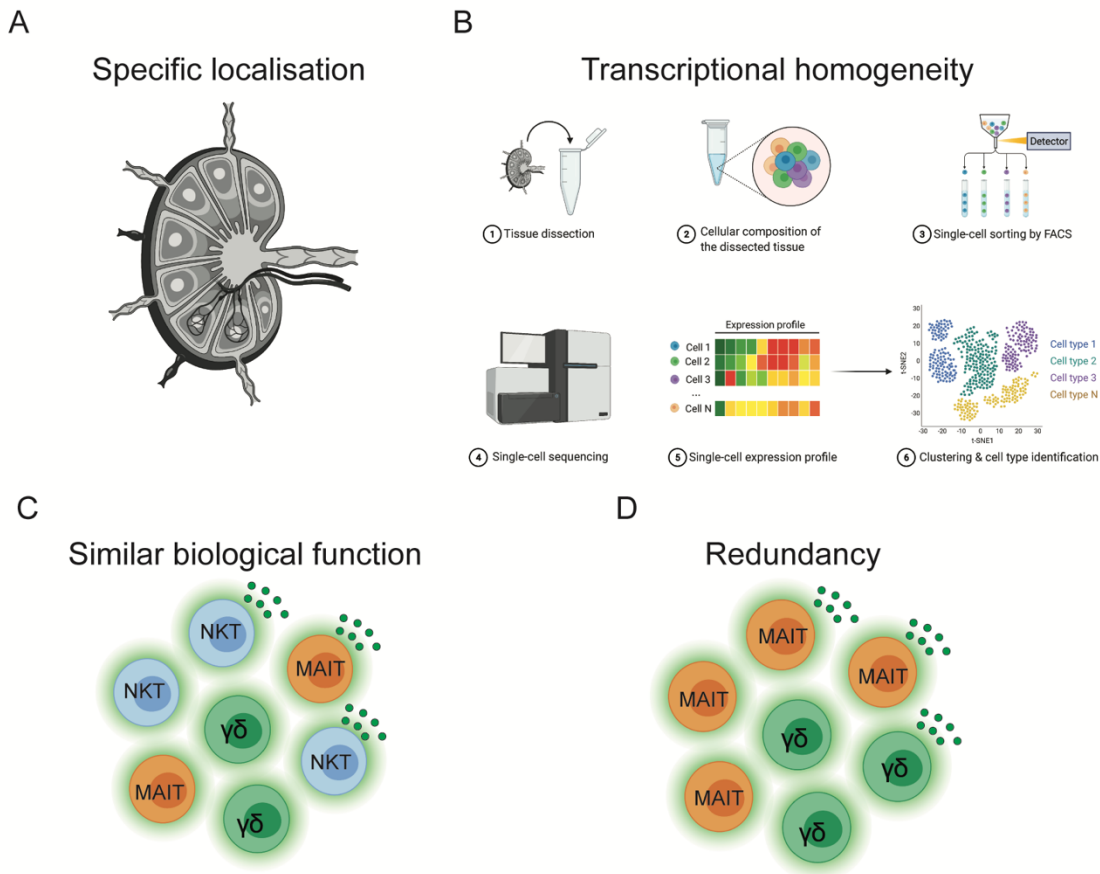


Figure 12: Schematic representation of the functional unit concept

Schematic of the requirements for cells to form a functional unit. A) Lymph node scheme to indicate specific localization. B) Display of scRNA-sequencing workflow to indicate analysis of transcriptional homogeneity. C) Display of 3 distinct cell types (MAIT cells, NKT cells, $\gamma\delta$ T cells), producing the same cytokines to indicate the similar biological function of a niche. D) Display of 2 cell types (MAIT cells, $\gamma\delta$ T cells), compensating in numbers and function of the unit.

Th17-like UTC localize in the interfollicular area in sdLN

Having proposed these requirements for forming a functional unit, we set out to test whether these strict definitions apply to UTC as a population. To investigate this hypothesis, we chose the Th17-like UTC population in the skin draining lymph nodes due to the following reasons: tools to visualize and investigate this unit are available with specific reporter mice; these cells showed the most striking tissue imprinting across lymph nodes even within the Th17-like phenotype; Th17-like UTC were absent in the circulatory pool of cells in contrast to Th1-like cells; and the skin draining lymph node displayed in our analysis the most significant TCR-based lineage alterations comparing different mouse facilities. As predicted by scRNA-sequencing (Fig. 5C), we could selectively identify the Th17-like UTC based on CXCR6, CD44, ITG β 7, IL-23R, IL-7R and IL-18R1 expression (Fig. 13A). This observation gave us the opportunity to visualize the localization of these cells using a *Cxcr6*^{GFP/wt} reporter mouse strain. Sections of the iLN harvested from this mouse strain

revealed the presence of GFP positive T cells in the interfollicular area (Fig. 13B), as it has been published before^{115,116}.

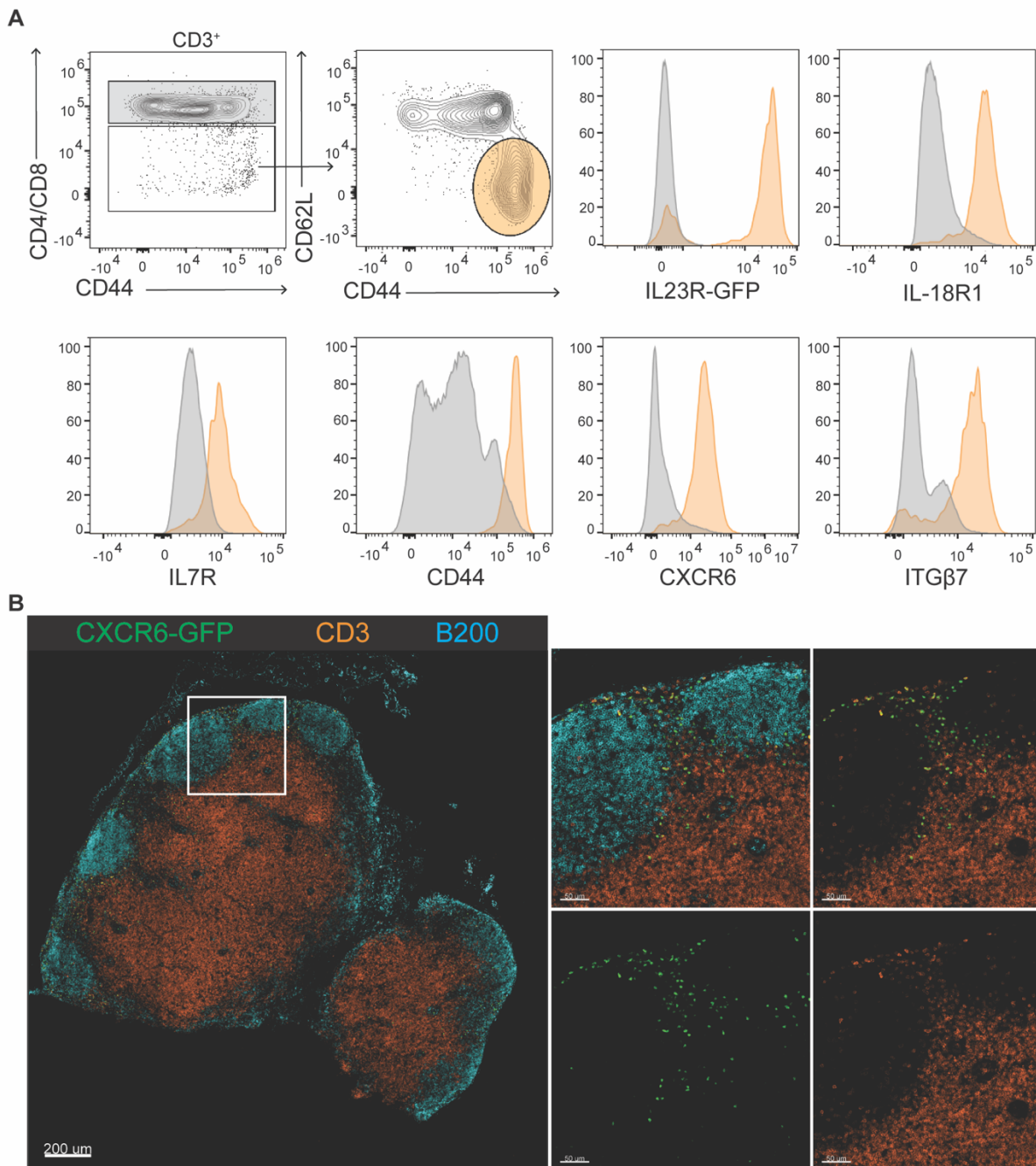


Figure 13: Th17-like UTC in skin draining lymph node have a specific localization

A) Representative flow cytometry plots and gating strategy of non-circulating UTC from the iLN of an *Il23r*^{GFP/wt} reporter mouse. Histograms display marker expression comparing conventional CD4/CD8⁺ T cells (grey) and non-circulating UTC (orange). B) Immunofluorescence image of the iLN from a *Cxcr6*^{GFP/wt} reporter mouse showing the localization of CXCR6⁺ UTC (CXCR6-GFP in green, B220 in blue, CD3 in orange). Scale bars represent 200 μm for overview and 50 μm for detailed images. Data display 1 representative experiment.

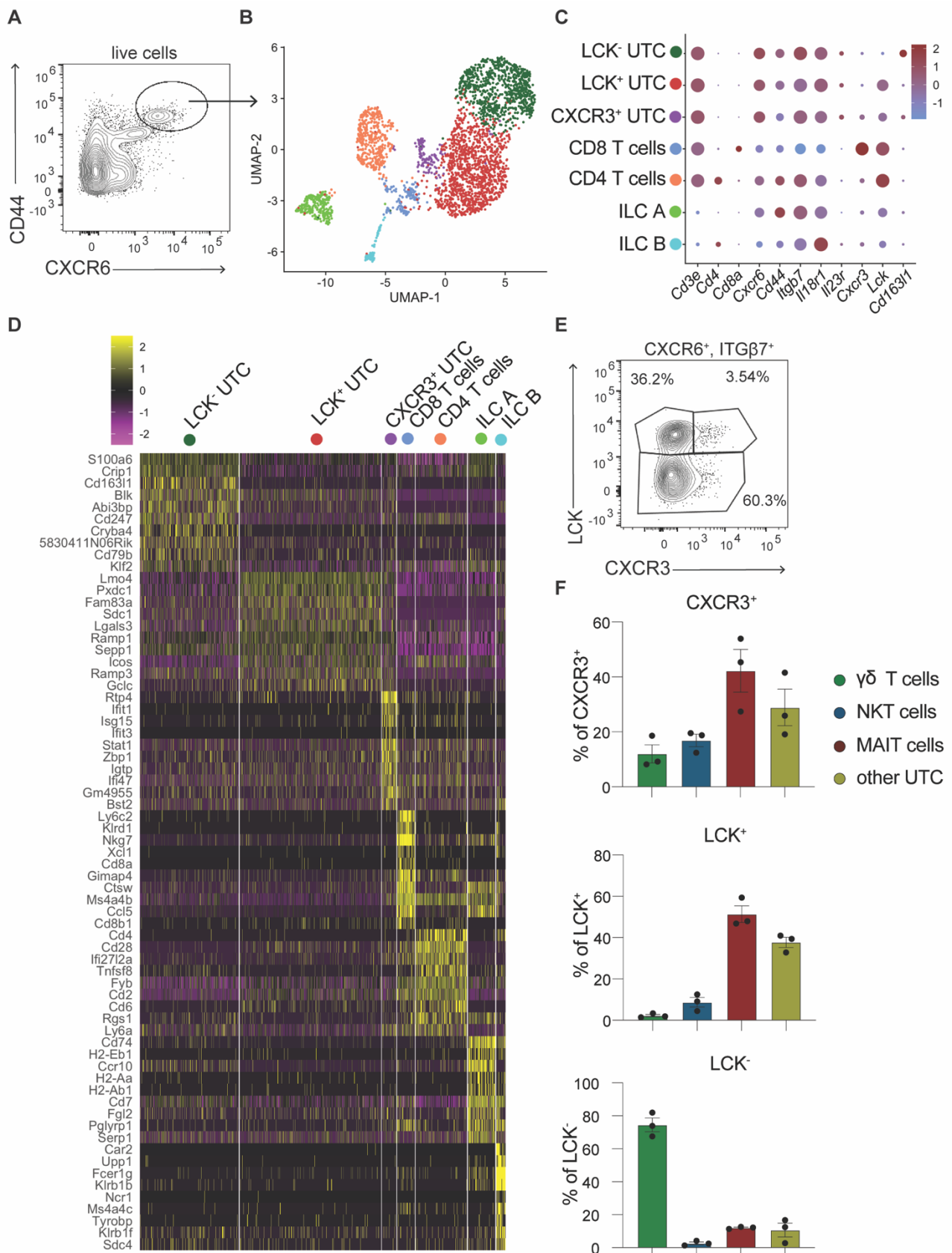


Figure 14: Transcriptional heterogeneity of Th17-like UTC does not represent TCR-based lineage identity

A) Flow cytometry plot representing the gating strategy for sorting the cells from the skin draining lymph nodes (sdLN). B) UMAP projection of 3032 single cells, color code based on cluster identity. C) Dot plot of selected marker genes associated with identified clusters. Color represents z-score mean expression values across clusters; dot size indicates fraction of cells in the cluster expressing respective genes. D) Heatmap displaying top 10 marker genes for each identified cluster. Color represents z-score mean expression values per cell. E) Representative flow cytometry plot of the UTC marker genes validation at protein level, pre-gated on CD3⁺ and CD4⁺ CD8⁻ cells. F) Quantitative analysis of TCR-based lineage frequencies among validated subsets. Data display 1 representative experiment with n = 3 (E, F) or n = 1 (A-D) mice. Bar graphs display mean value and error bars represent SEM.

Th17-like UTC encompass distinct TCR-based lineages in sdLN

Having established that the members of the Th17-like unit in the skin draining lymph node occupy a specific localization, we set out to investigate their transcriptional homogeneity. To this end we subjected CXCR6 high CD44 positive cells to scRNA-sequencing (Fig. 14A) and analyzed their transcriptome. The UMAP projection of unbiased clustering revealed, next to minor conventional T cell and ILC clusters, three distinct UTC clusters (Fig. 14B). These clusters were differentiated by the selective expression of *Cxcr3* in one cluster, the lack of *Lck* expression in the second, while the third cluster lacked *Cxcr3* expression but showed *Lck* expression (Fig. 14C). Next to these selected markers, the cluster showed a variety of other cluster specific genes, confounding the separation in further distinct clusters (Fig. 14D). The expression of the selected marker genes could be validated on protein level via flow cytometry (Fig. 14E). To test the hypothesis of transcriptional homogeneity across subsets within the functional unit, we analyzed the TCR-based lineage distribution within the identified clusters. Although there was a specific enrichment for certain lineages in subsets, e.g. around 50% of LCK positive UTC possessed a MAIT TCR and roughly 80% of LCK negative cells expressed a $\gamma\delta$ TCR, no subset was exclusively derived from one TCR-based lineage, as seen previously (Fig. 5E). This mixed lineage distribution further supports the concept of a functional unit for UTC.

Th17-like UTC produce IL-17 across TCR-based lineages in sdLN

Since the analyzed cell population could be identified by Th17-like markers (Fig. 7), we investigated the capacity of these cells to produce IL-17F *in vivo*. To this end we infected B6 WT mice subcutaneously in the footpad with *S. aureus*, harvested the pLN 4 h post infection and analyzed the cytokine production via flow cytometry (Fig. 15A). As seen in the *ex vivo* stimulation experiment (Fig. 2A), the majority of IL-17F producing cells were UTC, which expressed CXCR6 and ITG β 7 (Fig. 15B), two markers we used to identify the Th17-like niche (Fig. 13A). Next, we were interested in the TCR-based lineage contribution regarding the observed IL-17F response. We observed that all major TCR-based lineages, $\gamma\delta$ T cells, MAIT cells and NKT cells, as well as other UTC contributed to IL-17F production (Fig. 15C). Quantification of the distribution revealed that between 20% to 25% of the producing cells belonged to each lineage (Fig. 15D). Therefore,

we concluded that what we considered as the third requirement for a functional unit was valid for the Th17-like UTC in skin draining lymph nodes.

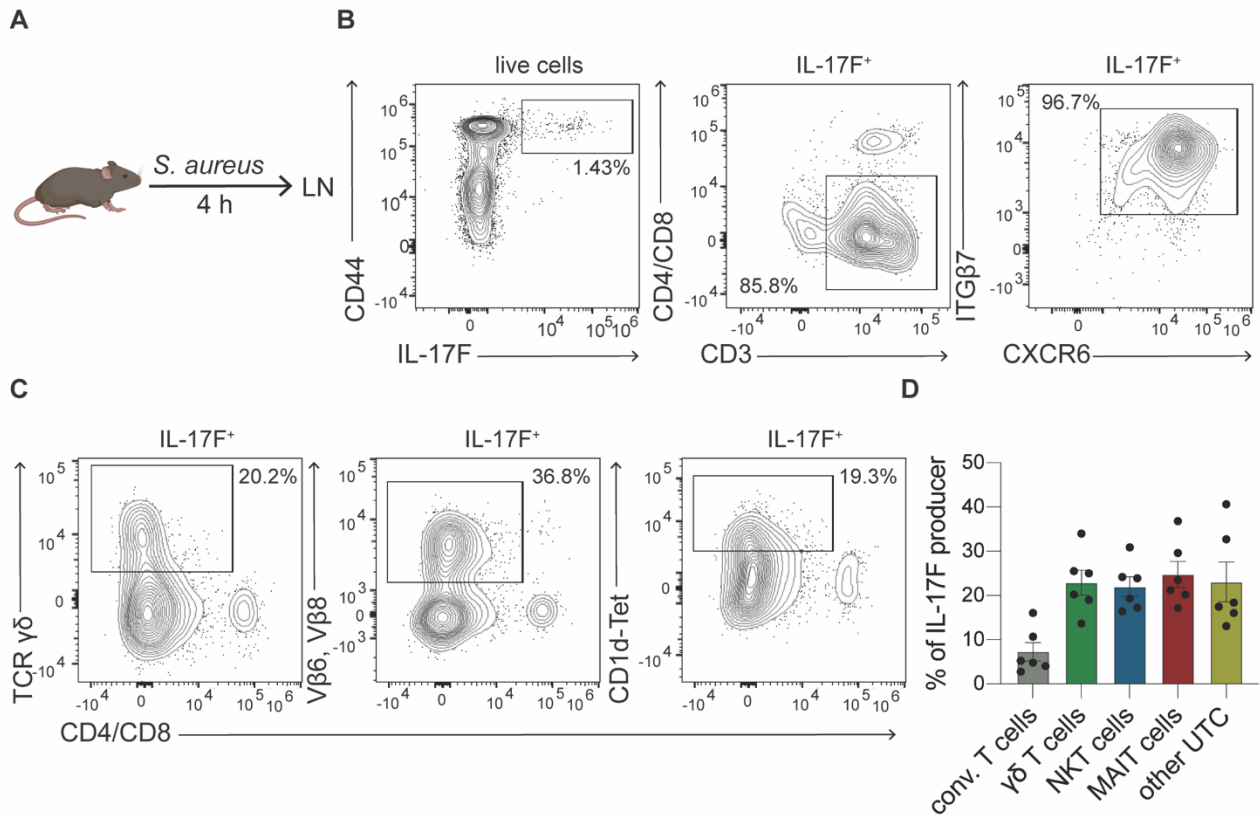


Figure 15: Th17-like UTC produce IL-17F after stimulation across TCR-based lineage identity
 A) Schematic of the experimental set up. B6 wt mice were subcutaneously infected with *S. aureus*. 4 h post-infection mice were sacrificed and draining LN cells were analyzed. B) Representative flow cytometry plot and gating strategy used to identify IL-17F producers as being mainly CD3⁺, CD4/ CD8⁻ UTC co-expressing CD44, ITGβ7 and CXCR6. C) Representative flow cytometry plots of UTC TCR-based lineages represented in IL-17F producing cells. D) Quantitative analysis of TCR-based lineage frequencies among IL-17F producers. Data display 2 experiments with n = 6 mice. Bar graphs display mean value and error bars represent SEM.

Th17-like UTC are compensated in numbers and function in sdLN

As a fourth requirement to classify UTC as being organized as functional units, we aimed to test whether cell numbers and function are compensated in the absence of a subset. To this end, we made use of mouse strains that specifically lack one of the major UTC TCR-based lineages. Mice having a deficiency in the TCR-delta gene are deficient for $\gamma\delta$ T cells¹¹⁷. CD1d-deficient mice lack the capacity to develop NKT cells¹¹⁸, while MR1-deficient animals are characterized by an absence of MAIT cells⁷⁴. To test for compensation of the Th17-like UTC in these strains, we analyzed the frequencies and absolute numbers of the whole unit (Fig. 16A and C) and its subsets (Fig. 16B and D). Cast/B6 strain was used as a wt control for MR1-deficient mice, due to a mixed background of the strain. Pre-gated on CD4 and CD8 negative T cells, we observed, as before, that the Th17-like niche encompassed around 50-60% of the UTC in skin draining lymph nodes in B6 WT mice (Fig. 16A).

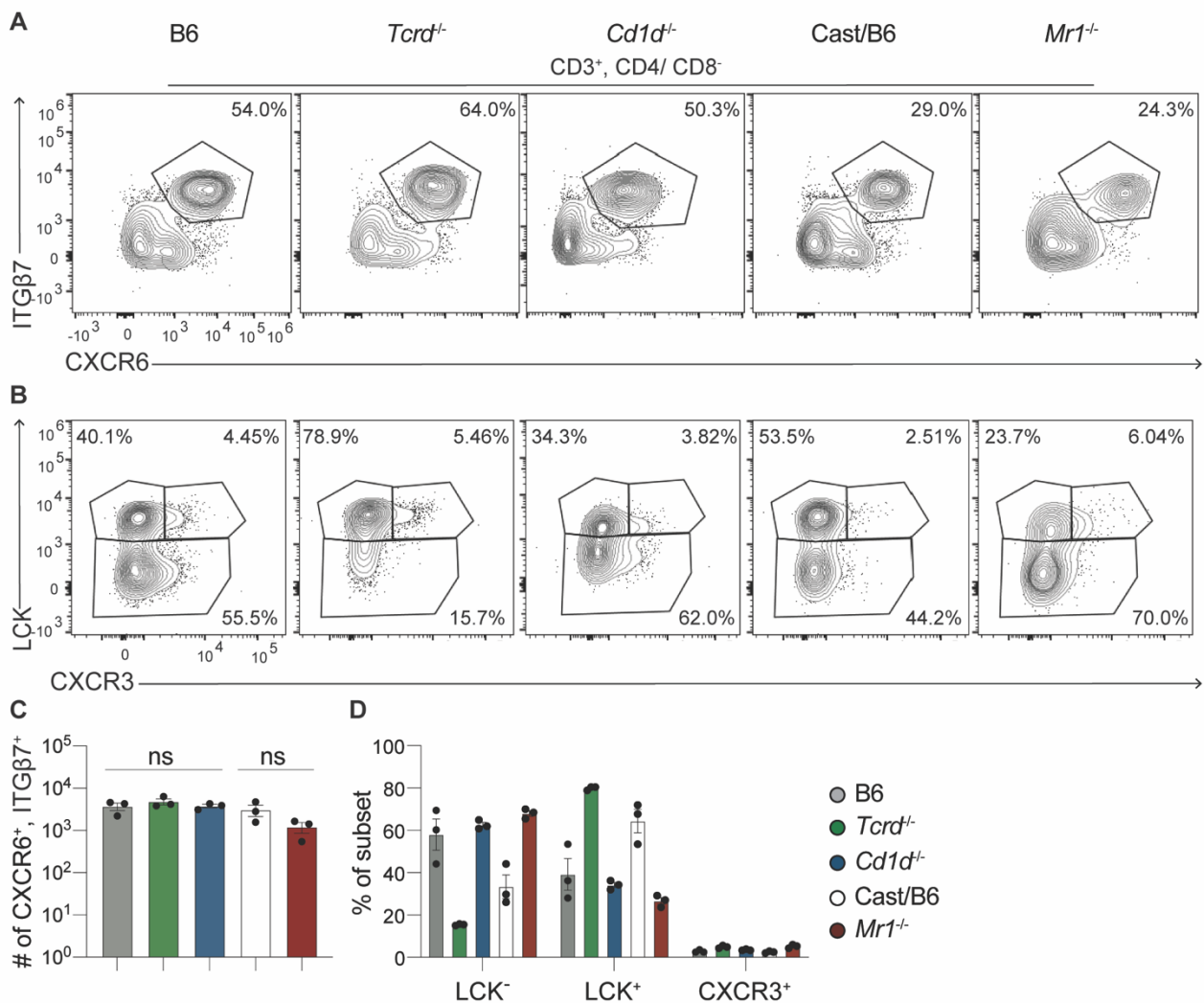


Figure 16: Numbers and subsets of Th17-like UTC are compensated in single TCR-based lineage deficient mice

A) Representative flow cytometry plots pre-gated on CD3⁺ and CD4/ CD8⁻ cells, displaying the IL-17 producing unit (CXCR6⁺, ITGβ7⁺) in control and single TCR-based lineage deficient mice. B) Representative flow cytometry plot displaying the identified subsets (based on LCK and CXCR3 expression, Fig. 14C, E) in control (B6 and Cast/B6) and single TCR-based lineage deficient mouse lines. C) Quantitative analysis of UTC from IL-17 producing unit in absolute numbers. D) Quantitative analysis of subset frequencies. Data display 1 representative experiment with n = 3 mice. Bar graphs display mean value and error bars represent SEM. Comparisons between groups were calculated using a non-paired student t-test. ns $p > 0.05$

In Cast/B6 control mice we observed a frequency of around 30%. Compared to control animals, the frequency of CXCR6, ITGβ7 positive UTC was not significantly altered in single TCR-based lineage deficient mice. More importantly, we observed that the three identified subsets, based on LCK and CXCR3 expression, were present in all analyzed strains (Fig. 16B). Therefore, we concluded that the absence of one major TCR-based lineage does not lead to the absence of a complete cluster. Furthermore, in addition to looking at the relative contribution of Th17-like cells to UTC, we analyzed their absolute numbers. As expected from the observation of similar

frequencies, we could not see significant differences in absolute cell numbers comparing the analyzed mouse strains to their respective control group (Fig. 16C). Quantifying the relative distribution of the subsets from the Th17-like unit, we were able to observe differences in the distribution (Fig. 16D). For example, $\gamma\delta$ T cell deficient animals showed a relative reduction of LCK negative cells compared to B6 wt control mice. In contrast, MR1-deficient mice, lacking MAIT cells, had an increase in the LCK negative cells compared to the Cast/B6 WT control group. Together, we concluded that in single TCR-based lineage deficient strains, the absolute number of Th17-like UTC was compensated and that no identified subset was lacking.

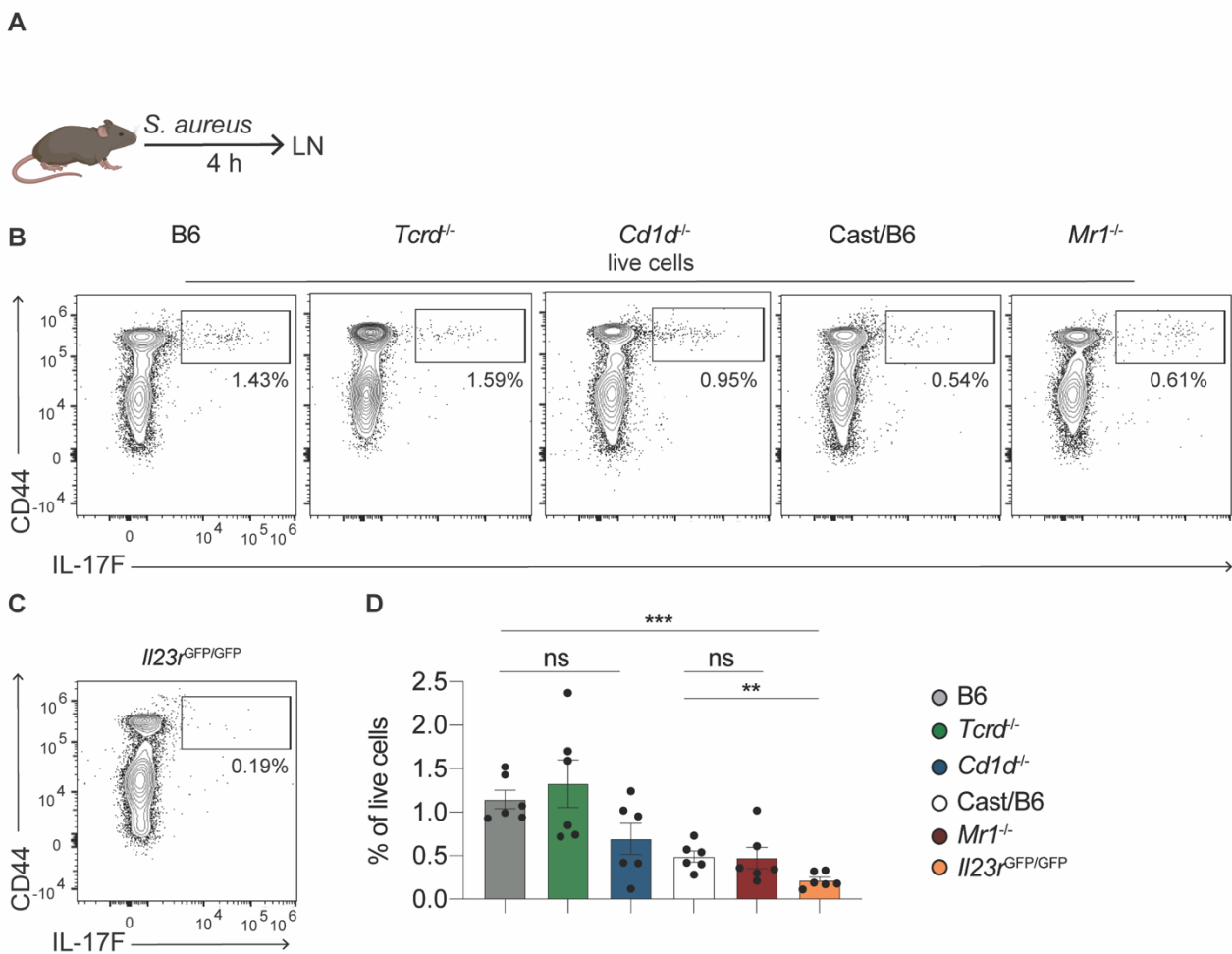


Figure 17: IL-17F response is compensated in single TCR-based lineage deficient mice

A) Schematic of the experimental set up. Mice were subcutaneously infected with *S. aureus*. 4 h post-infection the mice were sacrificed and draining LN cells were analyzed. B) Representative flow cytometry plots, pre-gated on live cells, displaying the IL-17F producing cells in control (B6 and Cast/B6) and single lineage deficient mouse lines. C) Representative flow cytometry plot, pre-gated on living cells, displaying IL-17F producing cells in IL-23R deficient (*Il23r*^{GFP/GFP}) mice. D) Quantitative analysis of IL-17F producing cell frequencies. Data display 2 representative experiments with $n = 6$ mice. Bar graphs display mean value and error bars represent SEM. Comparisons between groups were calculated using a non-paired student t-test. ns $p > 0.05$; ** $p < 0.01$; *** $p < 0.001$.

Next, we tested the functionality of the unit in terms of cytokine production in the single TCR-based lineage deficient strains. As before, we infected mice subcutaneously with *S. aureus* and analyzed the IL-17F production 4 h later via flow cytometry (Fig. 17A). We detected IL-17F production in all single TCR-based lineage deficient strains and their corresponding control groups after infection (Fig. 17B). IL-23R deficient (*Il23r^{GFP/GFP}*) mice served as a negative control (Fig. 17C), since IL-23 signaling is essential for cytokine induced IL-17 production¹¹⁹. As expected, the frequency of IL-17F producing cells was significantly reduced comparing IL-23R deficient mice to either B6 wt or Cast/B6 control (Fig. 17D). We detected no significant differences when comparing the single TCR-based lineage deficient mice and their respective controls regarding the frequency of IL-17F producing cells (Fig. 17D). In summary, we conclude that the lack of a certain TCR-based lineage does not impact the size or functionality of the analyzed unit.

All UTC units are compensated in single TCR-based lineage deficient strains

So far, we have tested the proposed requirements in forming a functional unit specifically for the Th17-like unit in skin draining lymph nodes. We observed that Th17 polarized UTC, identified by CXCR6, CD44 and ITGβ7 were located in a specific area of the lymph node, display transcriptional homogeneity with regards to their TCR-based lineage populations and were compensated in numbers and function. To generalize the observation for the Th17-like niche, we aimed to analyze the four proposed requirements additionally for the remaining UTC units in other lymph nodes and extend the analysis to the circulating part of these cells. Since at the current state we lack the tools to specifically investigate the localization of the other subsets, due to a lack of specific reporter mice, we aimed to at least address the compensation of the described units in single TCR-based lineage deficient mice.

To this end, we analyzed the previously described subsets (Fig. 5B) with the defined markers on a protein level via flow cytometry. Pre-gated on CD4 and CD8 negative T cells, a clear separation between circulating (CD62L positive) and non-circulating (CD62L negative, CD44 positive) UTC was seen in all analyzed strains (Fig. 18A). A shift towards relatively more circulating UTC was observed in Cast/B6 WT control and MR1-deficient animals. This observation is likely caused by the mixed genetic background of the mice.

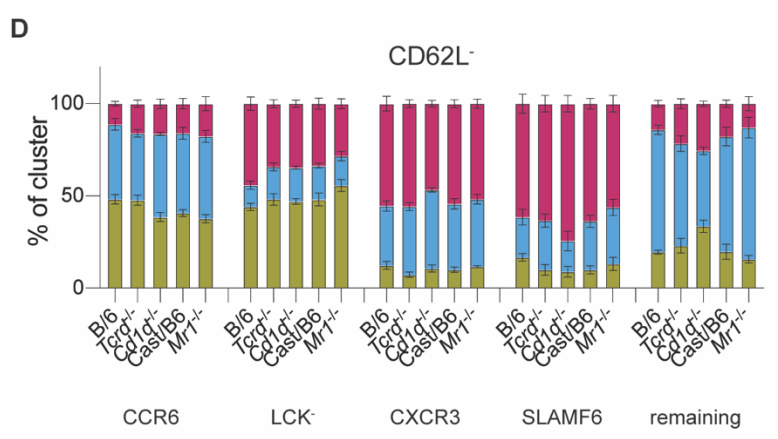
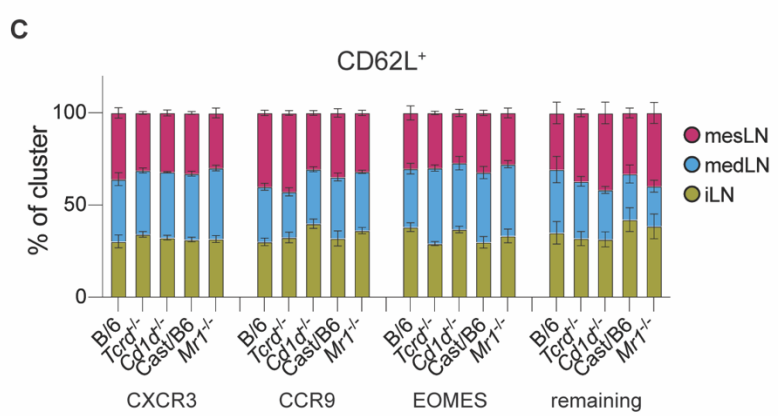
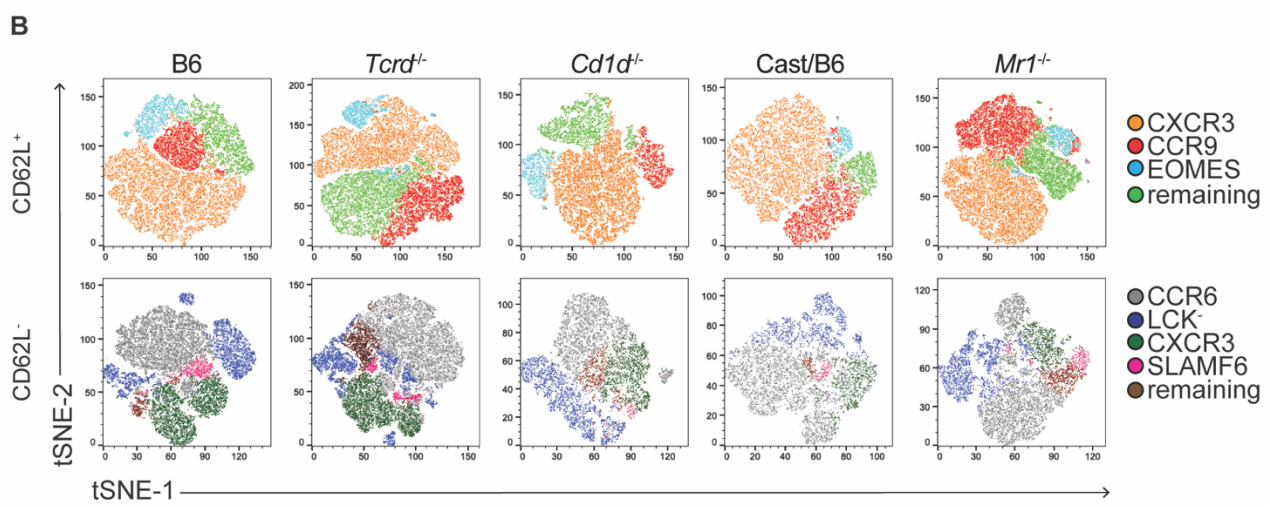
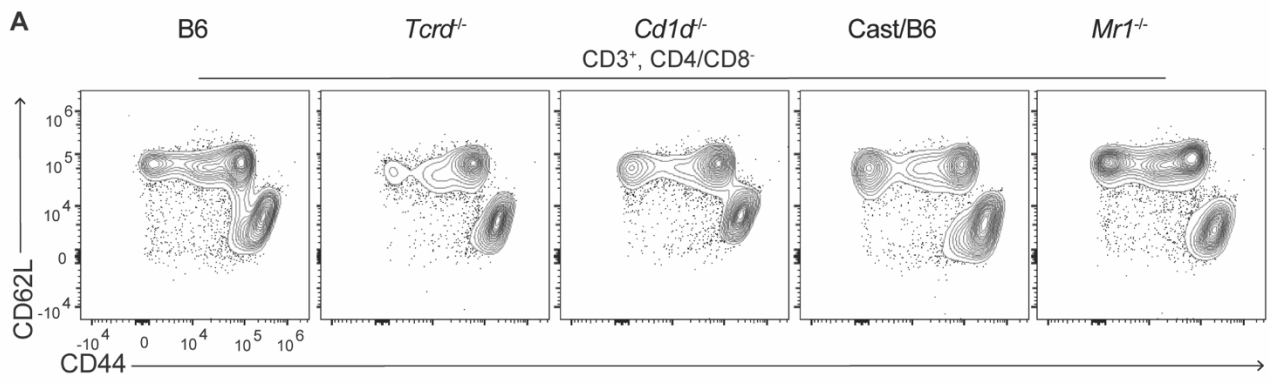


Figure 18: All UTC subsets are compensated in single TCR-based lineage deficient mice

A) Representative flow cytometry plots and gating strategy, pre-gated on CD3⁺ and CD4/CD8⁻ cells, displaying circulating (CD62L⁺) and non-circulating (CD62L⁻) UTC. Cells are derived from iLN, medLN and mesLN, comparing single T cell lineage deficient mice. B) tSNE projection of circulating (CD62L⁺, top) and non-circulating (CD62L⁻, bottom) UTC, color code based on protein validation (Fig. 5D). Displayed cells are derived from iLN, medLN and mesLN. C) Quantitative analysis of lymph node distribution across clusters of circulating UTC. D) Quantitative analysis of lymph node distribution across clusters of non-circulating UTC. Data display 2 representative experiments with n = 6 mice. Bar graphs display mean value and error bars represent SEM.

Investigating the subsets based on cluster defining markers (Fig. 5D), we observed that all subsets were present in control groups and single TCR-based lineage deficient animals (Fig. 18B). t-distributed stochastic neighbor embedding (tSNE) projection of the high-dimensional flow cytometry data demonstrated that for all analyzed mouse strains, the previously identified subsets form separate clusters and represent individual cell populations. To capture the complete spectrum of UTC, iLNs, medLNs and mesLNs were analyzed and displayed together. Taking a closer look at the cluster distribution across the lymph nodes, we observed that the CD62L positive subsets were equally distributed across lymph nodes (Fig. 18C). The non-circulating UTC displayed the predicted tissue specific distribution (Fig. 18D), which was observed in all single TCR-based lineage deficient mouse strains. Therefore, we concluded that all analyzed UTC subsets are compensated in single TCR-based lineage deficient animals and most likely form functional units as we could demonstrate for Th17-like UTC in skin draining lymph nodes.

Discussion

Summary

Taken together, we proposed and experimentally validated two novel concepts in this work. First, we demonstrated a so far unknown layer of heterogeneity among different lymph nodes imprinted by UTC. A site-specific Th-like phenotype composition of UTC resulted in unique innate cytokine profiles upon activation with the potential to directly impact on the innate and adaptive immune responses that are generated in distinct LNs. Second, our results indicated that the innate function of UTC argues for an organization within functional units rather than separate TCR-based lineages. We demonstrated that the three major UTC TCR-based lineages, $\gamma\delta$ T, MAIT and NKT cells shared transcriptional homogeneity, resided in the same microanatomical compartment, and compensated for each other in both numbers and function. This re-classification of UTC has major implications on interpreting previous results and designing future experiments when analyzing the functionality of these cells. Data from previous studies that were obtained using single TCR-based lineage deficient mouse models should be reevaluated and discussed in light of our results.

Lymph node heterogeneity

Previous studies have demonstrated that the immune response differs depending on the site of infection or antigen stimulus⁹⁹⁻¹⁰². Our results added to the previously obtained knowledge and offered new mechanistic insights on how this variance among lymph nodes is achieved. We showed that the UTC population of each lymph node is comprised of a common pool of circulating UTC (Fig. 6) and unique subsets of tissue-derived cells that reflect the UTC composition of the respective draining tissue (Fig. 10). The tissue-mirroring population thereby mimicked the behavior of DCs, that migrate constantly from the tissue to the draining lymph node, carrying antigens and transmitting information about the immunological state of the tissue⁶⁹. Which information and how exactly it can be transmitted via UTC needs be further investigated.

Direct evidence for migration from the tissue to the draining lymph node of UTC was not shown in this work. The overlap of Th-like phenotypes between tissue and draining lymph node can theoretically also be explained in other ways. For example, factors that imprint the tissue phenotype of UTC drain via the lymphatics to the lymph node and imprint the resident UTC in a similar way. To clarify whether UTC actively migrate from the tissue to the draining lymph node, colleagues and collaborators performed sophisticated photo-switching and transplantation experiments¹²⁰. The results of this set of experiments provided direct evidence that UTC migrate from several tissues to their draining lymph node.

Previous studies have demonstrated that this migration from tissues to the draining lymph nodes applies to skin-derived $\gamma\delta$ T cells¹¹⁰. Our study extends the previous observations to several tissues and all UTC lineages, identifying this behavior as a general principle of UTC biology. Since UTC, in particular MAIT and NKT cells, have been described as tissue resident⁷⁹, our results offer a novel conceptual view on the migrational behavior of these cells. The conclusion that these cells remain locally in their tissue was primarily derived from parabiosis experiments. In this approach, the blood-circulation of two mice is surgically connected, allowing for the exchange of circulating cells between them¹²¹. After several weeks, the immune cell composition of tissues can be assessed and based on congenital markers, it is possible to determine which fraction is derived from the host or the donor. The observation that UTC in tissues are largely comprised of host origin cells, demonstrates that they are not entering the tissue via the blood stream. Our data showing a migrational behavior from the tissue to the draining lymph node, most likely via lymphatic vessels, is in agreement with this previous data. However, considering our data and the previous results obtained from parabiosis experiments, the interpretation of the life cycle of UTC needs to be revised. These cells are not, as previously thought, purely tissue resident. Leaving the thymus after maturation, UTC seed niches in peripheral tissues and reside there. Over time, they migrate from these tissues to the draining lymph node and most likely die there. That the UTC die in the lymph node over time without leaving it again is speculation but considering the previous parabiosis

results⁷⁹, a valid conclusion. If the cells leave the lymph node to re-enter the tissue of origin, they need to do this via the blood stream. In the parabiosis set-up the circulation of UTC from the lymph node via the blood to the tissue would most likely have been detected.

An alternative explanation is that non-circulating UTC differentiate into the circulating ones in the lymph node and thereby feed into the pool of circulating cells that do not enter the tissue. This scenario is rather unlikely, because of the different Th phenotypes present in the circulating and non-circulating pool. Th17-like UTC are absent in the circulating compartment, based on our analysis (Fig. 7) and previous reports¹¹⁵. So far, there is no report to my knowledge, that shows convincingly a conversion of Th17-like into Th1-like UTC *in vivo*. Furthermore, for $\gamma\delta$ T cells it was shown that in the blood and partially lymphatic organs the transcriptional landscape of these cells resembles the more mature differentiation states in the adult thymus¹²². This argues for a direct thymic origin of these cells. Future experiments need to determine the functional role of continuous UTC migration from the tissue to the draining lymph node.

It needs to be considered that the experiments regarding the circulation and migrational behavior of UTC from the tissue to the lymph node were analyzed at steady state in this study (Fig. 5A). Whether the recruitment from the tissue to the lymph node is accelerated, blocked or unaltered during inflammatory conditions needs to be further investigated. Potentially, a conversion of Th17- into Th1-like UTC could also be induced during inflammatory conditions⁸⁵. However, under infectious conditions, others have shown that $\gamma\delta$ T cells can be recruited from the blood to the skin in a CCR2-dependent manner¹²³. Whether the recruited cells belong to the circulatory compartment or are derived from the lymph node under these inflammatory conditions needs to be determined by dedicated experiments. Also, it would be interesting to investigate whether the recruited UTC integrate permanently into the target organ and potentially bias the TCR and Th-like phenotype composition of the organ, or whether they transiently reside like short-lived effector cells and die after resolution of the infection.

Overall, the data presented here, demonstrates a novel, generalizable migration behavior of UTC and adds important knowledge to their life cycle. In light of our data, further questions and novel angles to study these cells and the overall setup of the immune system arise.

Functional unit concept of UTC

While studying the composition and migrational behavior of UTC, we realized that the observed heterogeneity and the TCR-based lineages are disconnected. Our comprehensive scRNA-sequencing analysis of UTC across lymph nodes and following flow cytometric validation demonstrates that the TCR-based lineage does not imprint the transcriptional identity of UTC (Fig. 5E). In our unbiased analysis, cells belonging to different lineages clustered together, belonging to the same cell type. This data is an extension of previous studies demonstrating transcriptional

similarities comparing different UTC lineages¹²⁴⁻¹²⁶, but it also goes beyond previous descriptions, offering for the first time a comprehensive overview of UTC composition and subsets across lymph nodes.

Next to the transcriptional overlap, we could also observe a disconnected layer of selection, comparing the Th-like phenotypes of UTC and their TCR-based lineage. While we observed, as others before^{80,81}, significant variation of TCR-based lineages comparing mice with different microbiota compositions, the Th-like phenotype of the cells remained unaffected (Fig. 11). These data indicate that the different immunological functions of UTC, one being part of the innate immune system and getting activated via cytokines, and the other part serving as adaptive immune cells reacting to specific antigens with their TCR, are likely controlled and selected via different mechanisms. The TCR composition of UTC residing in barrier tissues seems to be regulated via tissue-restricted antigens or stimulatory molecules as was proposed by other studies before^{127,128}. Specifically, development and maintenance of dendritic epidermal T cells is dependent on selection and upkeep of intraepithelial T cells protein 1 (Skint-1) expression in the epidermis^{89,129}. The mechanisms selecting the Th-like phenotype composition within a tissue remains largely unknown. Our data indicates for the first time that these features of UTC are independently controlled on a population level and will foster further studies trying to elucidate the molecular basis for this observation.

Focusing on the TCR-independent regulation of UTC, we propose, based on our data, a functional unit concept that encompasses all UTC TCR-based lineages. This study is the first to systematically investigate the functional, transcriptional and localization relationship between these lineages and we came to the conclusion that they belong to the same units. Demonstrating it for sdLN Th17-like UTC as an example, we showed that these cells share a localization (Fig. 13B), are transcriptionally homogenous (Fig. 14) and compensate for each other in numbers (Fig. 16) and function (Fig. 17). Investigating UTC as a unit and not as separate lineages, as several studies have been doing so far^{75,130,131}, offers explanations to open questions in the field, like why single TCR-based lineage deficient mice fail to show strong phenotypes in most disease or infection models. Furthermore, previously made observations would be offered a new interpretation as outlined below.

So far, it has been challenging to assign unique functions to UTC lineages¹³². In most cases, researchers identified a function of the cells and correlated their importance, rather than demonstrating the unique feature of the cell type. For example, IL-17 producing $\gamma\delta$ T cells have been described in the brain¹³³, where they contribute to neuronal development and anxiety behavior. The importance of IL-17 as a functional molecule was convincingly demonstrated using IL-17 deficient mouse models and since $\gamma\delta$ T cells are the main producers, the function was ascribed to these cells. Mice deficient for $\gamma\delta$ T cells showed only a milder version of the phenotype

and only acute depletion via antibodies of these cells revealed convincing results. Considering our data, it is questionable whether the IL-17 production is a unique feature of $\gamma\delta$ T cells in this tissue, or whether UTC in the brain are also organized as a functional unit.

The dependence of UTC on the microbiome during early life development in tissue seeding is well established⁸⁰. Germ-free mice, raised lacking a microbiome, have defects in developing MAIT cells. This observation could be ascribed to vitamin B6 metabolite producing bacteria which colonize the gut in microbiome sufficient mice⁸⁰. A different study observed that NKT cells increase in numbers in the absence of a microbiome⁸¹. It was concluded that the microbiome had an inhibitory effect on NKT cells seeding to the tissue. Considering our data, an alternative interpretation is that in germ-free mice NKT cells compensate for the absence of MAIT cells and therefore increase in numbers. To prove this hypothesis, dedicated experiments will need to be conducted. Nevertheless, our work offers an alternative interpretation of the data. This example demonstrates that considering UTC as functional units offers new perspectives on already existing data and eventually more studies might need to be reassessed in their interpretation.

Dedicated Th2-like UTC are absent outside the thymus of naïve mice

Next to the conceptual advance of this study, we provide a resource of the transcriptional UTC landscape across lymph nodes (Fig. 5D). Our single cell analysis can be used to identify new subsets of UTC and uncover their specific functions, work that would go beyond the scope of this thesis. The value and validity of this scRNA-sequencing atlas is shown in the fact that many already recognized subsets could be validated and confirmed⁷⁸. The rough classification of UTC into Th1-, Th2- and Th17-like cells was also seen in our data set, at least for the Th1- and Th17-like subsets (Fig. 7).

We failed to identify a Th2-like subset in our sequencing analysis based on published transcription factors or cytokines⁷⁸. To confirm the lack of Th2-like UTC we investigated further published data sets¹⁰⁴ and analyzed an IL-5 fate mapping mouse model (Fig. 8). The results indicate that in our analysis, opposed to previous studies investigating the thymus and periphery^{109,134,135}, Th2-like UTC are absent. A recent study analyzing the developmental trajectory of NKT cells in the thymus demonstrated that the Th2-like cells are rather an intermediate cellular state than a fixed identity of these cells¹³⁶, which might explain why we failed to identify these cells in the periphery. A further reason to the discrepancy with previous studies might lie in the utilized mouse models. As such, our study, as well as the study describing Th2-like NKT cells as an intermediate developmental state, were conducted in B6 mice, while Th2-like UTC have been primarily studied in Balb/C mice. This genetic background is described to have a prevalence for Th2 cells in general^{15,137}. This difference needs to be considered when comparing the data.

A complete analysis of the UTC composition in mouse models with different genetic backgrounds will be required to fully resolve the question on Th2-like UTC in the future. Our data offers the framework to design a comprehensive analysis for such future studies, aiming to elucidate the differences between mouse strains in detail.

Translation to humans

Mouse studies regarding UTC have been often drawn into question with regards to their translatability to humans, and therefore their value. Inter-species differences regarding UTC numbers, phenotype, tissue-distribution, and TCR-ligand recognition are important factors to take into consideration, which is why every mouse study needs to be evaluated carefully with regards to its interpretation for humans¹³⁸. To draw definite conclusions for the concepts described in this study, dedicated experiments and detailed analysis of human samples are necessary. Nevertheless, previous data obtained from humans indicate that the results presented in this study might also be valid in humans and therefore clinically relevant.

First, it was described that tissue residing UTC differ in their phenotype, TCR-repertoire, and transcriptional landscape from circulating UTC^{139,140}. This means, that in humans circulating and non-circulating UTC are segregated, like in mice (Fig. 6). Whether the tissue-residing UTC can also be found in the lymph nodes due to lymphatic migration needs to be determined. However, if it can be shown that UTC in human lymph nodes can be separated into a circulating and non-circulating population, the lymph node heterogeneity and all its consequences are translatable from our mouse study to humans. Furthermore, it would allow for the detailed study of tissue residing UTC in human lymph node samples. This would provide the advantage of having more samples available. Lymph node biopsies are a common medical procedure¹⁴¹, while obtaining solid organ samples from healthy donors is a rare case scenario. Additionally, from a technical point of view, isolating lymphocytes from lymphatic organs is a less complicated procedure than isolation from solid tissues, which also limits the introduction of technical bias in the analysis^{142,143}.

The second main aspect of our study is that UTC can be classified in functional units, independent of their TCR-based lineage. This aspect is harder to address in humans due to the lack of common markers to identify UTC beyond their TCRs. Human $\gamma\delta$ T, NKT and MAIT cells are studied using specific TCR antibodies and tetramers, like in many mouse studies. Our study benefited from the lack of CD4 and CD8 co-receptor expression in murine UTC, to identify them independently of their TCR. In humans most UTC express either CD8 or CD4^{144,145} which makes the analysis more challenging. Furthermore, no dedicated markers differentiating TCR lineages have been identified beyond their TCR, to my knowledge. However, the lack of specific markers might be an indication that the transcriptional homogeneity of UTC across lineages is also translatable to humans. To address this question in detail, a dedicated experiment analyzing these

cells on a single cell level needs to be conducted. Another indication that the functional unit concept for UTC applies to humans is derived from a patient study conducted by Howson *et al.*¹⁴⁶. One patient, that lacked MAIT cells due to genetic mutations in the *MR1* gene, showed a significant increase in $\gamma\delta$ T cells, which compensated for the function of MAIT cells in *ex vivo* experiments¹⁴⁶. This result resembles our data when analyzing single TCR-based lineage deficient mouse models. Of course, analyzing one patient provides only indications and not proof. Conducting a large-scale study with larger patient numbers is required for a convincing argument, but such a study may be difficult to conduct due to a lack of patients. To my knowledge, there is no disease described in humans caused by the lack of a specific UTC TCR-based lineage, which is why no patient registry exists. However, this absence of UTC associated diseases can be interpreted in two different ways. First, it might be that mutations causing a lack of MAIT, NKT or $\gamma\delta$ T cells are fatal, which might explain the lack of patients. Alternatively, the lack of a specific TCR-based lineage is compensated in numbers and function by the remaining ones and no clinical symptoms occur. Considering our data, classifying UTC into functional units, and the above-mentioned patient study¹⁴⁶, it is tempting to speculate that the compensation across UTC lineages is also applicable to humans.

Overall, it is impossible to conclude with certainty that the findings of this study are translatable to humans, without dedicated experiments demonstrating it. Nevertheless, the indications already present in the current literature, support the notion that most of the concepts described here for mouse UTC, will also apply to humans.

Clinical relevance

Assuming that the concepts proposed in this study are applicable to humans, it raises the question how clinically relevant these findings might be and how patients could potentially benefit from the gained knowledge. The implications for basic research were outlined above in detail, but the presented findings can have direct implications for patients and should direct the design of specific treatment strategies that harness the immune system.

The most recent clinical use of UTC lineages is the generation and administration of chimeric antigen receptor (CAR) T cells to treat cancer patients¹⁴⁷. CAR T cells are an individualized treatment strategy. Classically, endogenous conventional T cells are isolated from the patient, expanded *ex vivo* and transduced to express an antigen receptor specific for a tumor-antigen present in the patient¹⁴⁸. Since the patient's cells are used and the receptor can be individually designed to target antigens specific against the patient's tumor, high expectations were given to this treatment strategy. The success so far has been variable, depending on the type of tumor and other factors¹⁴⁹. To improve the CAR T cell treatment strategy, other cells like NK or UTC are currently investigated for their potential to treat patients^{147,150}.

Considering the results of our study, the usage of UTC as CAR T cell therapy might be more complex and would need further specifications. We show that UTC can be separated into circulating and non-circulating populations. Which one of these enters the tumor and resides in it, has not been investigated so far. To design optimal UTC CAR T cells, it might be beneficial to induce tissue specific phenotypes that promote the recruitment and potentially maintenance in the tissue-specific tumor microenvironment. As a conclusion, it could be beneficial that patients with colon carcinoma receive a colon specific type of UTC CAR T cells, while melanoma patients require a skin-specific UTC population. Therefore, an individualization of the therapy beyond receptor specificity might be required when utilizing UTC as CAR T cell therapy.

Other studies have described site-specific differences analyzing the immune response⁹⁹⁻¹⁰². Our study offers a molecular explanation for the observed differences and marks a starting point to study these and their impact in detail. Our data demonstrate that at least part of the lymph node heterogeneity is caused by different UTC subsets residing in the lymph nodes. Investigating these differences in more detail and obtaining a holistic overview of the caused heterogeneity, will pave the way for improved rational treatment designs. As an example, it can be beneficial to administer a vaccination via different routes, depending on whether more antibody producing B cells or memory T cells should be induced. Also, some vaccines might be more efficient in generating an immune response with long lasting memory at certain sites while failing to do so at others. Furthermore, adding adjuvants that site-specifically activate UTC, guiding the immune response in a favorable direction, can be investigated. This study can be used as a framework and provides a rational to investigate site-specific influences on vaccination outcomes in detail.

In conclusion, our study offers a rational to investigate the role of UTC in certain malignancies and clinical settings. Furthermore, it offers a framework for testing potential factors to consider when utilizing these cells as therapeutic agents.

Limitations of the study

This study, that investigated UTC biology in different lymph nodes, revealed a novel behavior of these cells and proposed a unifying concept with potential far reaching basic and clinical implications. Nevertheless, there are also certain limitations that need to be considered when interpreting the data. Most analyses of UTC were performed based on the identification of these cells via expression of CD3 and absence of CD4 and CD8, which would mark conventional T cells. For most UTC in mice, this classification is valid, but also in mice subsets of CD4 or CD8 positive UTC have been described^{151,152}. Focusing on our data, it cannot be excluded that these CD4 or CD8 positive UTC behave differently in terms of their migrational behavior. Furthermore, it is also possible that these subsets of UTC are not part of the functional units, but rather possess only TCR-based lineage specific functions. Dedicated experiments focusing on these cells are required

to clarify this remaining open question. Irrespective of the result, including or excluding CD4 and CD8 positive murine UTC does not jeopardize the significance of our findings for the majority of UTC.

Another limitation of our study is that we focused on the TCR-independent functions of T cells. The TCR of these cells is certainly critical for specific aspects of their biology and contributes to the immune response. Our proposed functional unit concept of UTC ignores this aspect, focusing solely on the innate function of UTC. During an immune response both functional aspects of these cells, adaptive response utilizing the TCR, and innate response reacting to cytokines, are integrated and probably influence the outcome of behavior of these cells in concert.

Nevertheless, isolating and separating the analysis of these two sides of UTC might offer certain benefits as well. Understanding in detail how and why UTC react the way they do is only possible by dissecting each stimulus they respond to. Here, we offer a framework that can clearly distinguish innate from adaptive features of UTC and thereby improve the interpretation of future studies.

Future directions

The findings presented here can be used for multiple future research projects, by directly addressing clinical issues and treatment options, or directing more basic molecular studies as mentioned in the discussion above. One important aspect, that was not mentioned so far, is a potential new approach to address the functions of UTC and their contribution to the immune response and homeostasis in general. So far, single TCR-based lineage deficient mouse models failed to reveal major specific contributions of these cells to either maintenance or immunity of the host¹³². Our study offers an explanation for this phenomenon, introducing the functional unit concept for UTC. Consequently, to fully understand the impact of UTC on immunity and tissue homeostasis, we need to generate and study a mouse model, that specifically lacks all UTC lineages. Crossing the three utilized single TCR-based lineage deficient mouse models used in this study, might be a potential approach to obtain such a mouse model. Analyzing the phenotype of mice lacking all UTC will likely offer a deeper understanding of their biology, revealing unknown functions.

With the data presented in this study we aim to introduce a novel concept for UTC biology and deepen our understanding on their behavior and pre-positioning in lymphatic organs. We are convinced that the presented findings offer a novel angle to study these cells and stimulate future research addressing their function and their clinical relevance for human diseases.

Material and Methods

Material

Table 1: Equipment

Device	Name and company
Autoclave	HX-430, Systec, Linden, Germany
Balance	CP2201, Sartorius, Göttingen, Germany
Cell sorter	Aria II, Becton-Dickinson, Franklin Lakes, NJ, USA
Centrifuge	Thermo Fisher Scientific, Waltham, MA, USA
Confocal Microscope	SP8, Leica, Hamburg, Germany
Cryostat	CM 3050S, Leica, Hamburg, Germany
Flow cytometers	Attune NxT Flow Cytometer, Thermo Fisher Scientific, Waltham, MA, USA Cytek Aurora 5-Laser, Cytek Biosciences, Amsterdam, The Netherlands
Freezer -20 °C	Liebherr, Biberach, Germany
Freezer -80 °C	VIP ECO ULT freezer, Panasonic, Avon Cedex, France
Ice machine	Ziegra, Isernhagen, Germany
Incubator cells	Binder, Tuttlingen, Germany
Incubator bacteria	MaxQ, Thermo Fisher Scientific, Waltham, MA, USA
IVC mice cage	Tecniplast Smartflow, Hohenpeißenberg, Germany
Neubauer chamber	Assistent, Karl Hecht GmbH, Sondheim, Germany
Pipette boy	Integra Biosciences, Biebertal, Germany
Pipette	Research plus (10, 20, 200, 1000), Eppendorf, Hamburg, Germany
Preparation instruments	F.S.T., Heidelberg, Germany
Refrigerator	Liebherr, Biberach, Germany
Sieves, steel	Mechanical Workshop, University Hospital Bonn, Germany
Spectrophotometer	Genesys 30, Thermo Fisher Scientific, Waltham, MA, USA
Vortex	neolab, Heidelberg, Germany
Water bath	Memmert, Schwabach, Germany
Workbench, sterile	Envair ECO, ENVAIR GmbH, Emmendingen, Germany

Table 2: Consumables

Consumables	Name and Company
Canula	100 Sterican, B. Braun, Melsungen, Germany
Cell strainer	Falcon cell strainer, Corning, NY, USA
Cover slips	controlled thickness 0.17 ±0.01 mm, CE, Assistent, Karl Hecht GmbH, Sondheim, Germany
Cryomolds	Tissue-Tek®, Sakura, Alphen aan den Rijn, Netherlands
Cryotubes	Cryopure 1.6ml, Sarstedt, Nümbrecht, Germany
FACS tubes	Sarstedt, Nümbrecht, Germany
FALCON tubes	15 ml, Greiner bio-one, Solingen, Germany 50 ml, Sarstedt, Nümbrecht, Germany

Injection Needles	27G, 25G, 20G, BD Microlance, Becton, Dickinson and Company, Franklin Lakes, NJ, USA
Microscopy slides	Superfrost Plus, VWR, Darmstadt, Germany
Nylon gauze	Labomedic, Bonn, Germany
Hydrophobic Barrier (PAP) Pen	ImmEdge™ Pen (H-4000), Vector Laboratories, Burlingame, CA, USA
Pestle	Fisher Scientific, Pittsburgh, PA, USA
Pipette tips	Ultratip 1000 µl, Greiner bio-one, Frickenhausen, Germany TipOne 200 µl, STARlab, Hamburg, Germany Pipette Tip 10 µl neutral, Sarstedt, Nümbrecht, Germany
Plastic pipettes	150 mm and 230 mm; Roth, Karlsruhe, Germany
Reaction tubes	microtubes (0.5 ml, 1.5 ml, 2 ml), Sarstedt, Nümbrecht, Germany
Syringes	2 ml/ 5 ml BD Discardit II, Becton-Dickinson, Heidelberg, Germany
Tissue culture plates	TPP Tissue culture testplates (96, 24, 6 wells), Trasadingen, Switzerland
Tissue grinder	Fisher Scientific, Pittsburgh, PA, USA

Table 3: Chemicals and reagents

Chemicals and reagents	Name and company
β-mercaptoethanol	Sigma Aldrich, St. Louis, MO, USA
Ammonium chloride (NH ₄ Cl)	Merck, Darmstadt, Germany
Bovine serum albumin fraction V	Roth, Karlsruhe, Germany
Brefeldin A (BFA)	Sigma Aldrich, Munich, Germany
Collagenase D	Roche, Basel, Switzerland
Dimethylsulfoxid (DMSO)	Roth, Karlsruhe, Germany
Dispase	Roche, Basel, Switzerland
DNase 1	Sigma-Aldrich, St. Louis, MO, USA
Diethiothreitol (DTT)	Sigma-Aldrich, St. Louis, MO, USA
Embedding medium	Tissue-Tek® O.C.T.™ Compound, Sakura, Alphen aan den Rijn, Netherlands
Ethanol 70% v/v	Otto Fischar, Saarbrücken, Germany
FCγ Block	Privigen, CSL Behring, Marburg, Germany
Fetal bovine serum (FBS)	Good Filtrated Bovine Serum, PAN Biotech, Aidenbach, Germany
Fluoromount-G	ebioscience, San Diego, CA, USA
Formaldehyde	Roth, Karlsruhe, Germany
Gelatin from cold water fish skin (GCWFS)	Sigma Aldrich, St. Louis, MO, USA
HEPES	Gibco, Thermo Fisher Scientific, Waltham, MA, USA
Ionomycin	Sigma-Aldrich, St. Louis, MO, USA
Ketamin	Ketanes® S, Pfizer, NY, USA
LB	LB Broth (Lennox), Invitrogen, Darmstadt, Germany
Liberase TL	Sigma Aldrich, St. Louis, MO, USA

L-Lysin	Sigma Aldrich, St. Louis, MO, USA
Normal Mouse Serum (NMS)	Life Technologies, Carlsbad, CA, USA
Penicillin/ Streptomycin/ Glutamine	Gibco, Thermo Fisher Scientific, Waltham, MA, USA
Percoll®	Sigma-Aldrich, St. Louis, MO, USA
Perm/Wash Buffer 10x	BD, Heidelberg, Germany
Phorbol Myristate Acetate (PMA)	Sigma Aldrich, St. Louis, MO, USA
Phosphate-buffered saline (PBS)	Biochrom AG, Berlin, Germany
Potassium bicarbonate (KHCO ₃)	Merck, Darmstadt, Germany
RPMI 1640 medium	Invitrogen, Darmstadt, Germany
Sucrose	Sigma Aldrich, St. Louis, MO, USA
Triton X-100	Promega, Madison, WI, USA
Trypan blue	Lonza, Cologne, Germany
Xylazine	Xylavet®, CP-Pharma, Burgdorf, Germany

Table 4: Buffer, media, solutions

Buffer, media, solutions	Composition
10x ACK lysis buffer	1.5 M NH ₄ Cl 100 mM KHCO ₃ 10 mM EDTA-Na ₂ in distilled water (pH value 7.2)
Blocking buffer	1% (v/v) FBS 1% (m/v) GCWFS 0.3 % (v/v) Triton-X 100 in PBS 1% NMS added directly before use
FACS buffer	2 % (v/v) FBS in 1x PBS
Intestine digestion buffer 1	1 mM EDTA 10 mM HEPES 0.15 % (w/v) DTT in RPMI 1640 medium preparation directly before use
Intestine digestion buffer 2	1 mM EDTA 10 mM HEPES in RPMI 1640 medium
Intestine digestion buffer 3	2 % (v/v) FBS 1.5 mg/ml Collagenase D 0.5 mg/ml Dispase 20 µg/ml DNase 1 1 mM EDTA 10 mM HEPES in RPMI 1640 medium preparation directly before use

LB medium	20 g/L LB in distilled water
Liberase digestion buffer	10 mM HEPES 125 µg/ml Liberase TL 20 µg/ml DNase 1 in RPMI 1640 medium preparation directly before use
PBS	137 mM NaCl 2.7 mM KCl 10 mM Na ₂ HPO ₄ 1.8 mM KH ₂ PO ₄ in distilled water
P-buffer	40.5 % (v/v) 0.1 M Na ₂ HPO ₄ 9.5 % (v/v) NaH ₂ PO ₄ in distilled water (pH value 7.4)
PLP	2.12 mg NaIO ₄ 3.75 ml P-buffer 3.75 ml L-Lysine 2.5 ml 10% formalin (pH value 7.4, adjusted with 10 M NaOH) preparation directly before use
T cell medium	8 % heat-inactivated FBS 50 µM β-Mercaptoethanol 4 mM L-Glutamin 100 U/ml Penicillin 100 µg/ml Streptomycin in RPMI 1640 medium

Table 5: Antibodies for flow cytometry

Antigen	Clone	Conjugate	Company
CCR6	29-2L17	PE	BioLegend
CCR9	CW-1.2	FITC	BioLegend
CD3 _ε	17A2	AF700	BioLegend
CD4	GK1-5 RM4-5	BV711 BV605	BioLegend
CD8 _α	53-6.7	BV711 BV605	BioLegend
CD44	IM7	BV785	BioLegend
CD45	30-F11	PB	BioLegend
CD45.2	104	FITC	BioLegend
CD62L	MEL-14	APC-Cy7 BV510 BV605 PE-Cy7	BioLegend
CXCR3	CXCR3-173	BV510	BioLegend
CXCR6	SA051D1	AF647	BioLegend

		BV421 PE PE-Dazzle594	
EOMES	Dan11mag	PE-Cy7	eBioscience
GM-CSF	MP1-22E9	PE	Thermo
IFN γ	XMG1.2	BV421	BioLegend
IL-17F	9D3.1C8	AF647	BioLegend
ITG β 7	FIB27	PerCp-Cy5.5	BioLegend
LCK	3A5	AF647	Santa Cruz
SLAMF6	13G3	BV711	BD Pharmigen
TNF α	MD6-XT22	PE -Cy7	BioLegend
TCR $\gamma\delta$	GL3	BV605 AF488 BUV805	BioLegend BD Biosciences
TCR V β 6	RR4-7	BUV395 FITC	BD Biosciences
TCR V β 8.1; 8.2	KJ16-133-18 MR5-2	FITC BUV395	BioLegend BD Biosciences

Table 6: Antibodies for Histology

Antigen	Clone	Conjugate	Company
B220	RA3-6B2	AF700	BioLegend
CD3 ϵ	17A2	BV421	BioLegend

Table 7: Tetramers

Molecule	Antigen	Conjugate	Company
CD1d	PBS-57	BV421	NIH Tetramer Core Facility

Table 8: Kits

Name	Company
Cytofix/ Cytoperm	BD Biosciences; Heidelberg, Germany
Zombie NIR™ Fixable Viability Kit	BioLegend; San Diego, CA, USA

Table 9: Software

Software	Company
Adobe Creative Cloud	Adobe, San Jos., CA, USA
Attune NxT Flowcytometry Software	Thermo Fisher Scientific; Waltham, MA, USA
Endnote 20	Clarivate Analytics, Philadelphia, PA, USA
Flowjo V10.7.1	BD Biosciences, Heidelberg, Germany
GraphPad Prism 8	GraphPad Software, La Jolla, CA, USA
Imaris	Bitplane
Leica LSX	Leica
Microsoft Office	Microsoft, Redmond, WA, USA
RStudio	RStudio Inc., Boston, MA, USA
SpectroFlo Software	Cytek Biosciences; Amsterdam, The Netherlands

Table 10: Viruses and bacteria

Pathogen	Description and Reference
Vaccinia virus	Vaccinia virus; kindly provided by Jonathan Yewdell, National Institute of Allergy and Infectious Diseases, Bethesda, MY, USA
<i>S. aureus</i> HG001	<i>S. aureus</i> ; kindly provided by Knut Ohlsen, Institute for Molecular Infection Biology, Würzburg, Germany

Mouse strains

All mice used were maintained under specific pathogen-free conditions at a certified Association for Assessment and Accreditation of Laboratory Animal Care-accredited animal facility (Animal facility Systems Immunology Würzburg or ZEMM animal facility Würzburg) in accordance with the institutional animal guidelines. Used mouse strains are listed below. All mice are on the genetic background of C57BL/6J, if not stated differently.

Table 11: Mouse strains

Mouse strain	Description and Reference
B6	C57BL/6J non-transgenic mice were purchased from Janvier Laboratories and used as wildtype controls (wt).
Cast/B6	Cast/B6 mice were kindly provided Lantz, O.. These mice have the same genetic background as the <i>Mr1</i> ^{-/-} strain.
<i>Cd1d</i> ^{-/-}	<i>Cd1d</i> ^{-/-} were purchased from Janvier Laboratories. The mice lack the expression of the genes CD1d1 and CD1d2. These mutations lead to the lack of NKT cells.
<i>Cxcr3</i> ^{GFP}	<i>Cxcr3</i> ^{GFP} mice were kindly provided by Satoskar, A.. A GFP gene cassette is expressed under the CXCR3 promoter and mice can be used as reporter line.
<i>Cxcr6</i> ^{GFP/wt}	<i>Cxcr6</i> ^{GFP/wt} were purchased from Janvier Laboratories. A GFP gene cassette is inserted and into the <i>Cxcr6</i> gene locus. Heterozygous this mouse strain can be used as a reporter line, homozygous it is a functional knock-out for CXCR6.
<i>Il23r</i> ^{GFP/GFP}	<i>Il23r</i> ^{GFP/GFP} mice were kindly provided by Zerneck, A.. A GFP gene cassette is inserted and into the <i>Il23r</i> gene locus. Heterozygous this mouse strain can be used as a reporter line, homozygous it is a functional knock-out for IL-23R.
<i>Il4</i> ^{GFP/wt}	<i>Il4</i> ^{GFP/wt} mice were kindly provided Voehringer, D.. A GFP gene cassette is inserted and into the IL4 gene locus. Heterozygous this mouse strain can be used as a reporter line, homozygous it is a functional knock-out for IL4.
<i>Mr1</i> ^{-/-}	<i>Mr1</i> ^{-/-} mice were kindly provided by Lantz, O.. The mice lack MR1 gene expression and thereby don't possess MR1-dependent T cells, including MAIT cells.
<i>Tcrd</i> ^{-/-}	B6.129P2 <i>Tcrdtm1</i> Mom/J mice were kindly provided by Prinz, I.. These mice harbor a mutation in the TCR delta gene and thereby lack gd T cells.

Methods

Virus preparation

Vaccinia virus was stored at -80 °C in cryo-conservation tubes. For usage, the virus stock was diluted in sterile PBS. Mice were injected with an infectious dose of 200 plaque forming units (PFU) subcutaneously or intranasally for 4 h.

Bacteria preparation

Staphylococcus aureus HG001 was stored at -80 °C in cryo-conservation tubes. For usage, a ring of cryo-conserved bacteria was placed into 50 ml LB medium and grown over night at 37° while shaking at a speed of 200 rounds per minute (rpm). To obtain a log culture, 100 µl of the over-night culture were diluted in 10 ml fresh LB medium. After 2 h, the growth of bacteria was measured by determining the optical density (OD) 600 using a spectrophotometer. The log-culture was diluted in PBS to obtain a concentration of 1×10^8 colony forming units (CFU) per 30 µl. Mice were injected with an infectious dose of 1×10^8 CFU subcutaneously for 4 h.

Treatment of mice

Footpad infection

To inject virus or bacteria subcutaneously into the footpad, mice were restrained. 10^8 CFU *S. aureus* or 200 PFU Vaccinia virus were diluted in 30 µl sterile PBS and injected into each footpad of the mice.

Intranasal infection

To infect with virus intranasally, the mice were anesthetized via intra peritoneal injection of 150 µl Ketamine/ Xylazine solution. The mice were monitored until no reflexes could be measured. 200 PFU Vaccinia virus were diluted in 25 µl sterile PBS and dropped into the nose of the mice. Afterwards, the mice were laid on their side in their cage and monitored until they woke up.

Isolation of lymphocytes from organs

Lymph nodes

To isolate cells from lymph nodes, organs were harvested from donor mice and placed into 150 µl FACS buffer containing 1.5 ml tubes on ice. Lymph nodes were mashed using a pestle

to create a single cell suspension. Afterwards, the cell suspension was transferred into a 96-well v-bottom plate and further processed for analysis.

Spleen

To isolate cells from spleen, organs were harvested and placed into PBS on ice until further processing. A single cell suspension was created by mashing the spleen over a metal sieve into a 50 ml tube. The mesh was washed with 20 ml FACS buffer and afterwards the cells were pelleted by centrifuging for 8 min at 1600 rpm. After discarding the supernatant, the pellet was resuspended in 2 ml 1x ACK buffer to lyse erythrocytes at room temperature. 5 min later 20 ml PBS was added, the cells were filtered into a new 50 ml tube and the cell suspension was centrifuged for 7 min at 1600 rpm. The pellet was resuspended in 1.5 ml FACS buffer. 150 μ l cell suspension was transferred into a 96-well v-bottom plate and further processed for analysis.

Skin

For isolation of resident cells from the skin, the ears of the mice were harvested and separated in order to expose the dermis. The ear skin was digested using 500 μ l liberase digestion solution per ear half for 90 min at 37 °C without shaking. The digestion was stopped by diluting with cold PBS supplemented with 50 μ M β -Mercaptoethanol. The digested tissue was mashed to obtain a single cell suspension over a metal sieve into a 50 ml tube. The sieve was washed with 20 ml PBS and the suspension centrifuged for 8 min at 1600 rpm to pellet the cells. The pellet was resuspended in 20 ml PBS, the cells were filtered into a new 50 ml tube and the cell suspension was centrifuged for 7 min at 1600 rpm. Afterwards, the pellet was resuspended in 150 μ l FACS buffer, transferred into a 96-well v-bottom plate, and further processed for analysis.

Lung

Before isolating lungs, mice were injected with 2 μ g anti-CD45 antibody (30-F11, Pacific Blue) in 100 μ l PBS intra-venously. 5 min post injection mice were sacrificed, and organs were harvested. For isolating the lung-resident cells, the lungs were pre-washed in cold PBS and chopped into small pieces in a 1.5 ml tube. The lungs were digested using 2 ml liberase digestion buffer per lung for 45 min at 37 °C shaking at 150 rpm. The digestion was stopped by diluting with cold PBS supplemented with 50 μ M β -Mercaptoethanol. For the lung, red blood cells were lysed as described for the spleen, using 1 ml 1x ACK buffer. The digested tissue was meshed to obtain a single cell suspension over a metal sieve. The sieve was washed with 20 ml PBS and the suspension centrifuged for 8 min at 1600 rpm to pellet the cells. The pellet was resuspended in 4 ml 40% Percoll and transferred into a 15 ml tube. 4 ml of 80% Percoll was carefully layered on top. For the density gradient centrifugation, the layered cells were centrifuged for 20 min at room

temperature and 2500 rpm. The acceleration was set to 1 and deceleration to 0. Afterwards, the interface was collected and diluted in 6 ml FACS buffer in a 15 ml tube. The cell suspension was centrifuged for 7 min at 1600 rpm. Afterwards, the pellet was resuspended in 150 μ l FACS buffer, transferred into a 96-well v-bottom plate, and further processed for analysis.

Intestine

The isolation of small intestine-resident cells was performed after removing the fat, the Payer's patches and the feces, and by exposing the internal side of the intestine. To isolate the intraepithelial lymphocytes (IELs), the small intestine pieces were transferred into a 50 ml tube and incubated in 30 ml intestine digestion buffer 1 for 30 min at 37° C and 120 rpm. To isolate the lamina propria lymphocytes, the intestinal pieces were transferred into a 50 ml tube containing 15 ml of intestine digestion buffer 2. After buffering the DTT containing intestine digestion buffer 1, the intestine pieces were chopped into smaller pieces and afterwards transferred into a 50 ml tube containing 25 ml intestine digestion buffer 3. The tissue pieces were incubated for 30 min at 37 °C at 120 rpm. The digested tissue was mashed to obtain a single cell suspension over a metal sieve. The sieve was washed with 20 ml PBS and the suspension centrifuged for 8 min at 1600 rpm to pellet the cells. The pellet was resuspended in 4 ml 40% Percoll and transferred into a 15 ml tube. 4 ml of 80% Percoll was carefully layered on top. For the density gradient centrifugation, the layered cells were centrifuged for 20 min at room temperature and 2500 rpm. The acceleration was set to 1 and deceleration to 0. Afterwards, the interface was collected and diluted in 6 ml FACS buffer in a 15 ml tube. The cell suspension was centrifuged for 7 min at 1600 rpm. Afterwards, the pellet was resuspended in 150 μ l FACS buffer, transferred into a 96-well v-bottom plate, and further processed for analysis.

Ex vivo stimulation of lymphocytes

Lymphocytes were isolated from inguinal, mediastinal or mesenteric lymph nodes and plated in a 96-well plate at a final concentration of 5×10^6 cells/ml in 200 μ L. Cell suspensions in T cell medium were plated and activated using 0.025 mg/ml phorbol myristate acetate (PMA), 1 mg/ml Ionomycin and cultured for 4 h hours at 37 °C. 1 mg/ml Brefeldin A (BFA) was added to the medium. Only 1 mg/ml BFA containing condition without PMA/ Ionomycin served as a control.

Histology

Fixation and embedding

For fixation, LNs were isolated and immediately fixed in 500 μ l of freshly prepared PLP buffer for 12 h at 4 °C. Samples were washed in PBS and afterwards dehydrated in 500 μ l 30 %

(v/v) sucrose at 4 °C overnight. Afterwards, samples were embedded in Tissue-Tek and stored at -80 °C for cryo-cutting and subsequent immunofluorescence staining.

Microscopy

30 µm sections were cut on the cryostat and adhered to Superfrost Plus object slides. Frozen sections were rehydrated with PBS for 10 min at room temperature, followed by permeabilization and blocking with blocking buffer containing 1 % normalized mouse serum (NMS) for up to 1 h at room temperature. Staining with fluorescently labelled antibodies was performed in blocking buffer (with 1 % NMS) at 4 °C overnight. Afterwards, sections were washed with PBS and mounted with Fluoromount-G. LN sections were imaged using Leica SP8 confocal microscope.

Flow cytometry

For staining surface molecules cells were transferred into a 96-well v-bottom plate. After centrifuging for 3 min at 1600 rpm cells were resuspended in 50 µl staining solution based on FACS buffer, containing the antibodies for the surface stain and Fc-block. Cells were incubated in the dark at 4 °C for 30 min. Afterwards, plates were centrifuged for 3 min at 1600 rpm. The pellets were resuspended in 150 µl FACS buffer and transferred into 5 ml tubes filtering through nylon gauze. The well plate was washed with additional 150 µl FACS buffer, which was transferred via the nylon gauze into the 5ml tube. The samples were analyzed using Cytex or Attune flow cytometers.

For intracellular proteins staining, the cells were differentially processed after the surface staining incubation. After washing once with FACS buffer, the cells were centrifuged for 3 min at 1600 rpm. Then, the cells were resuspended in 50 µl Cytofix/ Cytoperm to be fixed and permeabilized, and incubated for 20 min at 4 °C in the dark. After pelleting the cells, they were washed once with 1x Perm/ Wash and then resuspended in 50 µl Perm/ Wash-based intracellular staining solution which included the antibodies in appropriate concentration. The cells were incubated for 30 min at 4 °C in the dark. Afterwards, the cells were pelleted by centrifuging for 3 min at 1600 rpm. They were washed with 150 µl Perm/ Wash, then resuspended in 150 µl Perm/ Wash and transferred into 5 ml tubes prepared with 150 µl FACS buffer. They were processed by FACS analysis.

Tetramer staining

To identify NKT cells, CD1d tetramers loaded with PBS-57 were used. They were added in a 1:200 dilution to the surface staining solution and incubated for 30 min at 4 °C in the dark. After incubation the cells were washed as described for the surface staining and processed for further analysis.

scRNA-sequencing

Single-cell RNA-sequencing was performed with the help of the Helmholtz Institute for RNA-based Infection Research in Würzburg, the Core Unit Systems Medicine of the University of Würzburg and the Helmholtz Centre for Infection Research in Braunschweig.

Cell sorting

Lymph node cells were isolated as described above and stained as described in section Flow cytometry. Afterwards, the population of interest was sorted using a FACS Aria II cell sorter.

Hash tagging for scRNA-sequencing

To combine different lymph nodes for scRNA-sequencing, single cell suspensions were generated and together with the antibody mix for sorting, a specific TotalSeq™ Antibody mix was added and incubated for 30 min at 4 °C. After enriching for the populations of interest, the different samples were mixed in a 1:1:1 ratio and further processed for sequencing. The addition of the TotalSeq™ antibodies allowed for later identification of the tissue of origin for every single cell.

Dropseq

The single cells were encapsulated into droplets with the Chromium™ Controller and processed following manufacturer's specifications. Transcripts captured in all the cells encapsulated with a bead were uniquely barcoded using a combination of a 16 bp 10x Barcode and a 10 bp unique molecular identifier (UMI). To generate complementary desoxyribonucleic acid (cDNA) libraries the Chromium™ Single Cell 3' Library & Gel Bead Kit v2 for the CXCR6^{high}/CD44⁺ cells (Fig. 14) or v3 for the other samples (Fig. 5) was used following the detailed protocol provided by the manufacturer. Libraries were quantified by Qubit™ 3.0 Fluometer and quality was checked using 2100 Bioanalyzer with High Sensitivity DNA kit. Libraries were sequenced in 50 base pair paired-end mode with the NovaSeq 6000 platform. The sequencing data was demultiplexed using Cell Ranger software (version 2.0.2). The reads were aligned to mouse mm10 reference genome using STAR aligner. Aligned reads were used to quantify the expression level of mouse genes and generation of gene-barcode matrix. Subsequent data analysis was performed using Seurat R package (version 3.2)¹⁵³.

scRNA-sequencing analysis

Sample demultiplexing and doublet identification

To demultiplex hashing tags for each cell HTODemux function in Seurat package was used with standard parameters. Cross-sample doublet cell detection was performed based on

hashtag signal. Cells that were classified as 'singlet' and identified by hashtags were retained and used for downstream analysis¹⁵³.

scRNA-sequencing analysis workflow

Quality control was performed, and viable cells were selected by excluding cells with UMI counts lower than 1000 and above 27000, as well as cells having more than 5% of mitochondrial transcripts for the steady state CXCR6^{high}/ CD44⁺ cells (Fig. 14). For the data set comparing lymph nodes (Fig. 5) cells with UMI counts lower than 800 and above 3000, as well as cells having more than 6% of mitochondrial transcripts and more than 12000 (tissue-derived) or 10000 (circulating) total transcripts were excluded. Circulating and tissue-derived samples (Fig. 5) were combined using the merge function in Seurat. 2000 most variable genes were used for downstream analysis to calculate principal components, after log-normalization and scaling. Principle component analysis (PCA) was used for dimensionality reduction and to visualize a uniform manifold approximation and projection (UMAP) of the identified clusters. For the sample comparing distinct lymph nodes (Fig. 5), contaminating clusters containing B cells, monocytes and classical T cells were removed from the analysis based on marker genes.

Pathway and Gene set enrichment analysis

Significant differentially expressed genes were defined by the FindMarker function in Seurat using only.pos = T, min.pct = 0.25, logfc.threshold = 0.25 as parameters. The genes were visualized using either the in Seurat implemented heatmap function or using EnhancedVolcano¹⁵⁴. For pathway analysis, the significant differentially expressed genes were analyzed using the Enrichr tool^{155,156}. The BioPlanet 2019 database¹⁵⁷ was used as a reference to test for enrichment with standard Enrichr settings. The p-value was calculated from a Fisher's exact test. For gene set enrichment analysis, differentially expressed genes were analyzed using the GSEA MSigDB software^{158,159}.

Visualization

The graphs were partially created with BioRender.com.

Statistical analysis

Data, with the exception of scRNA-sequencing data, were analyzed using GraphPad Prism 8. Non-paired Student t-test (two-tailed) was used to determine statistical significance between two groups. Stars indicate significances (* $p < 0.05$, ** $p < 0.01$, *** $p < 0.001$). Error bars indicate the standard error of the mean (SEM).

Abbreviations

%	percent
°C	degree Celsius
APC	antigen presenting cells
ATP	adenosine-triphosphate
BFA	brefeldin A
CAR	chimeric antigen receptor
CCL	C-C motif chemokine ligand
CCR	C-C motif chemokine receptor
CD	cluster of differentiation
cDNA	complementary deoxyribonucleic acid
CFU	colony forming units
CSF1	colony-stimulating factor 1
CXCR	C-X-C motif chemokine receptor
DAMP	danger associated molecular patterns
DC	dendritic cells
DETC	dendritic epidermal T cells
DMSO	dimethylsulfoxid
DN	double negative
DTT	diethiothreitol
Eomes	eomesodermin
FBS	fetal bovine serum
Fcεr1g	Fc epsilon receptor 1g
GalCer	galactosylceramid
Gata3	GATA binding protein 3
GCWFS	gelatin from cold water fish skin
GFP	green fluorescent protein
GM-CSF	granulocyte-macrophage colony-stimulating factor
h	hour
Id2	inhibitor of DNA binding 2
IELs	intraepithelial lymphocytes
IFN	interferon
IL	interleukin
IL-18R1	interleukin 18 receptor 1
IL-18rap	interleukin18 receptor associated protein
IL-18BP	interleukin 18 binding protein
ILC	innate lymphoid cells
iLN	inguinal lymph nodes
Iono	ionomycin
ITG	integrin
Klf2	krüppel like factor 2
Lck	lymphocyte-specific protein tyrosine kinase
LN	lymph nodes
LPS	lipo-polysaccharide
Ly6a	lymphocyte antigen 6A
MAIT	mucosal associated invariant T
MAP	mitogen-activated protein
medLN	mediastinal lymph nodes
mesLN	mesenteric lymph nodes
mg	milligram
MHC	major histocompatibility complex
min	minute
ml	milliliter

MR1	major histocompatibility complex class I-related
MyD88	myeloid differentiation primary response 88
NF κ B	nuclear factor 'kappa-light-chain-enhancer' of activated B-cells
NK	natural killer
Nkg7	natural killer cell granule protein 7
NKT	natural killer T
NMS	normal mouse serum
NOD	nucleotide-binding and oligomerization domain
OD	optical density
PAMP	pathogen associated molecular patterns
PBS	phosphate-buffered saline
PFU	plaque forming units
pLN	popliteal lymph nodes
PMA	phorbol myristate acetate
RIG-I	retinoic acid-inducible gene I
Rora	RAR related orphan receptor A
Rorc	RAR related orphan receptor C
rpm	rounds per minute
<i>S. aureus</i>	staphylococcus aureus
scRNA	single cell ribonucleic acid
sdLN	skin draining lymph nodes
Sell	selectin L
Skint-1	selection and upkeep of intraepithelial T-cells protein 1
SEM	standard error of the mean
Slamf6	SLAM Family Member 6
SPF	specific pathogen free
Tbx21	T-Box transcription factor 21
TCR	T cell receptor
Th	T helper cell type
TIR	toll/interleukin-1 receptor
TLR	toll-like receptor
TRIF	TIR-domain-containing adapter-inducing interferon- β
tSNE	t-distributed stochastic neighbor embedding
TNF- α	tumor necrosis factor alpha
μ l	microliter
μ M	micromolar
μ m	micrometer
UMAP	uniform manifold approximation and projection
UMI	unique molecular identifier
UTC	unconventional T cells
Vim	vimentin
wt	wild type
Zbtb16	zinc finger and BTB domain-containing protein 16

Publication list

- Ataide, M. A.* , Knopper, K.* , Cruz de Casas, P.* , ... , Gasteiger, G., Saliba, A. E., Kastenmuller, W. (2022). Functional unit concept of unconventional T lymphocytes reveals site-specific immunity differing between lymph nodes. *under revision*, *authors contributed equal
- Dahling, S.* , Mansilla, A. M.* , Knopper, K.* , Grafen, A., ... , Kastenmuller, W. (2022). Type 1 conventional dendritic cells maintain and guide the differentiation of precursors of exhausted T cells in distinct cellular niches. *Immunity*, 55(4), 656-670 e658. <https://doi:10.1016/j.immuni.2022.03.006>; *authors contributed equal
- Giampaolo, S., Knöpper, K., ... , Serfling, E., Klein-Hessling, S. (2022). NFATc1 induction by an intronic enhancer restricts NKT gd T cells formation. *submitted*
- Peters, A. E., Knopper, K., Grafen, A. & Kastenmuller, W. (2021). A multifunctional mouse model to study the role of Samd3. *Eur J Immunol*. <https://doi:10.1002/eji.202149469>
- Kienle, K., ... , Knopper, K., ... , Kastenmuller, W., & Lammermann, T. (2021). Neutrophils self-limit swarming to contain bacterial growth in vivo. *Science*, 372(6548). <https://doi.org/10.1126/science.abe7729>
- Groh, J., Knöpper, K., ... , Saliba, A.-E., Kastenmüller, W., & Martini, R. (2021). Accumulation of cytotoxic T cells in the aged CNS leads to axon degeneration and contributes to cognitive and motor decline. *Nature Aging*, 1(4), 357-367. <https://doi.org/10.1038/s43587-021-00049-z>
- Ataide, M. A., Komander, K., Knopper, K., ... , Kastenmuller, W. (2020). BATF3 programs CD8(+) T cell memory. *Nat Immunol*, 21(11), 1397-1407. <https://doi.org/10.1038/s41590-020-0786-2>
- Zeis, P., Lian, M., Fan, X., ... , Knopper, K., ... , Gasteiger, G. (2020). In Situ Maturation and Tissue Adaptation of Type 2 Innate Lymphoid Cell Progenitors. *Immunity*, 53(4), 775-792 e779. <https://doi.org/10.1016/j.immuni.2020.09.002>
- Fulle, L., ... , Knopper, K., ... , Forster, I. (2018). CCL17 exerts a neuroimmune modulatory function and is expressed in hippocampal neurons. *Glia*, 66(10), 2246-2261. <https://doi.org/10.1002/glia.23507>

References

- 1 Janssen, L. M. A., van der Flier, M. & de Vries, E. Lessons Learned From the Clinical Presentation of Common Variable Immunodeficiency Disorders: A Systematic Review and Meta-Analysis. *Front Immunol* **12**, 620709, doi:10.3389/fimmu.2021.620709 (2021).
- 2 Rottem, M., Gershwin, M. E. & Shoenfeld, Y. Allergic disease and autoimmune effectors pathways. *Dev Immunol* **9**, 161-167, doi:10.1080/1044667031000137638 (2002).
- 3 Bretscher, P. & Cohn, M. A theory of self-nonself discrimination. *Science* **169**, 1042-1049, doi:10.1126/science.169.3950.1042 (1970).
- 4 Zindel, J. & Kubes, P. DAMPs, PAMPs, and LAMPs in Immunity and Sterile Inflammation. *Annu Rev Pathol* **15**, 493-518, doi:10.1146/annurev-pathmechdis-012419-032847 (2020).
- 5 Poltorak, A. *et al.* Defective LPS signaling in C3H/HeJ and C57BL/10ScCr mice: mutations in Tlr4 gene. *Science* **282**, 2085-2088, doi:10.1126/science.282.5396.2085 (1998).
- 6 Eltzschig, H. K., Sitkovsky, M. V. & Robson, S. C. Purinergic signaling during inflammation. *N Engl J Med* **367**, 2322-2333, doi:10.1056/NEJMra1205750 (2012).
- 7 Hoshino, K. *et al.* Cutting edge: Toll-like receptor 4 (TLR4)-deficient mice are hyporesponsive to lipopolysaccharide: evidence for TLR4 as the Lps gene product. *J Immunol* **162**, 3749-3752 (1999).
- 8 Rehwinkel, J. & Gack, M. U. RIG-I-like receptors: their regulation and roles in RNA sensing. *Nat Rev Immunol* **20**, 537-551, doi:10.1038/s41577-020-0288-3 (2020).
- 9 Zelensky, A. N. & Gready, J. E. The C-type lectin-like domain superfamily. *FEBS J* **272**, 6179-6217, doi:10.1111/j.1742-4658.2005.05031.x (2005).
- 10 Chen, G., Shaw, M. H., Kim, Y. G. & Nunez, G. NOD-like receptors: role in innate immunity and inflammatory disease. *Annu Rev Pathol* **4**, 365-398, doi:10.1146/annurev.pathol.4.110807.092239 (2009).
- 11 Kawasaki, T. & Kawai, T. Toll-like receptor signaling pathways. *Front Immunol* **5**, 461, doi:10.3389/fimmu.2014.00461 (2014).
- 12 Spits, H. *et al.* Innate lymphoid cells--a proposal for uniform nomenclature. *Nat Rev Immunol* **13**, 145-149, doi:10.1038/nri3365 (2013).
- 13 Hulsmans, M. *et al.* Macrophages Facilitate Electrical Conduction in the Heart. *Cell* **169**, 510-522 e520, doi:10.1016/j.cell.2017.03.050 (2017).
- 14 Mogensen, T. H. Pathogen recognition and inflammatory signaling in innate immune defenses. *Clin Microbiol Rev* **22**, 240-273, Table of Contents, doi:10.1128/CMR.00046-08 (2009).
- 15 Gasteiger, G., Fan, X., Dikiy, S., Lee, S. Y. & Rudensky, A. Y. Tissue residency of innate lymphoid cells in lymphoid and nonlymphoid organs. *Science* **350**, 981-985, doi:10.1126/science.aac9593 (2015).
- 16 Zeis, P. *et al.* In Situ Maturation and Tissue Adaptation of Type 2 Innate Lymphoid Cell Progenitors. *Immunity* **53**, 775-792 e779, doi:10.1016/j.immuni.2020.09.002 (2020).
- 17 Lammermann, T. *et al.* Neutrophil swarms require LTB4 and integrins at sites of cell death in vivo. *Nature* **498**, 371-375, doi:10.1038/nature12175 (2013).
- 18 Brinkmann, V. *et al.* Neutrophil extracellular traps kill bacteria. *Science* **303**, 1532-1535, doi:10.1126/science.1092385 (2004).
- 19 Thiam, H. R., Wong, S. L., Wagner, D. D. & Waterman, C. M. Cellular Mechanisms of NETosis. *Annu Rev Cell Dev Biol* **36**, 191-218, doi:10.1146/annurev-cellbio-020520-111016 (2020).
- 20 Kiessling, R., Klein, E. & Wigzell, H. "Natural" killer cells in the mouse. I. Cytotoxic cells with specificity for mouse Moloney leukemia cells. Specificity and distribution according to genotype. *Eur J Immunol* **5**, 112-117, doi:10.1002/eji.1830050208 (1975).

- 21 Bottcher, J. P. *et al.* NK Cells Stimulate Recruitment of cDC1 into the Tumor Microenvironment Promoting Cancer Immune Control. *Cell* **172**, 1022-1037 e1014, doi:10.1016/j.cell.2018.01.004 (2018).
- 22 Cunningham-Rundles, C. & Ponda, P. P. Molecular defects in T- and B-cell primary immunodeficiency diseases. *Nat Rev Immunol* **5**, 880-892, doi:10.1038/nri1713 (2005).
- 23 Mombaerts, P. *et al.* RAG-1-deficient mice have no mature B and T lymphocytes. *Cell* **68**, 869-877, doi:10.1016/0092-8674(92)90030-g (1992).
- 24 Muramatsu, M. *et al.* Class switch recombination and hypermutation require activation-induced cytidine deaminase (AID), a potential RNA editing enzyme. *Cell* **102**, 553-563, doi:10.1016/s0092-8674(00)00078-7 (2000).
- 25 Revy, P. *et al.* Activation-induced cytidine deaminase (AID) deficiency causes the autosomal recessive form of the Hyper-IgM syndrome (HIGM2). *Cell* **102**, 565-575, doi:10.1016/s0092-8674(00)00079-9 (2000).
- 26 Hodgkin, P. D., Heath, W. R. & Baxter, A. G. The clonal selection theory: 50 years since the revolution. *Nat Immunol* **8**, 1019-1026, doi:10.1038/ni1007-1019 (2007).
- 27 Lythe, G., Callard, R. E., Hoare, R. L. & Molina-Paris, C. How many TCR clonotypes does a body maintain? *J Theor Biol* **389**, 214-224, doi:10.1016/j.jtbi.2015.10.016 (2016).
- 28 Khan, U. & Ghazanfar, H. T Lymphocytes and Autoimmunity. *Int Rev Cell Mol Biol* **341**, 125-168, doi:10.1016/bs.ircmb.2018.05.008 (2018).
- 29 Takaba, H. & Takayanagi, H. The Mechanisms of T Cell Selection in the Thymus. *Trends Immunol* **38**, 805-816, doi:10.1016/j.it.2017.07.010 (2017).
- 30 Kurd, N. & Robey, E. A. T-cell selection in the thymus: a spatial and temporal perspective. *Immunol Rev* **271**, 114-126, doi:10.1111/imr.12398 (2016).
- 31 Godfrey, D. I., Kennedy, J., Suda, T. & Zlotnik, A. A developmental pathway involving four phenotypically and functionally distinct subsets of CD3-CD4-CD8- triple-negative adult mouse thymocytes defined by CD44 and CD25 expression. *J Immunol* **150**, 4244-4252 (1993).
- 32 Dudley, E. C., Petrie, H. T., Shah, L. M., Owen, M. J. & Hayday, A. C. T cell receptor beta chain gene rearrangement and selection during thymocyte development in adult mice. *Immunity* **1**, 83-93, doi:10.1016/1074-7613(94)90102-3 (1994).
- 33 Nakagawa, Y. *et al.* Thymic nurse cells provide microenvironment for secondary T cell receptor alpha rearrangement in cortical thymocytes. *Proc Natl Acad Sci U S A* **109**, 20572-20577, doi:10.1073/pnas.1213069109 (2012).
- 34 von Boehmer, H. *et al.* Pleiotropic changes controlled by the pre-T-cell receptor. *Curr Opin Immunol* **11**, 135-142, doi:10.1016/s0952-7915(99)80024-7 (1999).
- 35 Klein, L., Kyewski, B., Allen, P. M. & Hogquist, K. A. Positive and negative selection of the T cell repertoire: what thymocytes see (and don't see). *Nat Rev Immunol* **14**, 377-391, doi:10.1038/nri3667 (2014).
- 36 Janeway, C. A., Jr. The T cell receptor as a multicomponent signalling machine: CD4/CD8 coreceptors and CD45 in T cell activation. *Annu Rev Immunol* **10**, 645-674, doi:10.1146/annurev.iy.10.040192.003241 (1992).
- 37 Gay, D. *et al.* Functional interaction between human T-cell protein CD4 and the major histocompatibility complex HLA-DR antigen. *Nature* **328**, 626-629, doi:10.1038/328626a0 (1987).
- 38 Roche, P. A. & Furuta, K. The ins and outs of MHC class II-mediated antigen processing and presentation. *Nat Rev Immunol* **15**, 203-216, doi:10.1038/nri3818 (2015).
- 39 Zhu, J., Yamane, H. & Paul, W. E. Differentiation of effector CD4 T cell populations (*). *Annu Rev Immunol* **28**, 445-489, doi:10.1146/annurev-immunol-030409-101212 (2010).
- 40 Hsieh, C. S. *et al.* Development of TH1 CD4+ T cells through IL-12 produced by Listeria-induced macrophages. *Science* **260**, 547-549, doi:10.1126/science.8097338 (1993).

- 41 Zheng, W. & Flavell, R. A. The transcription factor GATA-3 is necessary and sufficient for Th2 cytokine gene expression in CD4 T cells. *Cell* **89**, 587-596, doi:10.1016/s0092-8674(00)80240-8 (1997).
- 42 Harrington, L. E. *et al.* Interleukin 17-producing CD4⁺ effector T cells develop via a lineage distinct from the T helper type 1 and 2 lineages. *Nat Immunol* **6**, 1123-1132, doi:10.1038/ni1254 (2005).
- 43 Hansen, T. H. & Bouvier, M. MHC class I antigen presentation: learning from viral evasion strategies. *Nat Rev Immunol* **9**, 503-513, doi:10.1038/nri2575 (2009).
- 44 Vyas, J. M., Van der Veen, A. G. & Ploegh, H. L. The known unknowns of antigen processing and presentation. *Nat Rev Immunol* **8**, 607-618, doi:10.1038/nri2368 (2008).
- 45 Kisielow, P. *et al.* Ly antigens as markers for functionally distinct subpopulations of thymus-derived lymphocytes of the mouse. *Nature* **253**, 219-220, doi:10.1038/253219a0 (1975).
- 46 van Stipdonk, M. J., Lemmens, E. E. & Schoenberger, S. P. Naive CTLs require a single brief period of antigenic stimulation for clonal expansion and differentiation. *Nat Immunol* **2**, 423-429, doi:10.1038/87730 (2001).
- 47 Eickhoff, S. *et al.* Robust Anti-viral Immunity Requires Multiple Distinct T Cell-Dendritic Cell Interactions. *Cell* **162**, 1322-1337, doi:10.1016/j.cell.2015.08.004 (2015).
- 48 Robbins, S. H., Terrizzi, S. C., Sydora, B. C., Mikayama, T. & Brossay, L. Differential regulation of killer cell lectin-like receptor G1 expression on T cells. *J Immunol* **170**, 5876-5885, doi:10.4049/jimmunol.170.12.5876 (2003).
- 49 Joshi, N. S. & Kaech, S. M. Effector CD8 T cell development: a balancing act between memory cell potential and terminal differentiation. *J Immunol* **180**, 1309-1315, doi:10.4049/jimmunol.180.3.1309 (2008).
- 50 Netea, M. G., Schlitzer, A., Placek, K., Joosten, L. A. B. & Schultze, J. L. Innate and Adaptive Immune Memory: an Evolutionary Continuum in the Host's Response to Pathogens. *Cell Host Microbe* **25**, 13-26, doi:10.1016/j.chom.2018.12.006 (2019).
- 51 Behr, F. M. *et al.* Tissue-resident memory CD8(+) T cells shape local and systemic secondary T cell responses. *Nat Immunol* **21**, 1070-1081, doi:10.1038/s41590-020-0723-4 (2020).
- 52 Bretscher, P. A. A two-step, two-signal model for the primary activation of precursor helper T cells. *Proc Natl Acad Sci U S A* **96**, 185-190, doi:10.1073/pnas.96.1.185 (1999).
- 53 Lenschow, D. J., Walunas, T. L. & Bluestone, J. A. CD28/B7 system of T cell costimulation. *Annu Rev Immunol* **14**, 233-258, doi:10.1146/annurev.immunol.14.1.233 (1996).
- 54 Curtsinger, J. M. *et al.* Inflammatory cytokines provide a third signal for activation of naive CD4⁺ and CD8⁺ T cells. *J Immunol* **162**, 3256-3262 (1999).
- 55 Curtsinger, J. M. & Mescher, M. F. Inflammatory cytokines as a third signal for T cell activation. *Curr Opin Immunol* **22**, 333-340, doi:10.1016/j.coi.2010.02.013 (2010).
- 56 Dong, C. Cytokine Regulation and Function in T Cells. *Annu Rev Immunol* **39**, 51-76, doi:10.1146/annurev-immunol-061020-053702 (2021).
- 57 Miyajima, A., Kitamura, T., Harada, N., Yokota, T. & Arai, K. Cytokine receptors and signal transduction. *Annu Rev Immunol* **10**, 295-331, doi:10.1146/annurev.iy.10.040192.001455 (1992).
- 58 Spangler, J. B., Moraga, I., Mendoza, J. L. & Garcia, K. C. Insights into cytokine-receptor interactions from cytokine engineering. *Annu Rev Immunol* **33**, 139-167, doi:10.1146/annurev-immunol-032713-120211 (2015).
- 59 Okamura, H. *et al.* A novel costimulatory factor for gamma interferon induction found in the livers of mice causes endotoxic shock. *Infect Immun* **63**, 3966-3972, doi:10.1128/iai.63.10.3966-3972.1995 (1995).
- 60 Fantuzzi, G., Reed, D. A. & Dinarello, C. A. IL-12-induced IFN-gamma is dependent on caspase-1 processing of the IL-18 precursor. *J Clin Invest* **104**, 761-767, doi:10.1172/JCI7501 (1999).

- 61 Dinarello, C. A., Novick, D., Kim, S. & Kaplanski, G. Interleukin-18 and IL-18 binding protein. *Front Immunol* **4**, 289, doi:10.3389/fimmu.2013.00289 (2013).
- 62 Novick, D. *et al.* Interleukin-18 binding protein: a novel modulator of the Th1 cytokine response. *Immunity* **10**, 127-136, doi:10.1016/s1074-7613(00)80013-8 (1999).
- 63 Girard-Guyonvarc'h, C. *et al.* Unopposed IL-18 signaling leads to severe TLR9-induced macrophage activation syndrome in mice. *Blood* **131**, 1430-1441, doi:10.1182/blood-2017-06-789552 (2018).
- 64 Tan, J. T. *et al.* IL-7 is critical for homeostatic proliferation and survival of naive T cells. *Proc Natl Acad Sci U S A* **98**, 8732-8737, doi:10.1073/pnas.161126098 (2001).
- 65 Xie, X. *et al.* Single-cell transcriptome profiling reveals neutrophil heterogeneity in homeostasis and infection. *Nat Immunol* **21**, 1119-1133, doi:10.1038/s41590-020-0736-z (2020).
- 66 Haring, J. S., Badovinac, V. P. & Harty, J. T. Inflaming the CD8+ T cell response. *Immunity* **25**, 19-29, doi:10.1016/j.immuni.2006.07.001 (2006).
- 67 Gallatin, W. M., Weissman, I. L. & Butcher, E. C. A cell-surface molecule involved in organ-specific homing of lymphocytes. *Nature* **304**, 30-34, doi:10.1038/304030a0 (1983).
- 68 Gasteiger, G., Ataide, M. & Kastenmuller, W. Lymph node - an organ for T-cell activation and pathogen defense. *Immunol Rev* **271**, 200-220, doi:10.1111/imr.12399 (2016).
- 69 Itano, A. A. *et al.* Distinct dendritic cell populations sequentially present antigen to CD4 T cells and stimulate different aspects of cell-mediated immunity. *Immunity* **19**, 47-57, doi:10.1016/s1074-7613(03)00175-4 (2003).
- 70 Druzd, D. *et al.* Lymphocyte Circadian Clocks Control Lymph Node Trafficking and Adaptive Immune Responses. *Immunity* **46**, 120-132, doi:10.1016/j.immuni.2016.12.011 (2017).
- 71 Holtkamp, S. J. *et al.* Circadian clocks guide dendritic cells into skin lymphatics. *Nat Immunol* **22**, 1375-1381, doi:10.1038/s41590-021-01040-x (2021).
- 72 Godfrey, D. I., Uldrich, A. P., McCluskey, J., Rossjohn, J. & Moody, D. B. The burgeoning family of unconventional T cells. *Nat Immunol* **16**, 1114-1123, doi:10.1038/ni.3298 (2015).
- 73 Bendelac, A. *et al.* CD1 recognition by mouse NK1+ T lymphocytes. *Science* **268**, 863-865, doi:10.1126/science.7538697 (1995).
- 74 Treiner, E. *et al.* Selection of evolutionarily conserved mucosal-associated invariant T cells by MR1. *Nature* **422**, 164-169, doi:10.1038/nature01433 (2003).
- 75 Chien, Y. H., Meyer, C. & Bonneville, M. gammadelta T cells: first line of defense and beyond. *Annu Rev Immunol* **32**, 121-155, doi:10.1146/annurev-immunol-032713-120216 (2014).
- 76 Rigau, M. *et al.* Butyrophilin 2A1 is essential for phosphoantigen reactivity by gammadelta T cells. *Science* **367**, doi:10.1126/science.aay5516 (2020).
- 77 Constantinides, M. G. & Belkaid, Y. Early-life imprinting of unconventional T cells and tissue homeostasis. *Science* **374**, eabf0095, doi:10.1126/science.abf0095 (2021).
- 78 Pellicci, D. G., Koay, H. F. & Berzins, S. P. Thymic development of unconventional T cells: how NKT cells, MAIT cells and gammadelta T cells emerge. *Nat Rev Immunol* **20**, 756-770, doi:10.1038/s41577-020-0345-y (2020).
- 79 Salou, M. *et al.* A common transcriptomic program acquired in the thymus defines tissue residency of MAIT and NKT subsets. *J Exp Med* **216**, 133-151, doi:10.1084/jem.20181483 (2019).
- 80 Legoux, F. *et al.* Microbial metabolites control the thymic development of mucosal-associated invariant T cells. *Science* **366**, 494-499, doi:10.1126/science.aaw2719 (2019).
- 81 Olszak, T. *et al.* Microbial exposure during early life has persistent effects on natural killer T cell function. *Science* **336**, 489-493, doi:10.1126/science.1219328 (2012).

- 82 Kohlgruber, A. C. *et al.* gammadelta T cells producing interleukin-17A regulate adipose regulatory T cell homeostasis and thermogenesis. *Nat Immunol* **19**, 464-474, doi:10.1038/s41590-018-0094-2 (2018).
- 83 Dillen, C. A. *et al.* Clonally expanded gammadelta T cells protect against *Staphylococcus aureus* skin reinfection. *J Clin Invest* **128**, 1026-1042, doi:10.1172/JCI96481 (2018).
- 84 Jameson, J. *et al.* A role for skin gammadelta T cells in wound repair. *Science* **296**, 747-749, doi:10.1126/science.1069639 (2002).
- 85 Marchitto, M. C. *et al.* Clonal Vgamma6(+)/Vdelta4(+) T cells promote IL-17-mediated immunity against *Staphylococcus aureus* skin infection. *Proc Natl Acad Sci U S A* **116**, 10917-10926, doi:10.1073/pnas.1818256116 (2019).
- 86 Mann, A. O. *et al.* IL-17A-producing gammadelta T cells promote muscle regeneration in a microbiota-dependent manner. *J Exp Med* **219**, doi:10.1084/jem.20211504 (2022).
- 87 Hinks, T. S. C. & Zhang, X. W. MAIT Cell Activation and Functions. *Front Immunol* **11**, 1014, doi:10.3389/fimmu.2020.01014 (2020).
- 88 McWilliam, H. E. *et al.* The intracellular pathway for the presentation of vitamin B-related antigens by the antigen-presenting molecule MR1. *Nat Immunol* **17**, 531-537, doi:10.1038/ni.3416 (2016).
- 89 McKenzie, D. R. *et al.* Normality sensing licenses local T cells for innate-like tissue surveillance. *Nat Immunol* **23**, 411-422, doi:10.1038/s41590-021-01124-8 (2022).
- 90 Wencker, M. *et al.* Innate-like T cells straddle innate and adaptive immunity by altering antigen-receptor responsiveness. *Nat Immunol* **15**, 80-87, doi:10.1038/ni.2773 (2014).
- 91 Tan, L. *et al.* Single-Cell Transcriptomics Identifies the Adaptation of Scart1(+) Vgamma6(+) T Cells to Skin Residency as Activated Effector Cells. *Cell Rep* **27**, 3657-3671 e3654, doi:10.1016/j.celrep.2019.05.064 (2019).
- 92 Gaud, G., Lesourne, R. & Love, P. E. Regulatory mechanisms in T cell receptor signalling. *Nat Rev Immunol* **18**, 485-497, doi:10.1038/s41577-018-0020-8 (2018).
- 93 Klose, C. S. N. & Artis, D. Innate lymphoid cells control signaling circuits to regulate tissue-specific immunity. *Cell Res* **30**, 475-491, doi:10.1038/s41422-020-0323-8 (2020).
- 94 Guilliams, M., Thierry, G. R., Bonnardel, J. & Bajenoff, M. Establishment and Maintenance of the Macrophage Niche. *Immunity* **52**, 434-451, doi:10.1016/j.immuni.2020.02.015 (2020).
- 95 Lavin, Y., Mortha, A., Rahman, A. & Merad, M. Regulation of macrophage development and function in peripheral tissues. *Nat Rev Immunol* **15**, 731-744, doi:10.1038/nri3920 (2015).
- 96 Rodda, L. B. *et al.* Single-Cell RNA Sequencing of Lymph Node Stromal Cells Reveals Niche-Associated Heterogeneity. *Immunity* **48**, 1014-1028 e1016, doi:10.1016/j.immuni.2018.04.006 (2018).
- 97 Pezoldt, J. *et al.* Neonatally imprinted stromal cell subsets induce tolerogenic dendritic cells in mesenteric lymph nodes. *Nat Commun* **9**, 3903, doi:10.1038/s41467-018-06423-7 (2018).
- 98 Esterhazy, D. *et al.* Compartmentalized gut lymph node drainage dictates adaptive immune responses. *Nature* **569**, 126-130, doi:10.1038/s41586-019-1125-3 (2019).
- 99 Hiltensperger, M. *et al.* Skin and gut imprinted helper T cell subsets exhibit distinct functional phenotypes in central nervous system autoimmunity. *Nat Immunol* **22**, 880-892, doi:10.1038/s41590-021-00948-8 (2021).
- 100 Abadie, V. *et al.* Original encounter with antigen determines antigen-presenting cell imprinting of the quality of the immune response in mice. *PLoS One* **4**, e8159, doi:10.1371/journal.pone.0008159 (2009).
- 101 Mullins, D. W. *et al.* Route of immunization with peptide-pulsed dendritic cells controls the distribution of memory and effector T cells in lymphoid tissues and determines the pattern of regional tumor control. *J Exp Med* **198**, 1023-1034, doi:10.1084/jem.20021348 (2003).

- 102 Rosenbaum, P. *et al.* Vaccine Inoculation Route Modulates Early Immunity and
Consequently Antigen-Specific Immune Response. *Front Immunol* **12**, 645210,
doi:10.3389/fimmu.2021.645210 (2021).
- 103 Janeway, C. A., Jr. Approaching the asymptote? Evolution and revolution in
immunology. *Cold Spring Harb Symp Quant Biol* **54 Pt 1**, 1-13,
doi:10.1101/sqb.1989.054.01.003 (1989).
- 104 Gaya, M. *et al.* Initiation of Antiviral B Cell Immunity Relies on Innate Signals from
Spatially Positioned NKT Cells. *Cell* **172**, 517-533 e520,
doi:10.1016/j.cell.2017.11.036 (2018).
- 105 Liu, Y. *et al.* A modified alpha-galactosyl ceramide for staining and stimulating natural
killer T cells. *J Immunol Methods* **312**, 34-39, doi:10.1016/j.jim.2006.02.009 (2006).
- 106 Stoeckius, M. *et al.* Simultaneous epitope and transcriptome measurement in single
cells. *Nat Methods* **14**, 865-868, doi:10.1038/nmeth.4380 (2017).
- 107 Hwang, S. T. *et al.* GlyCAM-1, a physiologic ligand for L-selectin, activates beta 2
integrins on naive peripheral lymphocytes. *J Exp Med* **184**, 1343-1348,
doi:10.1084/jem.184.4.1343 (1996).
- 108 Kharchenko, P. V., Silberstein, L. & Scadden, D. T. Bayesian approach to single-cell
differential expression analysis. *Nat Methods* **11**, 740-742, doi:10.1038/nmeth.2967
(2014).
- 109 Lee, Y. J., Holzapfel, K. L., Zhu, J., Jameson, S. C. & Hogquist, K. A. Steady-state
production of IL-4 modulates immunity in mouse strains and is determined by lineage
diversity of iNKT cells. *Nat Immunol* **14**, 1146-1154, doi:10.1038/ni.2731 (2013).
- 110 Laidlaw, B. J., Gray, E. E., Zhang, Y., Ramirez-Valle, F. & Cyster, J. G. Sphingosine-
1-phosphate receptor 2 restrains egress of gammadelta T cells from the skin. *J Exp
Med* **216**, 1487-1496, doi:10.1084/jem.20190114 (2019).
- 111 Nakamizo, S. *et al.* Dermal Vgamma4(+) gammadelta T cells possess a migratory
potency to the draining lymph nodes and modulate CD8(+) T-cell activity through TNF-
alpha production. *J Invest Dermatol* **135**, 1007-1015, doi:10.1038/jid.2014.516 (2015).
- 112 Gray, E. E. *et al.* Deficiency in IL-17-committed Vgamma4(+) gammadelta T cells in a
spontaneous Sox13-mutant CD45.1(+) congenic mouse substrain provides protection
from dermatitis. *Nat Immunol* **14**, 584-592, doi:10.1038/ni.2585 (2013).
- 113 Hufeldt, M. R., Nielsen, D. S., Vogensen, F. K., Midtvedt, T. & Hansen, A. K. Variation
in the gut microbiota of laboratory mice is related to both genetic and environmental
factors. *Comp Med* **60**, 336-347 (2010).
- 114 Qi, H., Kastenmuller, W. & Germain, R. N. Spatiotemporal basis of innate and adaptive
immunity in secondary lymphoid tissue. *Annu Rev Cell Dev Biol* **30**, 141-167,
doi:10.1146/annurev-cellbio-100913-013254 (2014).
- 115 Zhang, Y. *et al.* Migratory and adhesive cues controlling innate-like lymphocyte
surveillance of the pathogen-exposed surface of the lymph node. *Elife* **5**,
doi:10.7554/eLife.18156 (2016).
- 116 Gray, E. E., Friend, S., Suzuki, K., Phan, T. G. & Cyster, J. G. Subcapsular sinus
macrophage fragmentation and CD169+ bleb acquisition by closely associated IL-17-
committed innate-like lymphocytes. *PLoS One* **7**, e38258,
doi:10.1371/journal.pone.0038258 (2012).
- 117 Itohara, S. *et al.* T cell receptor delta gene mutant mice: independent generation of
alpha beta T cells and programmed rearrangements of gamma delta TCR genes. *Cell*
72, 337-348, doi:10.1016/0092-8674(93)90112-4 (1993).
- 118 Smiley, S. T., Kaplan, M. H. & Grusby, M. J. Immunoglobulin E production in the
absence of interleukin-4-secreting CD1-dependent cells. *Science* **275**, 977-979,
doi:10.1126/science.275.5302.977 (1997).
- 119 Cua, D. J. *et al.* Interleukin-23 rather than interleukin-12 is the critical cytokine for
autoimmune inflammation of the brain. *Nature* **421**, 744-748, doi:10.1038/nature01355
(2003).
- 120 Marco Ataíde, Konrad Knöpper, Paulina Cruz de Casas, Sarah Eickhoff, Milas Ugur,
Mangge Zou, Haroon Shaikh, Apurwa Trivedi, Anika Grafen, Immo Prinz, Knut Ohlsen,

- Andreas Beilhack, Jochen Huehn, Mauro Gaya, Antoine-Emmanuel Saliba, Georg Gasteiger, Wolfgang Kastenmüller. Lymphatic migration of unconventional T cells links tissue immunity to lymph node function. (2022).
- 121 Conboy, M. J., Conboy, I. M. & Rando, T. A. Heterochronic parabiosis: historical perspective and methodological considerations for studies of aging and longevity. *Aging Cell* **12**, 525-530, doi:10.1111/ace.12065 (2013).
- 122 Sagar *et al.* Deciphering the regulatory landscape of fetal and adult gammadelta T-cell development at single-cell resolution. *EMBO J* **39**, e104159, doi:10.15252/embj.2019104159 (2020).
- 123 McKenzie, D. R. *et al.* IL-17-producing gammadelta T cells switch migratory patterns between resting and activated states. *Nat Commun* **8**, 15632, doi:10.1038/ncomms15632 (2017).
- 124 Lee, M. *et al.* Single-cell RNA sequencing identifies shared differentiation paths of mouse thymic innate T cells. *Nat Commun* **11**, 4367, doi:10.1038/s41467-020-18155-8 (2020).
- 125 Gutierrez-Arcelus, M. *et al.* Lymphocyte innateness defined by transcriptional states reflects a balance between proliferation and effector functions. *Nat Commun* **10**, 687, doi:10.1038/s41467-019-08604-4 (2019).
- 126 Lee, Y. J. *et al.* Lineage-Specific Effector Signatures of Invariant NKT Cells Are Shared amongst gammadelta T, Innate Lymphoid, and Th Cells. *J Immunol* **197**, 1460-1470, doi:10.4049/jimmunol.1600643 (2016).
- 127 Asarnow, D. M., Goodman, T., LeFrancois, L. & Allison, J. P. Distinct antigen receptor repertoires of two classes of murine epithelium-associated T cells. *Nature* **341**, 60-62, doi:10.1038/341060a0 (1989).
- 128 Havran, W. L. & Allison, J. P. Developmentally ordered appearance of thymocytes expressing different T-cell antigen receptors. *Nature* **335**, 443-445, doi:10.1038/335443a0 (1988).
- 129 Turchinovich, G. & Hayday, A. C. Skint-1 identifies a common molecular mechanism for the development of interferon-gamma-secreting versus interleukin-17-secreting gammadelta T cells. *Immunity* **35**, 59-68, doi:10.1016/j.immuni.2011.04.018 (2011).
- 130 Crosby, C. M. & Kronenberg, M. Tissue-specific functions of invariant natural killer T cells. *Nat Rev Immunol* **18**, 559-574, doi:10.1038/s41577-018-0034-2 (2018).
- 131 Godfrey, D. I., Koay, H. F., McCluskey, J. & Gherardin, N. A. The biology and functional importance of MAIT cells. *Nat Immunol* **20**, 1110-1128, doi:10.1038/s41590-019-0444-8 (2019).
- 132 Mayassi, T., Barreiro, L. B., Rossjohn, J. & Jabri, B. A multilayered immune system through the lens of unconventional T cells. *Nature* **595**, 501-510, doi:10.1038/s41586-021-03578-0 (2021).
- 133 Alves de Lima, K. *et al.* Meningeal gammadelta T cells regulate anxiety-like behavior via IL-17a signaling in neurons. *Nat Immunol* **21**, 1421-1429, doi:10.1038/s41590-020-0776-4 (2020).
- 134 Lee, Y. J. *et al.* Tissue-Specific Distribution of iNKT Cells Impacts Their Cytokine Response. *Immunity* **43**, 566-578, doi:10.1016/j.immuni.2015.06.025 (2015).
- 135 Wang, H. & Hogquist, K. A. CCR7 defines a precursor for murine iNKT cells in thymus and periphery. *Elife* **7**, doi:10.7554/eLife.34793 (2018).
- 136 Bortoluzzi, S. *et al.* Brief homogeneous TCR signals instruct common iNKT progenitors whose effector diversification is characterized by subsequent cytokine signaling. *Immunity* **54**, 2497-2513 e2499, doi:10.1016/j.immuni.2021.09.003 (2021).
- 137 Hsieh, C. S., Macatonia, S. E., O'Garra, A. & Murphy, K. M. T cell genetic background determines default T helper phenotype development in vitro. *J Exp Med* **181**, 713-721, doi:10.1084/jem.181.2.713 (1995).
- 138 Holderness, J., Hedges, J. F., Ramstead, A. & Jutila, M. A. Comparative biology of gammadelta T cell function in humans, mice, and domestic animals. *Annu Rev Anim Biosci* **1**, 99-124, doi:10.1146/annurev-animal-031412-103639 (2013).

- 139 Lamichhane, R. *et al.* Human liver-derived MAIT cells differ from blood MAIT cells in their metabolism and response to TCR-independent activation. *Eur J Immunol* **51**, 879-892, doi:10.1002/eji.202048830 (2021).
- 140 Holtmeier, W. *et al.* The TCR-delta repertoire in normal human skin is restricted and distinct from the TCR-delta repertoire in the peripheral blood. *J Invest Dermatol* **116**, 275-280, doi:10.1046/j.1523-1747.2001.01250.x (2001).
- 141 Dogan, N. U., Dogan, S., Favero, G., Kohler, C. & Dursun, P. The Basics of Sentinel Lymph Node Biopsy: Anatomical and Pathophysiological Considerations and Clinical Aspects. *J Oncol* **2019**, 3415630, doi:10.1155/2019/3415630 (2019).
- 142 Mattei, D. *et al.* Enzymatic Dissociation Induces Transcriptional and Proteotype Bias in Brain Cell Populations. *Int J Mol Sci* **21**, doi:10.3390/ijms21217944 (2020).
- 143 Denisenko, E. *et al.* Systematic assessment of tissue dissociation and storage biases in single-cell and single-nucleus RNA-seq workflows. *Genome Biol* **21**, 130, doi:10.1186/s13059-020-02048-6 (2020).
- 144 Dias, J. *et al.* The CD4(-)CD8(-) MAIT cell subpopulation is a functionally distinct subset developmentally related to the main CD8(+) MAIT cell pool. *Proc Natl Acad Sci U S A* **115**, E11513-E11522, doi:10.1073/pnas.1812273115 (2018).
- 145 Godfrey, D. I., MacDonald, H. R., Kronenberg, M., Smyth, M. J. & Van Kaer, L. NKT cells: what's in a name? *Nat Rev Immunol* **4**, 231-237, doi:10.1038/nri1309 (2004).
- 146 Howson, L. J. *et al.* Absence of mucosal-associated invariant T cells in a person with a homozygous point mutation in MR1. *Sci Immunol* **5**, doi:10.1126/sciimmunol.abc9492 (2020).
- 147 Godfrey, D. I., Le Nours, J., Andrews, D. M., Uldrich, A. P. & Rossjohn, J. Unconventional T Cell Targets for Cancer Immunotherapy. *Immunity* **48**, 453-473, doi:10.1016/j.immuni.2018.03.009 (2018).
- 148 Fischer, J. W. & Bhattarai, N. CAR-T Cell Therapy: Mechanism, Management, and Mitigation of Inflammatory Toxicities. *Front Immunol* **12**, 693016, doi:10.3389/fimmu.2021.693016 (2021).
- 149 Marofi, F. *et al.* CAR T cells in solid tumors: challenges and opportunities. *Stem Cell Res Ther* **12**, 81, doi:10.1186/s13287-020-02128-1 (2021).
- 150 Xie, G. *et al.* CAR-NK cells: A promising cellular immunotherapy for cancer. *EBioMedicine* **59**, 102975, doi:10.1016/j.ebiom.2020.102975 (2020).
- 151 Nakamura, T. *et al.* CD4+ NKT cells, but not conventional CD4+ T cells, are required to generate efferent CD8+ T regulatory cells following antigen inoculation in an immune-privileged site. *J Immunol* **171**, 1266-1271, doi:10.4049/jimmunol.171.3.1266 (2003).
- 152 Rahimpour, A. *et al.* Identification of phenotypically and functionally heterogeneous mouse mucosal-associated invariant T cells using MR1 tetramers. *J Exp Med* **212**, 1095-1108, doi:10.1084/jem.20142110 (2015).
- 153 Stuart, T. *et al.* Comprehensive Integration of Single-Cell Data. *Cell* **177**, 1888-1902 e1821, doi:10.1016/j.cell.2019.05.031 (2019).
- 154 Blighe K., R. S., Lewis M. *EnhancedVolcano: publication-ready volcano plots with enhanced colouring and labeling*, (2019).
- 155 Kuleshov, M. V. *et al.* Enrichr: a comprehensive gene set enrichment analysis web server 2016 update. *Nucleic Acids Res* **44**, W90-97, doi:10.1093/nar/gkw377 (2016).
- 156 Chen, E. Y. *et al.* Enrichr: interactive and collaborative HTML5 gene list enrichment analysis tool. *BMC Bioinformatics* **14**, 128, doi:10.1186/1471-2105-14-128 (2013).
- 157 Huang, R. *et al.* The NCATS BioPlanet - An Integrated Platform for Exploring the Universe of Cellular Signaling Pathways for Toxicology, Systems Biology, and Chemical Genomics. *Front Pharmacol* **10**, 445, doi:10.3389/fphar.2019.00445 (2019).
- 158 Subramanian, A. *et al.* Gene set enrichment analysis: a knowledge-based approach for interpreting genome-wide expression profiles. *Proc Natl Acad Sci U S A* **102**, 15545-15550, doi:10.1073/pnas.0506580102 (2005).

- 159 Mootha, V. K. *et al.* PGC-1alpha-responsive genes involved in oxidative phosphorylation are coordinately downregulated in human diabetes. *Nat Genet* **34**, 267-273, doi:10.1038/ng1180 (2003).

Acknowledgement

During my PhD I have encountered many special people who supported me and helped me, but the person who I want to thank most for everything he did during this time is my PI, supervisor and mentor Wolfgang Kastenmüller. He accepted me into his group, trained me hands-on and formed me into the scientist I am today. I can't recall how many passionate and crazy scientific discussions we had over the past years, but I clearly remember that after every time we exchanged ideas and thoughts I could say: "Now I have learned something new." I truly hope that in the future we will continue having these discussions, because these are the times, I know I want to be a scientist. Thank you for sharing your passion and infectious enthusiasm with me.

Of course, my gratitude extends to the other members of my thesis committee Georg Gasteiger and Markus Sauer. Georg has been closely involved in many of my projects since the beginning and I have received a lot of great suggestions and encouragement from him. Markus always took time to listen to my project progress and I highly valued his feedback and suggestions during the years.

One person who shaped the course of my PhD and probably also the future of my scientific career is Emmanuel Saliba. Emmanuel revealed to me the fascinating world of scRNA-sequencing and together with his talented students he trained me in analyzing the data. For his patient and continued support, I will always be grateful.

Despite all the good times and discussions that I had with all my supervisors, I don't know whether I would have managed to obtain my PhD without the support and encouragement of my amazing colleagues. Most involved, especially over the last two years were Ana and Paulina. Paulina was a driving force behind the project I finally brought to paper here, and I don't want to know how it would have been without her. Her relentlessness and endurance transpired and kept me going even in the most difficult times and I am truly fortunate to have seen her growing into the amazing PhD student she is today. I know you will become a great scientist and I hope to witness your future development and achievements as your close friend.

Ana and I were working on a separate project together during the same time and I am so grateful to her for keeping up with me during these stressful periods. Together we went through a lot and even though it was very tough at times, I am more than glad to share this experience with her. I know that without her, I wouldn't have managed to keep on going. Being able to call you my friend makes my life brighter, and I am more than excited to see what greatness the future holds in store for you.

Every beginning is hard, especially when starting a PhD which usually doesn't get easier over time. Annika Peters took it upon her to train me in the beginning and introduce me to the real world of science and immunology. I will always look up to her and will never forget all the wisdom and guidance she offered me over the years.

Anika Grafen is the good soul of the lab, and her kind and positive energy often lifted my mood during difficult times. When I had problems, she always had open ears and helpful suggestions to offer. Because of this and many more things she is an important part I wouldn't want to miss during my PhD.

The real pioneer in the project you now hopefully have read is Marco. He produced many data, paved the way to make this project successful and was always available to me for advice and helpful discussion. Thank you for just being Marco.

Not many of my colleagues challenged me as often as my office mate and friend Lennart. We had many lively discussions together in the office and he made me strive to become a better scientist every day and I am glad he did.

My gratitude deeply extends to all former and current member of the group, Sarah, Sabrina Dähling, Lena, Milas, Jacob, Chloe, Ekaterina, Augusto, Kasia, Annerose, Anfei and Kathrin. All of you made this time wonderful and special to me. I feel like you guys are my second family.

The same goes of course to all the non-lab members who I was fortunate enough to spend time with during these years Sabrina Giampaolo, Melanie, Sigrun, Dou, Christin, Gosia, Jennifer, Andy, Reyna and Anne. I will never forget all the times we have laughed together, and I will always have a special place in my heart for you.

My family deserves the greatest gratitude from me. I know I can always count on them no matter how hopeless the situation might seem. And even though they still have no idea about what I am doing all the time, they never got tired of listening to my complaints or excitement. What more can a brother and son wish for?

Now that this chapter is about to close and a new one needs to open, I look back and I know, I wouldn't be the same person without any of you. I will always carry a piece of each and every one of you with me for the rest of my life. I couldn't ask for more than this present that you have given me. So, it comes from the bottom of my heart when I say

Thank you

Affidavit

I hereby confirm that my thesis entitled Lymph node heterogeneity is imprinted by unconventional T cells that are organized in functional units is the result of my own work. I did not receive any help or support from commercial consultants. All sources and / or materials applied are listed and specified in the thesis.

Furthermore, I confirm that this thesis has not yet been submitted as part of another examination process neither in identical nor in similar form.

Würzburg, 2022
Place, Date

Signature

Eidesstattliche Erklärung

Hiermit erkläre ich an Eides statt, die Dissertation Lymphknoten Heterogenität ist durch unkonventionelle T Zellen reguliert, welche in funktionellen Einheiten organisiert sind eigenständig, d.h. insbesondere selbständig und ohne Hilfe eines kommerziellen Promotionsberaters, angefertigt und keine anderen als die von mir angegebenen Quellen und Hilfsmittel verwendet zu haben.

Ich erkläre außerdem, dass die Dissertation weder in gleicher noch in ähnlicher Form bereits in einem anderen Prüfungsverfahren vorgelegen hat.

Würzburg, 2022
Ort, Datum

Unterschrift

KONRAD KNÖPPER

(Medical Biologist/ Immunologist)

27th of August 1993
Schiestlstr. 13A
97080, Würzburg

+49 152 54716879

konrad.knoepper@uni-wuerzburg.de

0000-0003-2076-2160

Software Skills

R	●●●●○○
MS Office	●●●●○○
Imaris	●●●●○○
GraphPad Prism	●●●●○○
Flowjo	●●●●○○
ImageJ	●●●○○○
Adobe Illustrator	●●●●○○

Laboratory Skills

scRNA-seq analysis	●●●●○○
RNA-seq analysis	●●●●○○
RT-PCR	●●●●○○
Western Blot	●●●○○○
ELISA	●●●●○○
IF Microscopy	●●●●○○
Flow Cytometry	●●●●○○
Skin 2P-Microscopy	●●●○○○
Mouse handling	●●●●○○
▪ acute infection	
▪ chronic infection	
▪ i.p. injection	
▪ i.v. injection	
▪ subcutaneous injection	
▪ intra nasal infection	

Education

- 10/2017 – today** **PhD student in Kastenmüller laboratory**
Max-Plank Research group of Systems Immunology, Würzburg
Applying diverse molecular and bioinformatic techniques to understand basic questions in T cell biology. Thesis title: *“Lymph node heterogeneity is imprinted by unconventional T cells that are organized in functional units”*
- 10/2015 – 09/2017** **Master study: Life and Medical Sciences, Bonn**
Master Thesis: *“Characterization of CCL17+ cells in skin using imaging and function analysis”* mentor: Prof. Irmgard Förster
- 10/2012 – 09/2015** **Bachelor study: Medical Biology, Essen**
Bachelor thesis: *“The double-edged sword of IFN γ in Melanoma”* mentor: Dr. Annete Paschen

Experiences

- 04/2016 – 09/2019** **Student assistant**
Support of ongoing research projects in the group of Prof. Irmgard Förster. Techniques: confocal microscopy, qRT-PCR
- 2015** **FELASA like B certificate**
Training for animal experiments, Essen
- 04/2014 – 09/2014** **Laboratory internship**
Internship in the group of Dr. Klump at University Hospital Essen. Involved in cloning projects

Awards, Honors and Memberships

- 2021** **Seed Grant project awarded in Single-Cell Biology**
- 2020** **2nd place imaging award**
EUREKA 2020, Würzburg
- 10/2013 – 09/2015** **Scholarship holder**
“UDE-stipendium”, Essen

KONRAD KNÖPPER

(Medical Biologist/ Immunologist)

Languages

German



English



References

Prof. Wolfgang Kastenmüller
wolfgang.kastenmueller@uni-wuerzburg.de
+49 931 31 81816

Prof. Georg Gasteiger
georg.gasteiger@uni-wuerzburg.de
+49 931 31 89740

Dr. Antoine-Emmanuel Saliba
emmanuel.saliba@helmholtz-hiri.de
+49 931 31 81341

Publications

- Ataide, M. A.*, **Knöpper, K.***, Cruz de Casas, P.*, ..., Gasteiger, G., Saliba, A. E., Kastenmuller, W. (2022). Functional unit concept of unconventional T lymphocytes reveals site-specific immunity differing between lymph nodes. *under revision*, *authors contributed equal
- Dahling, S.*, Mansilla, A. M.*, **Knopper, K.***, Grafen, A., ..., Kastenmuller, W. (2022). Type 1 conventional dendritic cells maintain and guide the differentiation of precursors of exhausted T cells in distinct cellular niches. *Immunity*, 55(4), 656-670 e658. doi:10.1016/j.immuni.2022.03.006 *authors contributed equal
- Giampaolo, S., **Knöpper, K.**, ..., Serfling, E., Klein-Hessling, S. (2022). NFATc1 induction by an intronic enhancer restricts NKT $\gamma\delta$ T cells formation. *submitted*
- Peters, A. E., **Knopper, K.**, Grafen, A. & Kastenmuller, W. (2021). A multifunctional mouse model to study the role of Samd3. *Eur J Immunol*. <https://doi:10.1002/eji.202149469>
- Kienle, K., ..., **Knopper, K.**, ..., Kastenmuller, W., & Lammermann, T. (2021). Neutrophils self-limit swarming to contain bacterial growth in vivo. *Science*, 372(6548). <https://doi.org/10.1126/science.abe7729>
- Groh, J., **Knöpper, K.**, ..., Saliba, A.-E., Kastenmüller, W., & Martini, R. (2021). Accumulation of cytotoxic T cells in the aged CNS leads to axon degeneration and contributes to cognitive and motor decline. *Nature Aging*, 1(4), 357-367. <https://doi.org/10.1038/s43587-021-00049-z>
- Ataide, M. A., Komander, K., **Knopper, K.**, ..., Kastenmuller, W. (2020). BATF3 programs CD8(+) T cell memory. *Nat Immunol*, 21(11), 1397-1407. <https://doi.org/10.1038/s41590-020-0786-2>
- Zeis, P., Lian, M., Fan, X., ..., **Knopper, K.**, ..., Gasteiger, G. (2020). In Situ Maturation and Tissue Adaptation of Type 2 Innate Lymphoid Cell Progenitors. *Immunity*, 53(4), 775-792 e779. <https://doi.org/10.1016/j.immuni.2020.09.002>
- Fulle, L., ..., **Knopper, K.**, ..., Forster, I. (2018). CCL17 exerts a neuroimmune modulatory function and is expressed in hippocampal neurons. *Glia*, 66(10), 2246-2261. <https://doi.org/10.1002/glia.23507>